

Analysis of G- Quadruplex Formation in mRNA Transcripts of Phospholemman/*FXVD1*

by

Hansraj DHAYAN

Submitted in partial fulfilment of the requirements of the University of Hertfordshire
for the degree of Master of Science by Research

Title of sponsoring department: School of Life Sciences
Name of company/institution: University of Hertfordshire
Date: 27th November 2013

UNIVERSITY OF HERTFORDSHIRE

Research Degrees Board

Name of Candidate: HANSRAJ DHAYAN

**Award of the degree of: MSc by Research in Molecular Biology, Biophysics
and Biochemistry**

DECLARATION REGARDING FINAL SUBMISSION

My submission for examination was temporarily bound.

I confirm that the contents of my final, approved submission are identical with the version submitted for examination, except where amendments have been made to meet the requirements of the examiners.

Signed:



Date: 10th June 2014

ABSTRACT

G-quadruplexes are higher-order nucleic acid structures formed by tetrads of guanine bases (G-tetrads) through non-canonical base interactions. Two G-tetrads are stabilised by a potassium-ion sandwiched between the tetrads. It has emerged from recent studies that G-quadruplexes occur widely throughout the human genome and have significant biological roles. In this study the *FXVD1* pre-mRNA encoding the protein Phospholemman (PLM) is investigated. PLM is highly expressed in cardiomyocytes and forms a third subunit of the Na⁺/K⁺ pump (NKA). PLM is a major phosphorylation target and thus regulates NKA activity. *FXVD1* pre-mRNA was investigated for its ability to form G-quadruplexes. By computational analysis, it was found that *FXVD1* can fold into G-quadruplex and multiple sequence alignment of ortholog *FXVD1* sequences indicated that G-quadruplex-forming potential is conserved in evolution, hinting at a potential regulatory mechanism of *FXVD1* expression. Comparative analysis confirmed that *FXVD1*-009, a variant of *FXVD1*, is a product of alternative splicing of *FXVD1*'s pre-mRNA. G-quadruplex formation in human and bovine *FXVD1*-derived oligonucleotides was detected experimentally by non-denaturing polyacrylamide gel electrophoresis that showed an increased mobility rate of G-quadruplexes in contrast to controls. Further analysis by fluorescence emission spectroscopy confirmed G-quadruplex formation in the human and bovine *FXVD1*-oligonucleotides that was triggered by the presence of K⁺ ions. The results provided clear evidence of G-quadruplex formation *in vitro* and together with evolutionary conservation point to potential role in regulating expression of *FXVD1* possibly through alternative splicing and thus regulate indirectly the

activity of Na⁺/K⁺-ATPase. Further *in-vivo* works should address whether alternative splicing of *FXVD1* to *FXVD1-009* is associated with G-quadruplex formation.

Acknowledgements: Dr Andreas Kukol for giving me the opportunity to work on this project, Prof Anwar Baydoun for being the second supervisor, Prof Mire Zloh for his assistance, Jamie Stone & Deepika Saikrishnan for their support, 2G165 lab personnel, Chemistry Department for providing the fluorimeter

TABLE OF CONTENTS

SECTION	PAGE
1. INTRODUCTION	1
1.1 G-quadruplex Overview	1
1.2 G-quadruplex folding motif and prediction tools	3
1.3 Existence and significance of G-quadruplexes	6
1.4 Prevalence of G-quadruplex in RNA	8
1.5 <i>FXVD1/phospholemman</i>	11
1.5.1 <i>The phospholemman protein</i>	12
1.5.2 PLM primary, secondary and tertiary structure	13
1.6 Techniques for G-quadruplex detection	16
1.7 Aims and objective	19
2. MATERIALS & METHODS	20
2.1 MATERIALS	20
2.1.1 <i>Software, databases, web-servers</i>	20
2.1.2 Sample preparation	21
2.1.3 NATIVE PAGE	22
2.1.4 Fluorescence and UV-vis spectroscopy	23
2.1.5 Data processing	23
2.2 METHODS	24
2.2.1 <i>In-silico</i> analysis	24
2.2.2 G-quadruplex preparation	28
2.2.3 Native PAGE preparation	28

2.2.4 Detection of G-quadruplex by Native PAGE	29
2.2.5 Detection of G-quadruplex by fluorescence spectroscopy	30
3. RESULTS	32
3.1 <i>In-silico</i> analysis	32
3.1.1 QGRS mapper and Quadbase findings	32
3.1.2 Stability calculations of secondary/tertiary structures	43
3.1.3 Multiple Sequence Alignment GQS against orthologous <i>FXVD1</i> sequences	50
3.1.4 Alternative splicing	54
3.2 G-quadruplex detection by Native PAGE	59
3.3 Detection of G-quadruplexes by Fluorescence spectroscopy	64
4. DISCUSSION	67
4.1 Computational sequence Analysis	67
4.2 Stability calculations of secondary/tertiary structures	69
4.3 Evolutionary conservation of G-rich sequences in <i>FXVD1</i> pre-mRNA	70
4.4 Alternative splicing	70
4.5 Laboratory experimental results support G-quadruplex formation	71
4.6 Limitations and further work	75
5. REFERENCES	78
APPENDIX I: GQS mapping from Table 2 and conserved sequence from Table 6 in the <i>FXVD1</i> pre-mRNA of each ortholog	84
<i>Mus musculus FXVD1</i> pre-mRNA sequence	84

<i>Canis lupus familiaris</i> FXYD1 pre-mRNA sequence	86
<i>Pan troglodyte</i> FXYD1 pre-mRNA sequence	88
<i>Bos taurus</i> FXYD1 pre-mRNA sequence	90
<i>Rattus norvegicus</i> FXYD1 pre-mRNA sequence	92
<i>Monodelphis domestica</i> FXYD1 pre-mRNA sequence	94
<i>Felis catus</i> FXYD1 pre-mRNA sequence	96
<i>Otolemur garnetti</i> FXYD1 pre-mRNA sequence	97
<i>Tursiops truncatus</i> FXYD1 pre-mRNA sequence	98
<i>Equus caballus</i> FXYD1 pre-mRNA sequence	100
<i>Ailuropoda melanoleuca</i> FXYD1 pre-mRNA sequence	102
<i>Pongo abelii</i> FXYD1 pre-mRNA sequence	103
<i>Oryctolagus cuniculus</i> pre-mRNA sequence	105
<i>Gorilla gorilla gorilla</i> pre-mRNA sequence	106
<i>Sus scrofa</i> FXYD1 pre-mRNA sequence	108
<i>Ovis aries</i> FXYD1 pre-mRNA sequence	110
APPENDIX II: FXYD1 variant 009 pre mRNA sequence	112

List of Tables

Table	Title	Page
1	G-scores for <i>H. sapiens</i>' <i>FXVD1</i> pre-mRNA	34
2	Highest scoring GQS from <i>FXVD1</i> orthologs	37
3	GQS located in UTR regions of orthologues <i>FXVD1</i> pre-mRNA	40
4	GQS predicted for <i>H. sapiens</i>' <i>FXVD1</i> mRNA	42
5	MFE structure generated by RNAfold and other secondary structures for oligonucleotide considered for laboratory work	43
6	Genomic location and G-scores of the conserved sequences with respect to the highest scoring GQS of <i>H. sapiens</i>	51
7	Consensus sequence obtained after aligning each GQS from Table 2	52
8	MFE and secondary structures of the variant <i>FXVD1-009</i> sequence	57
9	Student 2-tailed-t-test of R_f values for samples in the presence of K^+ containing buffer against samples in K^+ free buffer	62
10	Student 2-tailed-t-test of R_f values for samples incubated in different concentration of K^+ containing buffer	62

List of Figures

Figure	Title	Page
1	Schematic representation of G-quartet and G-quadruplex	2
2	Intramolecular RNA G-quadruplex	4
3	Proposed roles of G-quadruplexes associated with UTR regions of RNA	8
4	Genomic location and gene structure of <i>FXYD1</i>	11
5	Primary and tertiary structure of PLM	13
6	3-D cartoon graphic of the anti-parallel intramolecular G-quadruplex formed by 2KM3	17
7	<i>H. sapiens'</i> <i>FXYD1</i> pre-mRNA sequence in the QGRS mapper analyzer box	24
8	<i>H. sapiens'</i> FASTA <i>FXYD1</i> pre-mRNA to be analysed by Quadbase	25
9	MFE structures for controls and Bovine_PLM sequence	46
10	3 lowest energy state structures for Human_PLM sequence	47
11	Human_PLM sequence aligned against remaining orthologs	50
12	Comparison of <i>FXYD1</i> and <i>FXYD1-009</i> pre-mRNA sequences that map the Human_PLM sequence	56
13	Native 30% PAGE of samples in the presence and absence of K ⁺	59
14	Barchart comparing R _f for samples under different K ⁺ conditions	61
15	Emission spectrum of samples in the presence and absence of K ⁺	64
16	Emission spectra of Quinine in the absence or presence of K ⁺	66
17	Schematic illustration of the <i>intermolecular</i> G-quadruplex formed by – VE_A	73

List of abbreviations

Acronym	Definition
PLM	Phospholemman
GQS	G-quadruplex forming sequences
+VE	Positive control
-VE_A	Negative control A
-VE_B	Negative control B
MFE	Minimum Free Energy
QGRS	Quadruplex forming G-Rich Sequences
MSA	Multiple Sequence Alignment
TrisOAc	Tris Acetate buffer
KCl	Potassium Chloride
KOAc	Potassium acetate
NKA	Sodium Potassium pump/ Na^+/K^+ -ATPase
PAGE	Poly Acrylamide Gel Electrophoresis
DNA	Deoxyribonucleic Acid
RNA	Ribonucleic Acid
mRNA	messenger Ribonucleic acid
UTR	Untranslated region
ETDA	Ethylenediaminetetraacetic acid

1. INTRODUCTION

1.1 G-quadruplex overview

If there is something in particular that intrigues scientists about Guanine rich (G-rich) nucleic acid sequences, it is their ability to form higher order secondary structures called G-quadruplexes (Phong Lan Thao, Mergny, & Alberti, 2011; Stegle, Payet, Mergny, MacKay, & Huppert, 2009; Tluckova et al., 2013; Yuan et al., 2013; Zhang, Liu, Zheng, Hao, & Tan, 2013). G-rich nucleic acid sequences form G-quadruplexes when in the presence of cations, which help stabilizing the structures. G-tetrads, being the tetrahedral arrangement of four guanines residues linked via hydrogen bonds, are the building blocks of G-quadruplexes (Lech, Heddi, & Anh Tuan, 2013; Wu & Brosh, 2010). The role of cations is to stabilize the G-tetrads by sitting in their core (Figure 1A). Stacks of G-tetrads are called G-quadruplexes and a minimum of two G-tetrads are required to form a stable G-quadruplex. Structural polymorphisms in G-quadruplexes have been previously reported and some of the variants are shown in Figure 1B (Musetti, Krapcho, Palumbo, & Sissi, 2013; Palacky, Vorlickova, Kejnovska, & Mojzes, 2013; Xu, Xu, Shang, Feng, & Zhou, 2012).

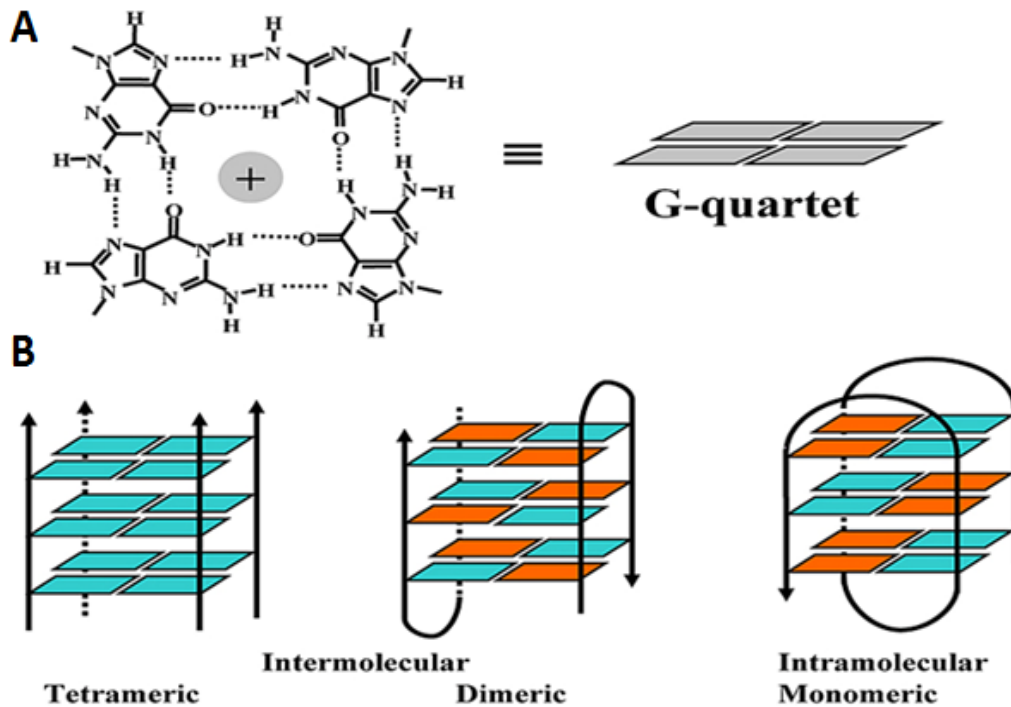


Figure 1: (A) Schematic representation of a G-quartet. Four guanines are linked together via hydrogen bonds (dotted lines) and the quartet is stabilised by a cation, K^+ . (B) G-quartets stack to form G-quadruplexes. Three different types of G-quadruplex are shown here. Intermolecular tetrameric G-quadruplex involves 4 separate strands of nucleic acid with the participation of one guanine residue from each strand in the G-quartets. Dimeric G-quadruplex involves participation of two separate strands with two guanines (*Anti* and *Syn*) from each strand participating in the G-quartets. Intramolecular monomeric G-quadruplex involves only one strand. *Anti*-guanines are coloured cyan and *Syn* guanines are coloured orange. Adapted from Moon & Jarstfer (2007).

1.2 G-quadruplex folding motif and prediction tools

In order for any nucleic acid to fold into G-quadruplex, the sequence of the latter should be rich in guanine residues and the arrangement of guanines within the nucleic acid should comply with particular motifs. Many algorithms have been developed to identify nucleic acid sequences rich in guanines with the appropriate motifs, and allow easy prediction of *intramolecular* G-quadruplex formation. Algorithms such as Quadruplex forming G-Rich sequences (QGRS) mapper (Kikin O, D'Antonio & Bagga, 2006), Quadfinder (Scaria, Hariharan, Arora & Maiti, 2006), QuadPredict (Wong, Stegle, Rodgers & Huppert, 2010), G-Rich sequence Database (GRSD), G-Rich Sequences UTR DataBase (GRS UTRdb), non-B DNA Motif Search Tool (nBMST), Quadbase and others are readily available on the internet (Kostadinov, Malhotra, Viotti, Shine, D'Antonio & Bagga, 2006). The most common folding motif was devised by Kikin *et al.* (2006) and is as follows: $G_x N_{y_1} G_x N_{y_2} G_x N_{y_3} G_x$. G stands for guanine and N stands for any other nucleotide residue, subscripts denote the number of occurrences of these nucleotides. According to the folding rule, x should be at least two as a minimum of two quartets is required to stack on top of each other to form a G-quadruplex. N is representative of the other bases involved in the loops of the G-quadruplex, N can be any base including guanine. Y1, Y2 & Y3 is the number of the different residues that participate in the three different loops, and can vary.

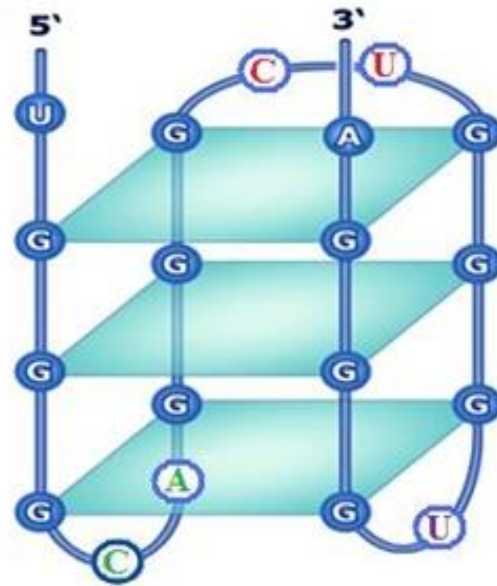


Figure 2: Intramolecular G-quadruplex formed by a RNA molecule with the sequence: 5'-UGGGCAGGGCUUGGGUGGGA-3'. This particular intramolecular RNA (5'-UGGGCAGGGCUUGGGUGGGA-3') G-quadruplex corresponds to the motif $G_3N_2G_3N_2G_xN_1G_x$. Note that the first base 5'-U and last base A-3' did not participate in the G-quadruplex structure. (Adapted and edited from GRS UTRdb Database, 2007)

Lorenz *et al.* (2011) stated that most of the putative G-quadruplex forming sequences in RNA are more likely to form secondary structures based on conventional base pairing rather than G-quadruplexes. The Vienna RNA package developed by Lorenz *et al.* (2013) provides a suitable platform for detecting secondary structures in sequences based on thermodynamic parameters and properties; it also allows users to predict the formation of G-quadruplexes alongside other possible competing secondary structures. The three main types of computational structural predictions are based on (i) Zuker & Stiegler's (1981) Minimum Free Energy (MFE) algorithm, which will predict a single structure for a particular sequence based on its MFE requirement (ii) McCaskill's (1990) Partition Function algorithm, providing

statistical insights about the base pairing probabilities in RNA ensembles allowing the prediction of more than one secondary structures within the same species of RNA (iii) Suboptimal Folding algorithm (Wuchty, Fontana, Hofacker, & Schuster, 1999) that computes structures within a given range of optimal energy, hence allowing users to screen for competing secondary structures with respect to G-quadruplex in RNA molecules. All of the three prediction methods are implemented in the Vienna RNA package, mostly independent of each other such as predicting MFE structure of a particular sequence or sometimes combined when for instance predicting structures in a particular sequence over a range of optimal energy. The webserver of the Vienna RNA package provides a suitable platform for users to predict structures in desired RNA sequences and is available at <http://rna.tbi.univie.ac.at/>.

1.3 Existence and significance of G-quadruplexes

There have been reports in the past about the existence of G-quadruplexes occurring *in-vitro* (Yuan, Tian, Chen, Yan, Xing, Zhang, Zhai, Xu, Wang, Weng, Yuan, Feng & Zhou, 2013; Biffi, Tannahill, McCafferty & Balasubramanian, 2013; Xu, Suzuki, Ito & Komiyama, 2010). *In-silico* analysis of the human genome has revealed many potential sequences that can fold into G-quadruplex, with quite a large fraction falling into gene promoter regions of DNA and UTR, exon, intron and exon-intron boundary regions of pre-mRNAs (Beaudoin *et al.*, 2010; Johnson *et al.*, 2010; Onyshchenko *et al.*, 2009). The biological significance of these G-quadruplexes has been discussed in literatures. Controversies have revolved around G-quadruplex as being a potential down-regulator of gene expression. These structures may have a specific role like the hairpin-stem loops that form within palindromic sequences and aid terminating translation in prokaryotes (Wilson *et al.*, 1995). Many roles have been associated to G-quadruplexes. Some of the proposed functions associated with G-quadruplex formation include: G-quadruplexes can up-regulate genes by keeping promoter or upstream regions of genes in a more open structure, therefore enabling easy access for transcriptional factors to bind (Du, Zhao, & Li, 2008). With the recent advances in molecular techniques and latest technological assets, G-quadruplexes' existence within cells and elucidation of the roles of some G-quadruplexes have been characterised. The formation of a G-quadruplex structure within a promoter region has been reported to sterically hinder access to negative regulators and enhance gene expression following the work led by Gu, Lin, Xu, Yu, Du, Zhang, Yuan & Gao in 2012. Their work led to the proposition that the formation of a G-quadruplex in the rat relaxin-1 (*RLN1*) gene promoter restricts access to the transcriptional activator STAT3. STAT3 is known to negatively regulate the expression of

relaxin-1 and Gu *et al.*, (2012) hypothesized that G-quadruplex formation in the RLN1 promoter region led to enhanced expression of relaxin-1. Down regulation of genes has also been reported to be associated with G-quadruplexes, for example in case of the oncogene *c-myc* (Ou *et al.*, 2007). Ou and colleagues (2007) reported that the stabilisation of a G-quadruplex within the *c-myc* gene promoter lead to its down regulation. G-quadruplexes are largely unexploited in the cancer therapeutics field. Reports have confirmed the fact that telomeric ends of *Homo sapiens* chromosomes are guanine rich and have the potential to fold into G-quadruplexes (Zhu, Xiao & Liang, 2013; Long, Parks, Bagshaw & Stone, 2013). The survival of cancer cells depends on the enzymatic action of telomerase on telomeric ends of chromosomes (Shay, Zhou, Hiyama & Wright, 2001). Telomerase is known to elongate ends of telomeres and helping cancer cells to survive. Stabilized G-quadruplexes in telomeres will inhibit telomerase and eventually stops telomeric elongation that will prove difficult for the cancer cells to survive (Li, Xiang, Zhang & Tang, 2012). It was the report published by Siddiqui-Jain, Grand, Bearss & Hurley in 2002 that drew major attention to considering G-quadruplexes as potential target for anti-cancer drugs. The former group successfully stabilised a G-quadruplex entity upstream the promoter of the pro-oncogene *c-myc*, using the ligand porphyrin TMPyP4. The stable G-quadruplex suppressed the expression of *c-myc* significantly, and their work was the first direct evidence of ligand mediated G-quadruplex stabilisation in the *c-myc* promoter region.

1.4 Prevalence of G-quadruplex in RNA

RNA G-quadruplexes have been reported in the past and the high occurrence of G-quadruplex in UTR regions of RNA has led to hypothesizing on their role as translational regulators (Huppert *et al.*, 2008, Bugaut & Balasubramanian, 2012). Huppert, Bugaut, Kumari & Balasubramanian (2008), proposed that G-quadruplex in 5'-UTRs of RNA can down regulate translation by caging the 5'-cap end or by disrupting small ribosome subunits (Figure 3A). Alternatively, Huppert *et al.* (2008) proposed that G-quadruplexes in the 3'-UTR region of template DNA can effectively allow mRNA processing, by supporting the cleavage of pre-mRNA at the polyadenylation site (Figure 3B).

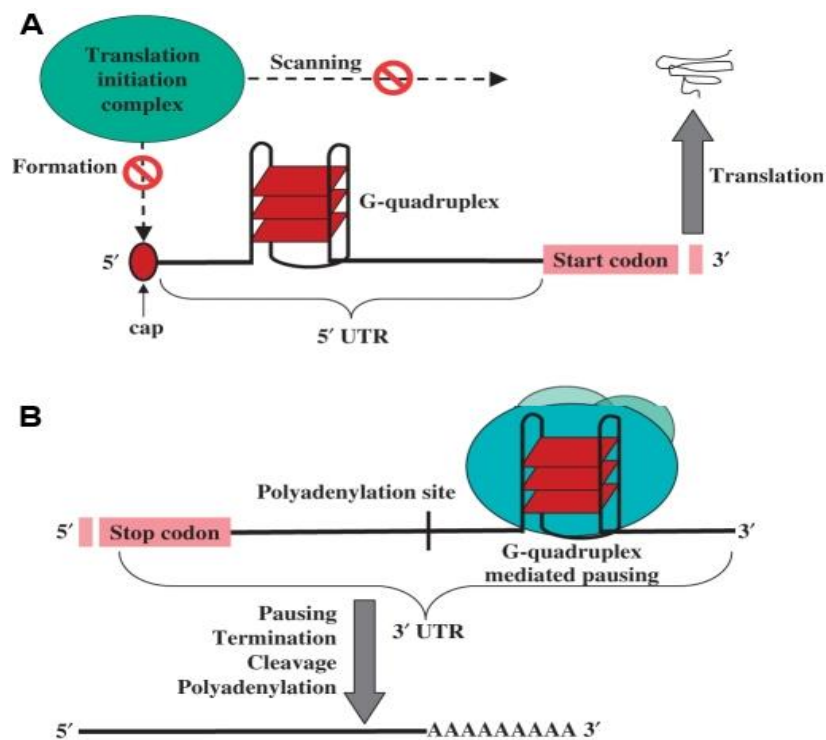


Figure 3: Proposed roles of G-quadruplexes associated with UTR regions of RNA. **(A)** G-quadruplex formation within the 5'-UTR region of an mRNA molecule. Cap-dependent initiation of translation is compromised in this instance, by the presence of the G-quadruplex that restricts the initiation complex to scan along the mRNA for the start codon.

Translation is prevented in this instance. **(B)** Formation of a G-quadruplex in the 3' region of the template DNA strand, just after the polyadenylation site. The presence of the G-quadruplex pauses RNA polymerase complex and allows effective termination of transcription. Adapted and Edited from Huppert *et al.*, (2008)

As previously stated, some G-quadruplexes and their *in-vivo* roles have been characterised in the past. Kumari, Bugaut, Huppert & Balasubramanian (2007) reported that G-quadruplex within the 5'-UTR of the *NRAS* oncogene reduces expression of the latter. Another group of researchers proposed that G-quadruplexes in RNA leads to alternative splicing. Marcel *et al.* (2011) reported that the formation of a G-quadruplex in the pre-mRNA of tumour suppressor protein, P53, leads to alternative splicing. Eventually this has an impact on the type of P53 that is formed. The usual form of p53 is FSP53, which is a fully processed mRNA, while P5312 is the alternative form that is derived from a partially unspliced pre-mRNA. The P5312 form retains its intron two, which is not spliced. The finding from Marcel & colleagues' work led to the suggestion that G-quadruplex formation in intron three of the pre-mRNA has an impact on the splicing frequency of intron two. The more G-quadruplex that was stabilized in intron three, the more FSP53 was made. Another group of researchers have also demonstrated that G-quadruplex formation led to alternative splicing patterns in hTERT intron 6, which caused down regulation of the activity of telomerase in A549 carcinoma cells (Gomez *et al.*, 2004). Bugaut *et al.* (2012) reported that a significantly large number of clinically important genes have been analysed and shown to have sequences that can form G-quadruplexes, especially post transcriptional. Previous reports supported the fact that conformational changes within mRNA molecules have the potential of regulating protein formation (Gray & Hentze, 1994; Van der velden & Thomas, 1999). Van der velden

et al. (1999) reported that the 5'-UTR of most mRNA is an important site where ribosomes will bind to initiate protein synthesis and any structural changes, G-quadruplexes in this instance, will affect this process. Many of the genes proposed by Bugaut *et al.*,(2012) fall into the oncogene family and the study and elucidation of G-quadruplexes in these genes is of clinical importance.

1.5 *FXVD1/phospholemman*

One clinically important gene, highly expressed in cardiomyocytes is the *FXVD1* gene. *FXVD1* codes for the protein phospholemman (PLM) and is part of the *FXVD* family, which are involved mainly in regulating the Na^+/K^+ -ATPase in different tissues (Teriete, Franzin, Choi, & Marassi, 2007; Cheung, 2010). *FXVD1* is located on chromosome 19 in *Homo sapiens* (Figure 4).

A.



B.



Figure 4: Genomic location of *FXVD1* in Chromosome 19 of *Homo sapiens* and the structure of the *FXVD1* gene. **A.** Chromosome 19 of *Homo sapiens* showing the genomic location (red rectangle) of the *FXVD1* gene on the q arm of chromosome 19 (Adapted and edited from Ensembl 2013). **B.** Gene structure of the *H. sapiens FXVD1* gene located in the region chr19: 35,138,789-35,143,055. The *FXVD1* gene is represented by the green line and green rectangles. The coding regions are represented by the red rectangles from the red line,

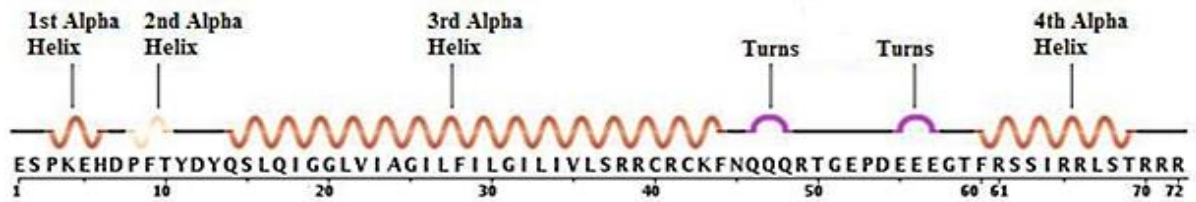
which translate to phospholemman. Introns are represented by the solid horizontal black lines at the bottom, while exons are located between the introns boundaries, red vertical lines at the top. The coding exons are exons 2 to 8. (Adapted and edited from NCBI 2014).

1.5.1 *The phospholemman protein*

Phospholemman (PLM) is 72 residues long and a single-span transmembrane protein. Characterised by Larry Jones in 1985, PLM is an important phosphorylation target of protein kinase A/C (PKA/PKC) (Crambert, Füzesi, Garty, Karlish & Geering, 2002). PLM is part of the Na⁺/K⁺-ATPase (NKA) ion pump and contributes to the proper functioning of NKA (Fuller *et al*, 2004; Silverman *et al*, 2005). PLM is therefore considered as a key physiological regulator of cardiomyocytes and poses as a potential target site for cardiac therapeutics (Shattock, 2009). The 72-residue single-span transmembrane protein forms alpha helical tetramers *in vitro* (Beevers & Kukol, 2006) and *in vivo* (Bossuyt, Despa, Martin, & Bers, 2006; Song, Pallikkuth, Bossuyt, Bers, & Robia, 2011).

1.5.2 PLM primary, secondary and tertiary structure

A



B

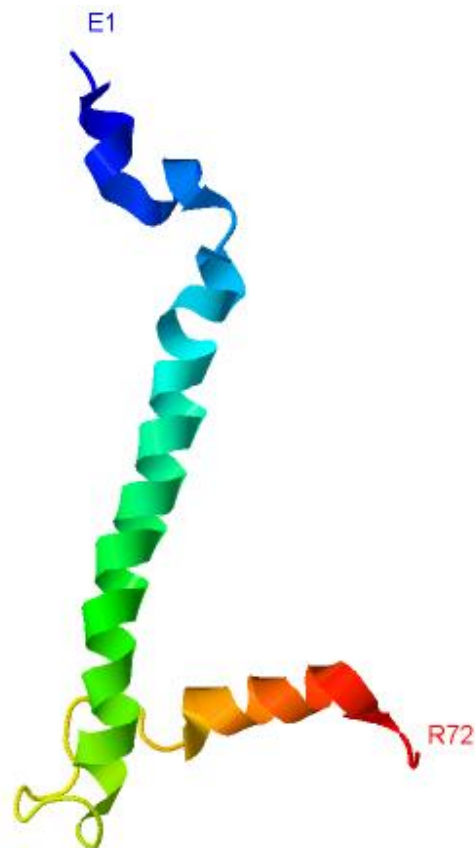


Figure 5: (A) Primary and tertiary structure of PLM showing the 72 amino acid residues. (B)

The cartoon 3-D structure of the PLM monomer obtained by NMR spectroscopy in detergent micelles. The polypeptide chain is made up of one long transmembrane alpha helix and

three shorter helices that are connected by turns. Adapted from RCSB Protein Data Bank (2013).

The transmembrane domain of PLM was shown to form tetramers in lipid bilayers (Beevers & Kukol, 2006). Using site specific infrared dichroism combined with molecular modelling (reviewed in Kukol, 2005) an atomic model of the tetramer was obtained that revealed the potential to interact with NKA, which was proposed to lead to a subsequent dissociation of the tetramer (Beevers & Kukol 2007). Further *in vivo* studies have shown that a tetramer exists *in vivo* and that there is a delicate balance between monomer and tetramer, which also depends on the phosphorylation of PLM (Song *et al.*, 2011). X-ray crystallography studies of the sodium-pump (NKA) in other tissues and species have shown that monomeric *FXVD1* (PLM) homologs, such as *FXVD2* in porcine renal tissue (Morth *et al.*, 2007) and *FXVD10* in the shark rectal gland (Shinoda, Ogawa, Cornelius, & Toyoshima, 2009) act as a third subunit of NKA. NKA exchanges three Na^+ ions against two K^+ ions that are pumped back into the cell and ensures the resting electrical membrane potential of cells is maintained. When not phosphorylated, PLM reduces the NKA pump's affinity for intracellular Na^+ . This will cause an overload of intracellular Na^+ and create an ionic imbalance, eventually causing accumulation of Ca^{2+} ions. Contrary to when PLM is phosphorylated, this intracellular accumulation of Na^+ ions is reduced as affinity of the NKA pump for sodium ions is restored. Protein kinase A activation reduces K_M of NKA for Na^+ , while protein kinase C activation increases v_{max} (Han, Bossuyt, Despa, Tucker, & Bers, 2006). The transmembrane domain of PLM on its own is responsible for changes in the sodium affinity (Lifshitz, Lindzen, Garty, & Karlsh, 2006). As previously stated, an imbalance of Na^+ will lead to accumulation of Ca^{2+} , which is reported to lead to arrhythmia (Parham,

Mehdirad, Biermann, & Fredman, 2006; Thandroyen *et al.*, 1991). Any factors that cause an increase in intracellular Na^+ ions will cause a build-up of Ca^{2+} inside cells. Previous papers have reported that G-quadruplex formation is positively correlated with the concentration of cations, especially K^+ ions (Kan *et al.*, 2006; Samatanga *et al.*, 2013), which have been proposed to be the best stabilizers of G-quartets, eventually G-quadruplexes, when compared to other cations such as Na^+ , Ca^{2+} , Li^+ etc (Sun *et al.*, 2013; Nguyen Thuan, Haselsberger, Michel-Beyerle, & Anh Tuan, 2011).

1.6 Techniques for G-quadruplex detection

Detection of G-quadruplex ensembles within nucleic acid species made use of biophysical, biochemical and molecular assays as well as bioinformatics-based predictions. As previously stated, the prediction of G-quadruplex in nucleic acid sequences can be done by computational techniques (Kikin *et al.*, 2006; Lorenz *et al.*, 2011). Biophysical assays exploit the different physical properties of G-quadruplexes compared to normal DNA/RNA. Such assays include circular dichroism spectroscopy (Paramasivan, Rujan, & Bolton, 2007; Randazzo, Spada, & da Silva, 2013) and light absorption (UV/VIS) spectroscopy (Goncalves, Ladame, Balasubramanian, & Sanders, 2006; Rubis *et al.*, 2009) that investigated the interactions of different ligand with G-quadruplex forming sequences. UV melting (Liu *et al.*, 2012; Mergny & Lacroix, 2009) experiments were aimed at measuring the folding and unfolding of G-quadruplexes under different cations concentration over a range of temperatures. Nuclear Magnetic Resonance (NMR) spectroscopy (Adrian, Heddi, & Anh Tuan, 2012; da Silva, 2007), can be used to detect the presence of G-quadruplexes due to characteristic resonances in the 1-dimensional spectrum. Upon the formation of G-quadruplexes, the imino guanine protons become trapped within the G-quadruplex entity and cannot be exchanged with the H₂O present in the buffer. This signal can be detected within the chemical shift range of 10-12 ppm, by a proton 1-D NMR spectrum. 2-D NMR techniques have been used to determine the three-dimensional structure of an anti-parallel intramolecular G-quadruplex (PDB-ID: 2KM3, fig. 6) derived from human telomeric ends (Lim, Alberti, Guedin, Lacroix, Riou, Royle, Mergny & Phan, 2009). The 2KM3 sequence was used as positive control in this work.

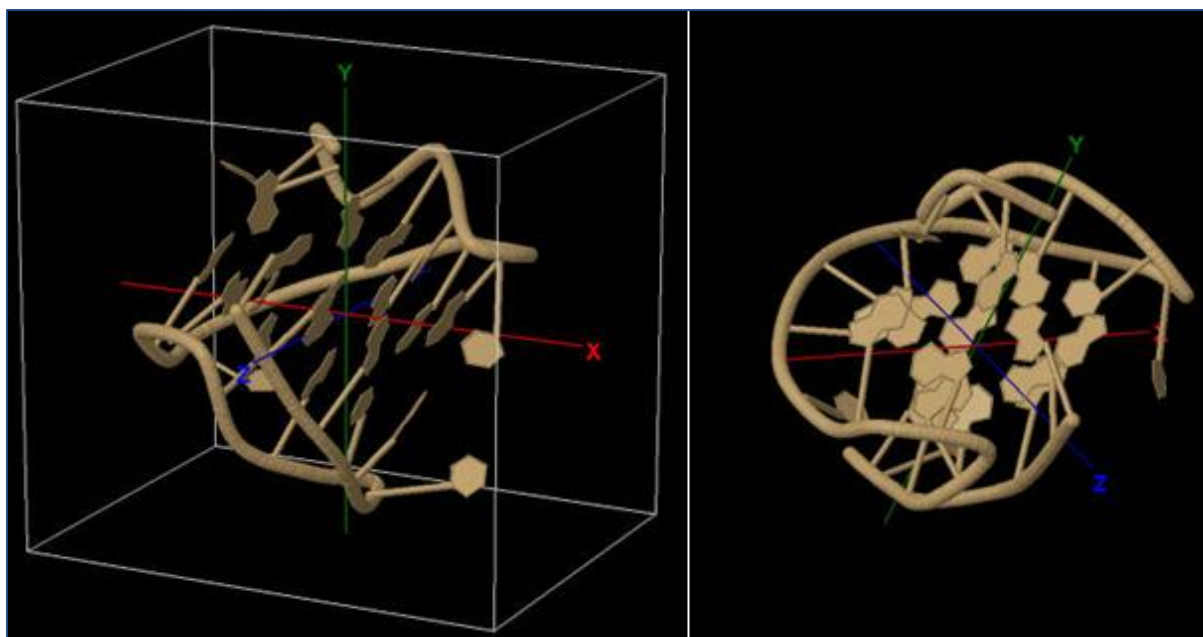


Figure 6: Cartoon representations of 3D structure of an anti-parallel intramolecular G-quadruplex formed from DNA viewed in two orientations (left and right part) (adapted and edited from RCSB PDB, 2013).

Other techniques used included surface plasmon resonance (Redman, 2007), isothermal titration calorimetry (Musetti *et al.*, 2013), mass Spectrometry (G. Yuan, Zhang, Zhou, & Li, 2011) and others. One of the most widely employed techniques used in the detection of G-quadruplex is fluorescence spectroscopy (Hong *et al.*, 2008; Tseng *et al.*, 2013; Vummidi, Alzeer, & Luedtke, 2013). The most commonly used fluorescence technique is based on the Förster resonance energy transfer (FRET) technique. A donor and an acceptor fluorophore are attached on either the 5' or the 3' ends of nucleic acids. In the G-quadruplex the 5' and 3' ends of the nucleic acid come into close proximity that allows FRET to occur. In one of the few *in vivo* studies, Xu *et al* (2010) investigated whether G-quadruplex can be formed *in vivo* by Telomeric Repeat-containing RNA (TERRA). A modified TERRA oligonucleotide containing

a pyrene monomer on each end was used and G-quadruplex formation will bring the monomers close together to form a pyrene dimer that emits light at wavelength 480 nm. Xu *et al* have found that TERRA can form G-quadruplex *in vivo*. Another approach utilises intrinsic fluorescence of nucleic acids, which has the advantage that it does not require labelling. G-quadruplexes are known to have increased fluorescence intensities. Nguyen Thuan *et al.* (2011) reported increased intrinsic fluorescence emission of previously characterised G-quadruplex structures.

Biochemical and molecular techniques include assays such as Polymerase Chain Reaction (PCR) stop assay (Ou *et al.*, 2007; Yan *et al.*, 2010), nuclease assays (Zhou *et al.*, 2013), Gel electrophoresis (Lin *et al.*, 2010; Moon & Jarstfer, 2010; Viglasky, Bauer, Tluckova, & Javorsky, 2010), antibody engineering (Biffi *et al.*, 2013) etc. The PCR stop assay gives information about ligand that can stabilize G-quadruplexes. PCR products are screened and any disturbance of the enzymatic activity of polymerase in guanine rich regions are attributed to stabilized G-quadruplexes by the ligand in that specific region. Nuclease assays enables detection by using restriction endonucleases to cut nucleic acid at specific sites. G-quadruplexes can restrict endonucleases and running the products on gels will generate a distinct band in nucleic acids that formed G-quadruplex, while nucleic acid that did not form G-quadruplex will produce more bands. Antibodies that selectively bind G-quadruplexes have been engineered and allowed easy detection of G-quadruplexes. The method is however very expensive. The basic principle resembles that of Enzyme Linked Immunosorbent Assay (ELISA). The engineered antibody will bind the G-quadruplex DNA, and usually the antibody is conjugated with a molecule that will allow visual detection. In early 2013, Biffi *et al.*, have reported the development of a specific antibody that has high

selectivity for DNA G-Quadruplexes. This labelled antibody allowed the visual detection of DNA G-quadruplexes inside human cancer cells. Gel electrophoresis is by far the easiest way to detect G-quadruplex formation within nucleic acid. Cheap and reliable, this simple method exploits the electrophoretic migration properties of compact vs. linear species in gels. G-quadruplex species have been reported to migrate faster on Poly Acrylamide Gel (PAGE) than non-G-quadruplex species. PAGE is preferred to other gels mainly because the nucleic acid sequences used for G-quadruplex assays are relatively short and PAGE gives better resolution.

1.7 Aim

The aim of this work was to investigate whether or not *FXVD1* pre-mRNA can form G-quadruplexes. This work took into account the ability of the *FXVD1* gene to form G-quadruplex and various techniques used to detect G-quadruplex formation. The initial stages involved *in-silico* analysis of *FXVD1* pre-mRNA and ortholog sequences using QGRS mapper, Quadbase and the Vienna RNA Package. Later stages involved the detection of G-quadruplexes in synthetic oligonucleotides by native PAGE and intrinsic fluorescence spectroscopy.

2. MATERIALS & METHODS

2.1 MATERIALS

2.1.1 Software, databases, web-servers

Algorithms and software used for G-quadruplex prediction:

1. G-quadruplex online prediction algorithm; QGRS mapper (<http://bioinformatics.ramapo.edu/QGRS/analyze.php>) (Kikin *et al.*, 2006)&Quadbase (http://quadbase.igib.res.in/proquad/quad_input.jsp) (Yadav *et al.*, 2008)
2. Vienna RNA Package version 2.1.2 (Lorenz *et al.*, 2011)

FXVD1 pre-mRNA sequences and control sequence database:

1. *FXVD1* pre-mRNA sequence accession numbers for *H. sapiens* (ENST00000351325), *M. musculus*(ENSMUSG00000036570), *C. familiaris*(ENSCAFT00000011368), *P. troglodytes*(ENSPTRT00000020057), *B. taurus*(ENSBTAG00000017816), *R. norvegicus*(ENSRNOG00000021079), *M. domestica*(ENSMODT00000033163), *F. catus*(ENSFCAG00000008890), *O. garnettii*(ENSOGAG00000014401), *E. caballus*(ENSECAG00000014815), *A. melanoleuca*(ENSAMEG00000000212), *P. abelii*(ENSPPYG00000009851), *O. cuniculus*(ENSOCUG00000022123), *G. gorilla*(ENSGGOT00000026217), *S. scrofa*(ENSSSCT00000027321), *O. aries*(ENSOARG00000004709), *T. truncates*(ENSTTRG00000001446)
2. *FXVD1* variant pre-mRNA sequence: *FXVD1*-009 (ENST00000589121)

3. Positive control DNA sequence, PDB ID: 2KM3, sequence from RSCB PDB

Web servers for sequence conversion, genome comparison and sequence alignment:

1. DNA<>RNA converting tool
(<http://www.attotron.com/cybertory/analysis/trans.htm>)
2. DNA/Protein sequence randomizer software (<http://www.cellbiol.com/python.html>)
3. Multiple Sequence Alignment of orthologous *FXYD1* sequences using the MAFFT web based alignment tool Version 7 available at (<http://mafft.cbrc.jp/alignment/server/>)
4. Pre-mRNA comparison of *FXYD1* and variant-009 using the 1000 genomes transcript comparison available at
(http://browser.1000genomes.org/Homo_sapiens/Gene/TranscriptComparison?db=core;g=ENSG00000266964;r=19:35629712-35634013;t=ENST00000589121;t1=ENST00000589121;time=1396457246372.372)

2.1.2 Sample preparation

Oligonucleotides used for laboratory analysis:

1. Oligonucleotides purchased from EurogentecLtd.(Southampton, UK) and used without further modification;
 - Positive (+VE) control DNA (**AGG-GCT-AGG-GCT-AGG-GCT-AGG-G**)purified by Reverse-phase cartridge purification (RP-Cartridge)
 - Negative control_A (-VE_A) DNA (**CGT-GGG-GAG-ATT-GGG-GAG-CGC-A**) purified by RP-Cartridge
 - Negative control_B (-VE_B) DNA (**GGT-GTG-CGT-GTG-CGA-GCG-AGA-GAG-**

AGU-GG) purified by RP-Cartridge

- *H. sapiens*FX $YD1$ (Human_PLM) RNA (**GGG-AGA-CUG-CGG-GUA-UUC-UGG-GGA-GAG-GG**) purified by Reversed Phase High Performance Liquid Chromatography (RP-HPLC)
- *B. Taurus* FX $YD1$ (Bovine_PLM) RNA (**GGG-CGC-GGG-GGG-UCG-GGG-AUC-GGG**) purified by RP-HPLC

Solutions used for preparing G-quadruplex samples:

1. 10 ml of 1M Potassium Chloride (KCl) solution
2. 20 ml of RNAase free H₂O
3. 500 ml of 1M Tris-Acetate Buffer (TrisOAc) pH 7.5
4. 100 ml of 1 M Potassium Acetate (KOAc)

NOTE: All solutions were autoclaved and kept at room temperature prior to use.

2.1.3 NATIVE PAGE

Solutions for preparing Native PAGE and staining:

1. 100 ml 40% acrylamide solution
2. 10 x TBE Buffer solution
3. 100 ml of 0.05M & 1M KCl/KOAc solution, sterile distilled water
4. Ammonium persulfate (APS) at 10% (w/v) in water
5. N,N,N',N'-tetramethylethylenediamine (TEMED)
6. Mini gel stop mix; 1 x TBE + 20% (w/v) sucrose + 10 % (w/v) Ficoll + 10mM EDTA and

0.25% (w/v) bromophenol blue

7. 1 x TBE gel running buffer
8. SYBR Green IS32717& SYBR Green II Nucleic Acid Stain S9430

2.1.4 Fluorescence and UV-vis spectroscopy

Equipments used for fluorescence spectroscopy:

1. Fluor cuvette Type C quartz glass with 10 mm light path
2. Perkin Elmer LS 55 fluorimeter
3. UV/VIS CARY 100 dual-beam spectrophotometer (Varian Inc.)
4. Quinine solution at 24 ppm

2.1.5 Data processing

Software used to process raw data from Native PAGE and Fluorescence spectroscopy:

1. Gene Tool Syngene (Copyright © 2009-2011 Syngene, A Division of Synoptics Ltd)
2. PerkinElmer UV WinLab Data Processor and Viewer Version1.00.00
3. Microsoft®Excel®2010 Version 14.0.7109.5000

2.2 METHODS

2.2.1 *In-silico* analysis

G-quadruplex prediction using QGRS mapper and Quadbase

The raw FASTA pre-mRNA sequences of the *FXYP1* orthologs were analysed online using QGRS mapper (Figure 7) and Quadbase prediction software (Figure 8).



Figure 7: *H. sapiens'* *FXYP1* pre-mRNA sequence (4286 bp) in the QGRS mapper analyzer

box.

The parameters were left at the defaults, with maximum length of potential of Quadruplex forming sequences set at 30 bases. The minimum G-group was set at 2, which is the minimum number of G-tetrads and finally the loop length was set between the range of 0 – 36 bases. Clicking on the “Analyze” button in the bottom right corner initiates screening of the sequence and search for putative G-quadruplex forming sequences (GQS). All the other orthologous *FXYD1* pre-mRNA sequences were analysed using the same settings as *H. sapiens*.

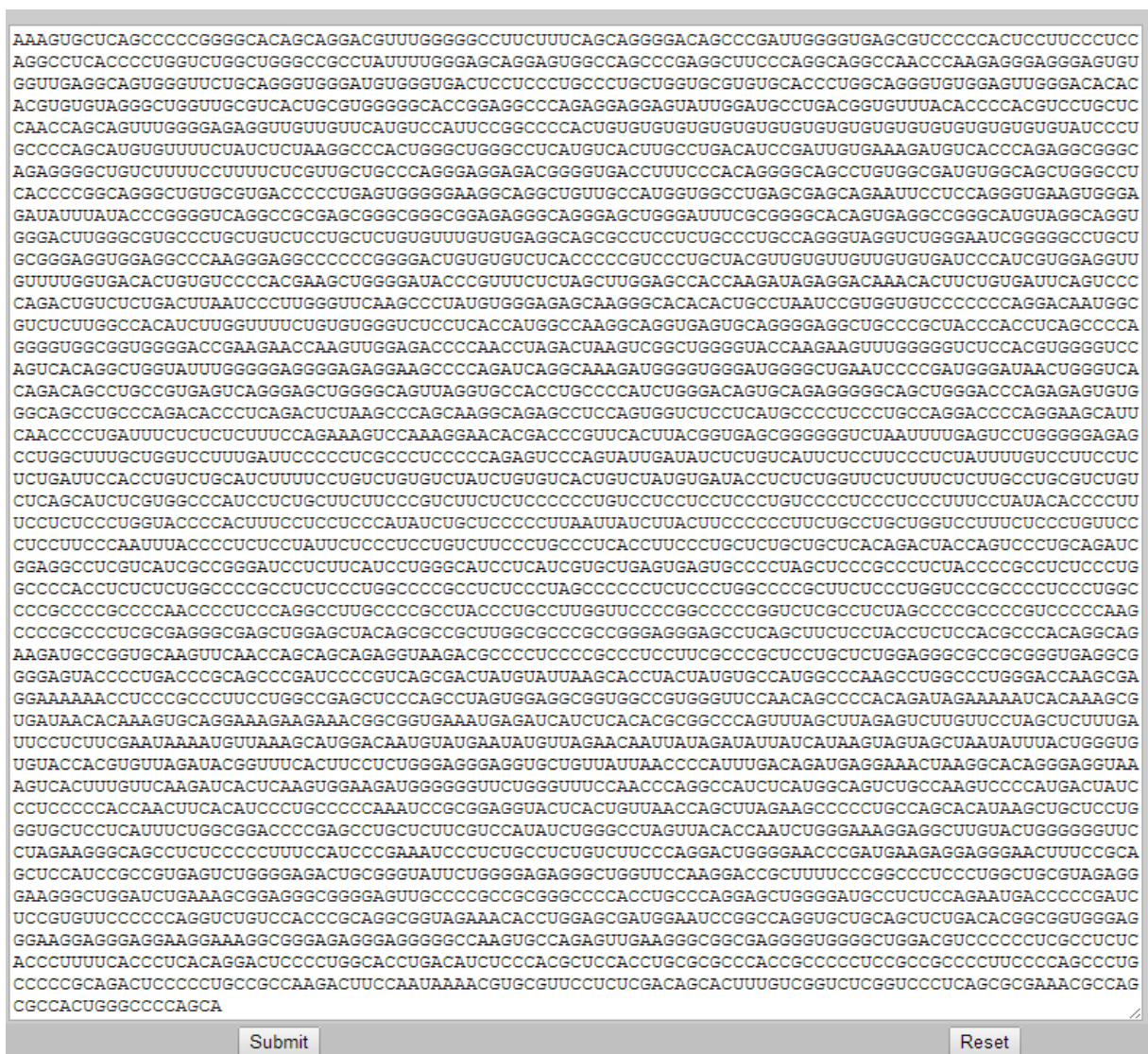


Figure 8: *H. sapiens*’ FASTA *FXYD1* pre-mRNA (4286 bp) in the Pattern finder search box of Quadbase that screens nucleic sequences for patterns that can form G-quadruplex.

The parameters were those of the default settings, which was between two and five guanines for the G-tetrads. The loop sizes were set between 1 and 7, 1 being the minimum and 7 the maximum integer available.

Prior to analysis by QGRS mapper and Quadbase the raw FASTA sequences were converted to RNA using the DNA<>RNA converter tool. The sequence of a +VE control DNA previously known to form a G-quadruplex was obtained from the RSCB Protein Database (NDB-ID: 2KM3) and was also analysed in QGRS mapper and Quadbase. A DNA/Protein randomiser tool was used to shuffle the sequence of the +VE control and generate possible sequences of a -VE control, -VE_A, which were of the same length as the +VE control and had the same base composition as the +VE control. Following analysis by QGRS mapper and Quadbase, a second -VE control, -VE_B, was also generated using the DNA/Protein randomiser based on the *H. sapiens*' highest scoring sequence generated by QGRS mapper.

G-quadruplex and secondary structures prediction using the Vienna RNA package

The *Vienna RNA package* was used to predict G-quadruplex and other secondary structures that are likely to compete against G-quadruplex formation. The +VE control, -VE_A, -VE_B, Human_PLM and Bovine_PLM were analysed using the RNAfold, RNAsubopt and RNAeval algorithms from the package. RNAplot option was used to produce graphical display of the proposed structures by RNAfold and RNAsubopt for all sequences.

The following command lines were used in the Command Prompt (Microsoft©) for the Human_PLM sequence:

```
1) C:\Users> rnafold -g < Human_PLM.txt
```

```
2) C:\Users> rnaeval -g < RNA_struct.txt
3) C:\Users> rnasubopt -e3 < Human_PLM.txt
4) C:\Users> rnaplot -o ps <RNA_struct.txt
```

The first commands predict the minimum free energy (MFE) structure of the sequence contained in the text file taking into account G-quadruplex formation (-g option) The second command calculates the energies of given secondary structures, taking into account G-quadruplex formation. The third command determines other secondary structures within 3 kcal/mol above the MFE structure. The same command lines were executed for the +VE, -VE_A, -VE_B and Bovine_PLM sequences. The last command line produces graphical display of secondary structures predicted by RNAfold and RNAsubopt in post script format (-o ps option).

Multiple sequence alignment by MAFFT web server version 7.0

The MAFFT web server was used to align all orthologous *FXVD1* pre-mRNA sequences. All parameters were the default settings. The slow iterative refinement method was used.

Pre-mRNA comparison of *FXVD1* and *FXVD1-009*

The mRNA and pre-mRNA sequences of *H. sapiens'* *FXVD1* and *FXVD1-009* were compared against each other to look for alternative splicing. Using the 1000 Genomes Transcript Comparison option, mutations were screened in potential G-quadruplex forming sequences from the pre-mRNA sequences of *FXVD1* and variant 009.

2.2.2 G-quadruplex preparation

G-quadruplex was induced by incubating the oligonucleotides in K^+ containing and K^+ free buffers (as controls). The G-quadruplex folding buffer contained K^+ (mixture of KCl and KOAc) at 0.1 or 0.05 M and 0.02 M TrisOAc pH 7.5. Controls were prepared in K^+ free buffer that contained 0.02 M TrisOAc pH 7.5 only. The samples were prepared in sterile microfuge tubes. The mixtures were heated at 90°C for 10 minutes to disrupt any intramolecular interactions. After heating, the -VE_A and -VE_B samples in K^+ containing buffer and all control samples were cooled to 4°C by keeping the tubes on ice, to disfavour formation of G-quadruplex. The +VE, Human_PLM and Bovine_PLM samples in K^+ containing buffer were allowed to cool down to 25°C over 2.5 hours by removing the heating block from the heating source. Once the samples reach the annealing temperature, the tubes were then stored at 0°C to preserve the G-quadruplex structures for later use.

All plastic wares were heated at 230°C, including pipette tips, to inactivate any RNAase.

2.2.3 Native PAGE preparation

30 % polyacrylamidegels were used to run the samples. Samples incubated in K^+ containing buffer were ran on separate gels from samples incubated in K^+ free buffer, to keep experimental conditions constant. Gels prepared for K^+ containing samples was made by adding 9.375 ml of 40% acrylamide solution + 1.250 ml of 10 x TBE supplemented with KCl & KOAc to match the concentration of K^+ of the folding buffers, e.g. for samples incubated in 0.1 M K^+ , 10 x TBE+0.1 M K^+ mixture was used for preparation of the gel. This was followed

by the addition of 1.875 ml of sterile distilled water and 150 μ l of 10% APS. This mixture was degassed under vacuum to remove any molecular oxygen that would inhibit the polymerisation process. Degassing was followed by the addition of 15 μ l of TEMED. Gels used for K^+ free samples were made in the same way as previously described for K^+ containing samples, except that the 10 x TBE was used without K^+ .

2.2.4 Detection of G-quadruplex by Native PAGE

Samples for electrophoresis were thawed at room temperature and 8 μ l of mini gel stop mix (1 x TBE + 20% (w/v) sucrose + 10 % (w/v) Ficoll + 10mM EDTA and 0.25% (w/v) bromophenol blue) was added to each tube. The final oligonucleotide concentration of each species was 3 μ M. After thoroughly mixing the samples with the dye, 10 μ g of each sample was loaded onto the gels. The gels were run in different tanks and the buffer used for non-G-quadruplex gels was 1 x TBE buffer, while G-quadruplex gels were ran using 1 X TBE containing either KCl and KOAc at a final concentration of 0.1M or 0.05 M. The buffers were pre-chilled at 4 $^{\circ}$ C to minimize overheating of the tanks. Electrophoresis was performed at 140V and the run time was on average 3-4 hours. Following electrophoresis each gel was removed and cut at the upper right hand corner to track orientation. The gels were stained using SYBR Green I RNA stain S9430 and SYBR Green I nucleic S32717 exposed at 254 nm for 15.5s.

The ratio of the distance migrated by each samples relative to the distance migrated by the tracking dye, R_f value, was calculated using the software Gene Tool Syngene (Copyright 2009-2011 Syngene, A Division of Synoptics Ltd). Student 2-tailed-t-test was carried out for the samples under different incubation conditions.

2.2.5 Detection of G-quadruplex by fluorescence spectroscopy

G-quadruplex induced and uninduced samples were prepared at a final oligonucleotide concentration of 1.5 μM for RNA species and 5.0 μM for DNA species. The reason behind the choice of these concentrations was that these are the minimum detectable concentrations for either RNA or DNA by the Perkin Elmer LS 55 fluorimeter. Buffers for non G-quadruplex samples was 0.02 M TrisOAc only and that of G-quadruplex samples was 0.02 M TrisOAc + 0.1 M K^+ . Samples prepared overnight were allowed to thaw and attain room temperature, 20°C, before readings were taken. Emission spectra were recorded over the wavelength range of 300-500 nm using a Perkin Elmer LS 55 in a Type C Fluor micro cuvette with a 10 mm light pathway. Samples were excited at a wavelength of 260 nm and both excitation and emission slit widths were set at 5 nm. The scan rate was 150 nm/min. Emission spectra of buffers were also recorded. UV-VIS spectra of each sample were recorded using a UV-VIS CARY 100 dual-beam spectrophotometer between the range of 200-400 nm with the appropriate buffer placed into the second beam.

The fluorescent compound quinine was used to test the fluorimeter by recording the emission spectra in the presence of either 0.02 M TrisOAc or 0.1 M K^+ and 0.02 M TrisOAc. The spectra were recorded by exciting Quinine at a final concentration of 0.6 ppm at

wavelength of 250 and 350 nm independently over the range 335-485 and 355-505 nm respectively. The scan speed was 150 nm/min and both excitation and emission slits were set at 5nm each.

The data generated by the fluorimeter were processed with PerkinElmer UV WinLab Data Processor and Viewer Version 1.00.00 into graphical display. The original spectra were processed using Microsoft Excel 2010 Version 14.0.7109.5000 to obtain smooth curves. Trendline with moving average of 30 data points per period was produced for each emission spectrum.

3. RESULTS

3.1 *In-silico* analysis

3.1.1 QGRS mapper and Quadbase findings

Analysis of orthologous *FXYD1* pre-mRNA sequences by QGRS mapper revealed several G-Quadruplex forming Sequences (GQS) for most organisms. The whole pre-mRNA sequence of *H. sapiens FXYD1* contains 41 GQS as seen in the FASTA sequence below:

```
AAAGUGCUCAGCCCCGGGGCACAGCAGGACGUUUGGGGGCCUUCUUUCAGCAGGGGACAGC  
CCGAUUGGGgugagcgcuccccacuccuucccuccaggccucaccccuggucuggcugggccc  
gccaauuuuugggagcaggaguggccagcccaggccuucccaggcaggccaacccaagaggga  
gggagugugguugaggcagugggguucugcaggguggggaugugggugacuccucccugcccug  
cuggugcgcugugcaccucggcaggguguggaguugggacacacacgcuguguagggcugguug  
cgucacugcgcugggggcaccggaggcccagaggaggaguauuggaugccugacgguguuuac  
acccacgcuccugcuccaaccagcaguuugggagagguuuguuuauuguccauucccgcc  
ccacuguguguguguguguguguguguguguguguguguguguaucccugcccagcaug  
uguuuucuaucucuaaggcccacugggcugggcccuaugucacuugccugacaucggauugu  
gaaagaugucaccagaggcgggcagaggggcugucuuuuuccuuuucugugcugcccagg  
gaggagacggggugacccuuuccacagggggcagccuguggcgauguggcagcugggcccucac  
cccggcagggcugugcgcugaccccugagugggggaaggcaggcuguugccaugguggccug  
agcgagcagaauuccuccagggugaagugggagauuuuauaccggggucagggccgcgagc  
gggcggggcggagagggcagggagcugggauuucgcggggcacagugaggccgggcauguagg  
caggugggacuuggggcgcugcccugcugucuccugcucuguguuugugugaggcagcgcucc  
ucugcccugccaggggagggucugggaaucgggggcccugcgcgggagguggaggcccaaggg  
aggccccccggggacugugugucucaccccgcuccugcuaacguuguguuugugugaucc  
caucguggagguuguuuugggagacacuguguccccacgaagcugggggauaccgguuucua  
gcuuggagccaccaagauagaggacaaacacuucugugauucaguccccagacugucucuga  
cuuaaucccuuggguucaagcccuauugugggagagcaagggcacacacugccuaaucggugg  
uguccccccagGACA AUGGCGUCUCUUGGCCACAUCUUGGUUUUCUGUGUGGGUCUCCUCA  
CCAUGGCCAAGGCAGgugagugcaggggaggcugcccgcuaaccaccucagcccaggggug  
gcgguggggaccgaagaaccaaguuggagaccccaccuagacuaagucggcugggguacca  
agaaguuuugggggucuccacguggggguccagucacaggcugguauuuugggggaggggagagg  
aagcccagaucaggcaagauggggguggggauggggcugaauccccgauggggauaacugggu  
cacagacagccugccgcugagucagggagcuggggcaguuaggugccaccugcccacucuggg  
acagugcagaggggggagcugggaccagagagugugggagccugcccagacaccucagac  
cucuaagcccagcaaggcagagccuccaguggucuccucaugcccucccugccaggacccc  
aggaagcauucaaccccugauuucucucucuuuccagAAAGUCCAAAGGAACACGACCCGUU  
CACUUACGgugagcgggggggucuaauuuugaguccgggggagagccuggcuuugcuggucc  
uuugauuucccccucgcccuccccagagucccagauugauaucucugucuuucccuucc
```

ucuaauuuuguccuuccucucugauuccaccugucugcaucuuuuccugucugugucuaucug
 ugucacugucuaugugauaccucucugguucucuuucucuuugccugcugucucagcauc
 ucguggcccauccucugcuucucccgucucucuccccuguccuccuccuccugucc
 cuccucccuuuccuaauacaccccuuuccucuccugguaccccauuuccuccuccauau
 cugcucccccuuaauuaucuuacuuucccccuucugccugcugguccuuucuccugucc
 uccuucccaauuuaccccucuccuaucuccuccugucuuuccugcccuaccuucccugc
 ucugcugcucacagACUACCAGUCCUGCAGAUCCGGAGGCCUCGCAUCGCCGGGAUCCUCU
 UCAUCCUGGGCAUCCUCAUCGUGCUGAGugagugcccuagcucccgcccucuaacccgccu
 cucccuggccccaccucucucuggccccgcccucucccuggccccgcccucuccuagcccc
 ucucccuggccccgcuucucccuggucccgccccucccuggccccgccccgcccccaaccuu
 ccaggccuugccccgccuaccucgcuugguuccccgccccggucucgcccuaagcccc
 gccccgucucccaagccccgccccucgagggcgagcuggagcuaacagcgcgcgucggcgc
 ccgcccggaggaggccucagcucuccuaccucuccacgcccacagGCAGAAGAUGC GGUG
 CAAGUUCAACCAGCAGCAGAGguaagacgccccuccccgcccuccuucgcccgcuccugcuc
 uggagggcgccgcccgggugaggggggaguaccccugaccgagcccgaucucccgucagcga
 cuauguaauaagcaccuacuaugugccauggcccaagccuggcccugggaccaagcgaggaa
 aaaaccuccccgcccuccuggccgagcucccagccuaguggaggcggguggccguggguucca
 acagccccacagauagaaaaucacaaagcgugauaacacaaagugcaggaaagaagaacg
 gcguguaaagagaucaucucacacgcccaguuuagcuaagagucuuuguuccuagcucu
 uugauuccucucgaauaaaauguaaagcauggacaauguaugaauauguagaacaauua
 uagauauaucauaaguagcuaauuuuacuggguguguaaccacguguuagauacgguu
 ucacuuccucugggaggaggugcuguuauuaaccccuuugacagauaggaaacuaaggc
 acagggagguaaagucacuuuguucaagaucacucaaguggaagauggggggguucuggguu
 ccaaccaggccaucuauugcagucugccaagucccaugacuauccuccccccaccaacu
 ucacauccugcccccaauuccgaggguacucacuguaaaccagcuuagaagccccugc
 cagcacauaagcugcuccugggugcuccucauuucuggcggaccccagaccugcucucguc
 cauaucugggcuaguuacaccaaucugggaaaggaggcuuguaucuggggggguuccuagaag
 ggcagccucuccccuuuccaucccgaauuccucugccucugucuucccagGACUGGGGAA
 CCCGAUGAAGAGGGGAACUUUCCGCAGCUCCAUCCGCCgugagucuggggagacugcggg
 uauucugggggagagggcugguuccaaggaccgcuuuuccggcccucccuggcugcguagag
 ggaagggcuggaucugaaagcggagggcggggaguugccccgcccggggccccaccugccca
 ggagcuggggggaugccucuccagaauagaccccgaucuccguguuccccccagGUCUGUCCAC
 CCGCAGGCGGUAGAAACACCUGGAGCGAUGGAAUCCGGCCAGgugcugcagcucugacacgg
 cggugggaggggaaggaggagggaaggaaaggcgggagagggagggggccaagugccagaguu
 gaagggcggcgagggguggggucggacgucccccucgcccucacaccuuuucaccucaca
 gGACUCCCUCCUGGACCUCAUCUCCACGCUCCACCUGCGCGCCACCGCCCCUCCGCCG
 CCCCUCUCCAGCCUGCCCCCGCAGACUCCCCUGCCGCCAAGACUUCCAAUAAAACGUGC
 GUUCCUCUCGACAGCACUUUGUCGGUCUCGGUCCUCAGCGCAAACGCCAGCGCACUGGG
 CCCCAGCA

Key: UTR region
 Intronic sequence
 Exonic translated sequence

In the above FASTA sequence, alternate exons are in uppercase and introns are in lowercase
 blue characters respectively. Purple uppercase characters represent UTR regions of the gene

and black uppercase characters represent translated region of the gene. Lowercase blue characters represent intron sequences of the gene. The predicted GQSs by QGRS mapper have been mapped and are underlined in the gene and have different G-scores as shown in Table 1. The most stable G-quadruplex in the gene is located in the intron between exon 6 and 7, highlighted yellow. Each GQS has different G-scores; influenced by several factors such as loop sizes, number of guanine residues taking part in G-quartet formation

The 41 GQSs obtained upon analysis of the pre-mRNA of *H. sapiens'* *FXVD1* sequence and their respective G-scores are listed in Table 1.

Table 1: List of all 41 GQSs and the G-scores for *H. sapiens'* *FXVD1* pre-mRNA predicted by QGRS mapper (Kikin *et al.*, 2006).

Length	GQS	G-Score
29	<u>GGGAGACUGCGGGU</u> AUUCU <u>GGGGAGAGGG</u>	39
24	<u>GGGCGGAGAGGGCAGGGAGCU</u> GGG	38
24	<u>GGGUUCUGCAGGGU</u> GGGAUGU <u>GGG</u>	36
30	<u>GGGUUGGGAU</u> GGGGCUGAAU <u>CCCCGAU</u> GGG	31
30	<u>GGGAGGAAGGAAAGG</u> CGGGAGAGGGAGGGG	31
11	<u>GGAGGUGGAGG</u>	21
11	<u>GGUGGCGGUGG</u>	21
11	<u>GGAGGCGGUGG</u>	21
14	<u>GGUGGGAGGGAAGG</u>	21
18	<u>GGCAGGGUGUGG</u> AGU <u>UGG</u>	20

13	<u>GGGGGAAGGCAGG</u>	20
25	<u>GGCAUGUAGGCAGGUGGGACUUGGG</u>	20
19	<u>GGGUAGGUCUGGGAAUCGG</u>	20
10	<u>GGGGGAGGGG</u>	20
16	<u>GGGCGGCGAGGGGUGG</u>	20
20	<u>GGGAGGGAGUGUGGUUGAGG</u>	19
28	<u>GGCAGCCUGUGGC GAUGUGGCAGCUGGG</u>	19
11	<u>GGAGGGCGGGG</u>	19
30	<u>GGCACCGGAGGCCAGAGGAGGAGUAUUGG</u>	18
21	<u>GGCGCCGCGGGUGAGGCGGGG</u>	18
19	<u>GGAAGAUUGGGGGUUCUGG</u>	18
22	<u>GGAGCGAUGGAAUCCGCCAGG</u>	18
14	<u>GGCGGGCAGAGGGG</u>	17
13	<u>GGAGGAGACGGGG</u>	17
30	<u>GGACAAUGGCGUCUCUUGGCCACAUCUUGG</u>	17
27	<u>GGCCAAGGCAGGUGAGUGCAGGGGAGG</u>	16
21	<u>GGAAACUAAGGCACAGGGAGG</u>	16
29	<u>GGCCCUCCUUGGCUGCGUAGAGGGAAGGG</u>	16
22	<u>GGCACAGCAGGACGUUUGGGGG</u>	15
25	<u>GGGAGCAGGAGUGGCCAGCCCGAGG</u>	15
16	<u>GGGAGGCCCCCCGGGG</u>	15
19	<u>GGGAGCUGGGCAGUUAGG</u>	15
23	<u>GGGGGAGAGCCUGGCUUUGCUGG</u>	15

24	<u>GGAAAGGAGGCUUGUACUGGGGGG</u>	15
24	<u>GGCCUCACCCCUGGUCUGGCUGGG</u>	14
19	<u>GGGGUCAGGCCGCGAGCGG</u>	13
18	<u>GGGGGUCUCCACGUGGGG</u>	12
25	<u>GGACAGUGCAGAGGGGGCAGCUGGG</u>	12
25	<u>GGUUUCACUCCUCUGGGAGGGAGG</u>	10
28	<u>GGACUGGGGAACCCGAUGAAGAGGGAGGG</u>	10
25	<u>GGCCCCACCUGCCAGGAGCUGGGG</u>	8

The GQS listed in Table 1 are sorted in the order of highest to lowest G-scoring. The underlined guanines are those taking part in G-tetrad formation to form G-quadruplexes. The highest scoring GQS from *H. sapiens* pre-mRNA is 29 bases long and has a G-score of 39. The G-quadruplex structure formed by the latter is comprised of 3 G-tetrads. The guanines are connected by loops of length 7, 6 and 4 bases in length.

The highest scoring GQS from each ortholog are listed in Table 2 alongside the controls used in this work.

Table 2: The highest scoring predicted GQS from *FXYD1* orthologs and their location within the gene. The analysis was performed with QGRS mapper (Kikin *et al.*, 2006).

Organism	Sequence of highest scoring GQS	G-score	Genomic location ¹
<i>Homo sapiens</i>	<u>GGGAGACUGCGGGU</u> <u>AUUCUGGGGAGAGGG</u>	39	Intronic (6:7)
<i>Mus musculus</i>	<u>GGGAGGAAGGAGGGAGAGGGU</u> <u>UUGGAGGG</u>	38	Intronic (7:8)
<i>Canis lupus</i>	<u>GGGGCGAAGGGU</u> <u>GGGCUGGGAUGGCCGGG</u>	42	3'-UTR
<i>Pan troglodytes</i>	<u>GGGAGACUGCGGGU</u> <u>AUUUUGGGGAGAGGG</u>	39	Intronic (6:7)
<i>Bos taurus</i>	<u>GGGCGCGGGGGGUC</u> <u>GGGGAUCGGG</u>	42	Intronic (6:7)
	<u>GGGCAGGUGAGGCUGGG</u>	21	Intronic (1:2)
	<u>GGAUGGAAGGUAGG</u>	21	Intronic (2:3)
<i>Rattus norvegicus</i>	<u>GGCGGUGGGGG</u>	21	Intronic (5:6)
	<u>GGCACGGGGAGGUAAGG</u>	21	Intronic (5:6)
	<u>GGGAGGAAGGAGGG</u>	21	Intronic (7:8)
	<u>GGCGGGUUGGAGGG</u>	21	Intronic (7:8)
<i>Felis catus</i>	<u>GGGAGACUUUGGGGGUUU</u> <u>GGGGUGAGGG</u>	40	Intronic (5:6)
<i>Otolemur garnettii</i>	<u>GGGCGCAGGGU</u> <u>GGGGUGGGUGAGGCCGGG</u>	40	Intronic (4:5)
<i>Tursiops truncatus</i>	<u>GGGAGUUAGGGGGUGC</u> <u>GGGCUGGG</u>	38	Intronic (2:3)
<i>Equus caballus</i>	<u>GGGAGUUGGGGAGUGGGG</u> <u>UUUGGG</u>	42	Intronic (3:4)
<i>Ailuropoda</i>	<u>GGGAGACUUCGGGUG</u> <u>UUUGGGGGUGAGGG</u>	40	Intronic (5:6)

<i>melanoleuca</i>			
	<u>GGGAGACUGCGGGUAUUUUGGGGAGAGGG</u>	39	Intronic (5:6)
<i>Pongo abelii</i>	<u>GGGUUGAAGGGCGGCGAGGGGUGGGG</u>	39	Intronic (6:7)
<i>Oryctolagus cuniculus</i>			
	<u>GGGAGAGUGGGUGGGGUCCUGGG</u>	40	Intronic (5:6)
<i>Gorilla gorilla gorilla</i>			
	<u>GGUGGC GGUGG</u>	21	Intronic (1:2)
<i>Sus scrofa</i>			
	<u>GGGGUGGGGGUGGGGGUGGGGG</u>	83	Intronic (2:3)
<i>Ovis aries</i>	<u>GGGCUGGGGCAAAGGGGGAGGG</u>	41	Intronic (1:2)
<i>Monodelphis domestica</i>			
	<u>GGGGUGGGGAGGAGGGAUGGG</u>	40	5'-UTR
	<u>GGGAGAUGGGGGGGGUAGGUGGG</u>	40	Intronic (2:3)
positive control²	<u>AGGGCTAGGGCTAGGGCTAGGG</u>	42	N/A
negative control³			
	CGTGGGGAGATTGGGGAGCGCA	0	N/A
negative control_B			
	GGTGTGCGTGTGCGAGCGAGAGAGAGTGG	0	N/A

¹The genomic location specifies the intron between the numbered exons

²The G-quadruplex structure of this DNA sequence was determined by nuclear magnetic resonance (Protein databank-ID: 2KM3)

³ All controls were DNA. The negative control_A is a randomised sequence with the same base composition as the positive control. The negative control_B has the same base composition as the *Homo sapiens* GQS.

In Table 2, the sequences that had highest scores within the whole pre-mRNA of respective organism are listed. The G-scores obtained from QGRS mapper for most organisms are comparable to that of the +VE control, with the exception of *R. norvegicus* and *G. gorilla*. The –VE controls have G-score of 0 as they cannot fold into G-quadruplex. Underlined are the guanine residues participating in the G-quartets. The genomic location of the GQSs is also listed in Table 2, with the majority of them being intronic. For instance the *M. musculus*' highest GQS is Intronic (7:8), which is indicative of the intron located between exon 7 & 8. *R. norvegicus* has 6 GQSs with G-scores of 21 each and are at different locations in the gene. *M. domestica* has its highest GQS occurring in the 5' UTR region while *C. Lupus* has its highest scoring GQS located in its 3'-UTR. *P. troglodyte*, *P. abelii* and *M. domestica* have 2 GQSs with highest G-score from different locations. *S. scrofa* possesses a GQS that has a score of 83, indicative of a very stable G-quadruplex. Quadbase does not have a scoring system unlike QGRS mapper; however the putative sequences predicted by Quadbase correlated with the highest scorers from QGRS mapper.

The QGS listed in Table 2 have been mapped for respective organisms (Appendix I).

With the exception of *F. catus*, *O. garnettii*, *T. truncatus*, *A. melanoleuca*, *O. cuniculus*, *G. gorilla* and *O. aries*, which lack UTR regions, every other orthologs that possess UTR regions in their *FXVD1* gene have GQS located in their UTR regions. However, given the low scores, it does not seem likely that these UTR GQS form stable G-quadruplexes when compared to the +VE control's G-score. The UTR GQSs from each ortholog are shown in Table 3.

Table 3: GQS located in UTR regions from the orthologs, revealed by QGRS mapper and Quadbase.

Organism	UTR GQS	UTR QGRS G-Score
<i>H. sapiens</i>	<u>GGCACAGCAGGACGUUUGGGGG*</u>	15
	<u>GGAGCGAUUGGAAUCCGGCCAGG**</u>	18
<i>M. musculus</i>	<u>GGGUGGAGCAUCCAGUUCUGGGCCAGGG*</u>	10
	<u>GGUGCACAGCUGGACAUUUGGGGG*</u>	13
	<u>GGAGGGAAAGAGAGCAGGGCAGAGG*</u>	13
<i>C. lupus</i>	<u>GGCGGCGCAGGACCAGCUCUGGAACAGGGG*</u>	18
	<u>GGCACAGCCGGACGUUUGGGGG*</u>	15
	<u>GGCGGUAGAGACACCUUGGCGGAUGG**</u>	11
	<u>GGGCUAGGCUGGGGGGCGGGGG**</u>	35
	<u>GGGGGCGAAGGGUGGGCUGGGAUGGCCGGG**</u>	42
<i>P. troglodytes</i>	<u>GGCACAGCAGGACGUUUGGGGG*</u>	15
	<u>GGAGCGAUUGGAAUCCGGCCAGG**</u>	18
<i>B. taurus</i>	<u>GGCAGCGCAGCCAGCUCUGGGCCAGGGGG*</u>	6
	<u>GGCCCCGGGGCACAGCCGGACGUUUGGG*</u>	20
	<u>GGCCUUCUUUCGGCAGGGG*</u>	19
	<u>GGCGGUAGAGACACCUUGGCGGAUGGG**</u>	11
	<u>GGCUGGGGGAGGGAGGAUAGAGG**</u>	21
	<u>GGGCAAAGGGCUGGGUAGCGGG**</u>	40
<i>R. norvegicus</i>	<u>GGCGGUAGAACCUCACCUGGCUCCAGG**</u>	8
<i>Felis catus</i>	N/A	N/A

<i>Otolemur garnettii</i>	N/A	N/A
<i>Tursiops truncatus</i>	N/A	N/A
<i>Equus caballus</i>	<u>GGCCCCUGGGCACAGCCGGACGUUGGG</u> *	20
<i>Ailuropoda melanoleuca</i>	N/A	N/A
	<u>GGAGUGGCCAGCCCGAGGCUUCCCAGG</u> *	15
	<u>GGGAGGGAGUGUGGUUGAGG</u> *	19
	<u>GGGUUCUGCAGGGUGGGAUGUGGG</u> *	36
<i>Pongo abelii</i>	<u>GGCAGGGUGUGGAGUUUGG</u> *	19
	<u>GGCACCGGAGGCCAGAGGAGGAGUACUGG</u> *	18
	<u>GGGACGACGGUGGUUGGGCGGGGGCGGGG</u> **	34
<i>Oryctolagus cuniculus</i>	N/A	N/A
<i>Gorilla gorilla gorilla</i>	N/A	N/A
	<u>GGGGAGGGGUGGGGUGGGG</u> *	63
<i>Sus scrofa</i>	<u>GGGAGGGGACACCGCUGAGGGCGG</u> *	13
	<u>GGGCCAGGGGUCCAGCCGGCCGUUUGGG</u> *	21
<i>Ovis aries</i>	N/A	N/A
<i>M. domestica</i>	<u>GGGUGGGGAGGAGGGAUGGG</u> *	40

* represents GQS from 5'UTR regions

** represents GQS from 3'UTR regions

Most orthologs have more than one GQS in their UTR regions that can fold into a G-quadruplex, but are relatively unstable in comparison to the GQS from Table 2. It is seen here that 5 organisms, namely (i) *C. lupus* (ii) *B. taurus* (iii) *M. domestica* (iv) *S. scrofa* & (v) *P. abelii* have GQS of G-scores comparable to the positive control in their UTR regions, indicative of the formation of highly stable G-quadruplexes.

Analysis of fully processed *FXYD1* human and ortholog mRNA did not contain high scoring GQS in comparison to the +VE control. The results for the mRNA of *H. sapiens* are shown in Table 4.

Table 4: GQS predicted by QGRS mapper for *H. sapiens'* fully processed mRNA

Length	GQS	G-Score
26	<u>GG</u> CAGCUG <u>GG</u> CCUCACCC <u>GG</u> CAG <u>GG</u>	15
13	<u>GGGG</u> AAG <u>GCAGG</u>	20
30	<u>GG</u> ACAAU <u>GG</u> CGUCUCU <u>GG</u> CCACAUCU <u>GG</u>	17
28	<u>GG</u> ACUG <u>GGG</u> AACCCGAUGAAGAG <u>GGAGGG</u>	10
22	<u>GG</u> AGCGAU <u>GG</u> AAUCC <u>GG</u> CCAG <u>GG</u>	18

Five potential GQS were predicted, but they have relatively low scores and the highest scoring one has a G-score of 20, which is about half of the score obtained for the +VE control's G-quadruplex. Also the GQSs have only 2 quartets (underlined guanines), making the G-quadruplexes less stable.

3.1.2 Stability calculations of secondary/tertiary structures

The calculations executed by RNAfold, RNAeval and RNAsubopt on the controls, Human_PLM and Bovine_PLM sequences confirmed the potential of the +VE control, Human_PLM and Bovine_PLM sequences to form G-quadruplexes. The calculated and proposed structure based Minimum Free Energy (MFE) calculation is listed in Table 5.

Table 5: Analysis of the oligonucleotide sequences considered for laboratory work by the Vienna RNA Package. The proposed dot bracket notation of the MFE structure generated by RNAfold and other secondary structures by RNAeval and RNAsubopt are shown.

Name	Dot bracket annotation ¹	Free Energy (kcal/mol)	Diversity of MFE structure ²	Frequency of MFE structure
+VE	.++++.....++++.....++++.....++++	-12.65	0.00	1.001
((((.....))))..	-3.80		
	..((((.....)))).....	-2.80		
	...((((.....)))).....	-2.10		
((..((((.....))))..)	-2.00		
-VE_A	.((((.....))))..	-0.30	4.10	0.259
	0.00		
	..((.(.....).))	0.30		
	((.....))..	0.30		

	(. ((. ((.....)) .) .)	0.30		
-VE_B	. ((. ((. ((.....)) .) .)	-2.70	4.68	0.385
	. ((. ((. ((.....)) .) .)	-2.20		
 ((. ((.....)) .) .)	-1.80		
 ((. ((.....)) .) .)	-1.60		
 ((. ((.....)) .) .)	-1.30		
Human ((. ((. ((.....)) .) .)	-4.30	1.69	0.476
_PLM ((. ((. ((.....)) .) .)	-4.10		
	+++.....+++.....+++.....+++	-3.51	0.01*	0.504**
	... ((. ((. ((.....)) .) .) .) ...	-2.90		
	... ((. ((. ((.....)) .) .) .) ...	-2.70		
Bovine	+++.....+++.....+++.....+++	-8.37	0.00	0.125
_PLM	... ((. ((. ((.....)) .) .)	-3.20		
	((. ((. ((.....)) .) .) .) ...	-2.50		
	... ((. ((.....)) .) .)	-2.30		
	. (((. ((.....)) .) .) .)	-2.20		

¹The symbols '(' and ')' represent canonical base pairs, '+' represents guanine bases taking part in G-tetrad formation, '.' represents unpaired bases.

² = diversity of the proposed structure, the average distance separating bases involved in pairing of the structure

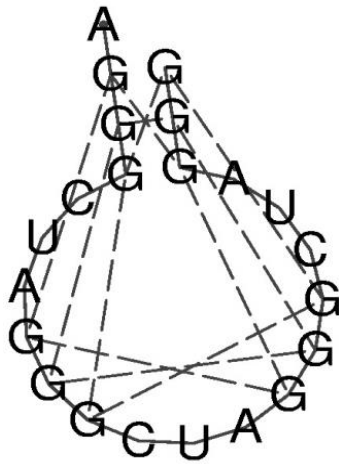
* diversity of the 3rd structure with respect to its MFE for Human_PLM sequence

** frequency of Human_PLM's 3rd structure after its MFE structure

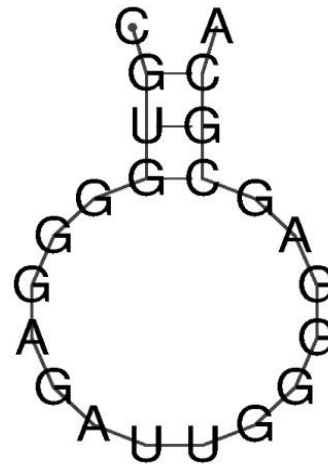
The data presented in Table 5 lists the MFE structures and other secondary structures according to their free energies. The results indicate that the +VE control forms a highly stable G-quadruplex, with a structural diversity of $d = 0.00$. The intramolecular G-quadruplex formed is the minimum energy requiring structure for the +VE control at -12.65 kcal/mol. For the Human_PLM sequence, G-quadruplex was the 3rd energy favourable entity, giving -3.51 kcal/mol. The highly stable G-quadruplex formed by Bovine_PLM, with diversity of $d = 0.0$, was its MFE structure, at -8.37 kcal/mol. The structures proposed for -VE_A and -VE_B are quite unstable, with high free energies. The frequencies of the MFE structures vary for the different species. The G-quadruplex for the +VE control is expected to be the only structure present with a frequency of 1.00. The MFE structure proposed for the remaining species will be in equilibrium with other structures as indicated by frequencies < 0.5 . All G-quadruplex entities have $d = 0.00$, which indicate highly stable G-quadruplexes from the +VE, Human_PLM and Bovine_PLM sequences.

The proposed MFE structure for the +VE, -VE_A, -VE_B and Bovine_PLM sequences was obtained by RNAplot and are shown below.

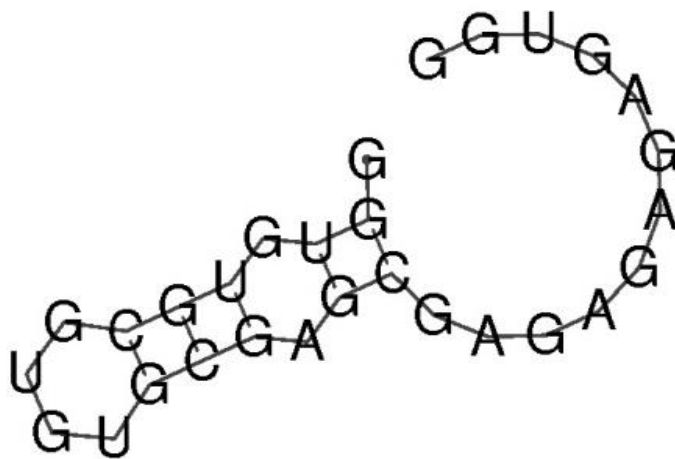
A.



B.



C.



D.

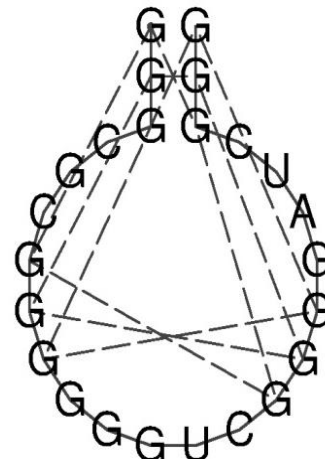


Figure 9: MFE structures generated by RNAplot as calculated by RNAfold and RNAsubopt. **A.** +VE control's intramolecular G-quadruplex at -12.00 kcal/mol. **B.** -VE_A MFE structure at -0.30 kcal/mol. **C.** Proposed -VE_B MFE ensemble at -2.70 kcal/mol. **D.** Intramolecular G-quadruplex entity formed by the Bovine_PLM sequence at -8.37 kcal/mol.

Graphical plots of the 3 lowest energy state structures for Human_PLM sequence were produced by RNAplot and are shown below.

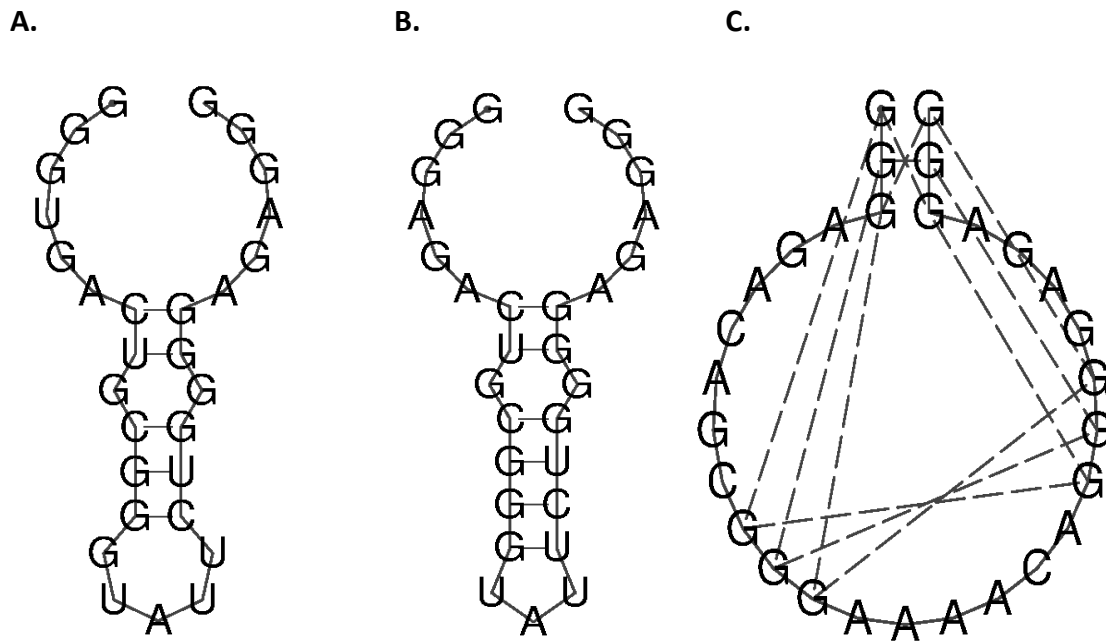


Figure 10: Graphical plot by RNAplot for the proposed secondary and G-quadruplex structures for Human_PLM sequence predicted by RNAfold and RNAsubopt. **(A)** MFE structure at -4.30 kcal/mol **(B)** second lowest energy state structure at -4.10 kcal/mol **(C)** G-quadruplex structure of Human_PLM at -3.51 kcal/mol.

In comparison to the G-quadruplex structure proposed for Human_PLM, the MFE and structure at -4.10 kcal/mol are relatively broader and longer in size. The G-quadruplex is compacter.

These MFE values were used to estimate the relative amount of secondary structure in equilibrium with G-quadruplex structure for Human_PLM, assuming that the MFE values correspond approximately to the free enthalpy of folding ΔG .

$$\Delta G = -RT \ln K$$

,where ΔG is the Gibbs free energy, R is the gas constant and T is temperature ($R = 1.987 \times 10^{-3} \text{ kcal K}^{-1} \text{ mol}^{-1}$, $T = 298 \text{ K}$) and K is the equilibrium constant.

$$K1 = \frac{[G4 \text{ emsemble}]}{[Non - folded]}$$

$$K2 = \frac{[2^\circ \text{ emsemble}]}{[Non - folded]}$$

$$\frac{K1}{K2} = \frac{[G4 \text{ ensemble}]}{[2^\circ \text{ ensemble}]}$$

$$K = e \left(\frac{-\Delta G}{RT} \right)$$

$$K1 = e \left(\frac{- \left(-3.51 \frac{\text{kcal}}{\text{mol}} \right)}{1.987E - 3 \frac{\text{kcal}}{\text{kmol}} \times 298 \text{ K}} \right) \equiv 375.33$$

$$K2 = e \left(\frac{- \left(-4.30 \frac{\text{kcal}}{\text{mol}} \right)}{1.987E - 3 \frac{\text{kcal}}{\text{kmol}} \times 298 \text{ K}} \right) \equiv 1425.06$$

$$\frac{375.33}{1425.06} = \frac{G4 \text{ ensemble}}{2^\circ \text{ emsemble}}$$

$$2^\circ \text{ emsemble} = (3.80)G4 \text{ emsemble with } \Delta G - 4.30 \text{ kcal/mol}$$

Or
$$2^\circ \text{ emsemble} = (2.71)G4 \text{ emsemble with } \Delta G - 4.10 \text{ kcal/mol}$$

The calculation revealed that the other two lower energy secondary structures exist at about a fourfold higher concentration than G-quadruplex for Human_PLM. Or in other words, the concentration of the G-quadruplex species takes approximately 25% of the concentration of all molecular species. The two secondary structures are likely to compete against G-quadruplex formation in Human_PLM.

3.1.3 Multiple Sequence Alignment of GQS from Table 2 against orthologous *FXYD1* pre-mRNA sequences

The MSA carried out using the MAFFT server shows G-rich regions that are conserved across the genome of the orthologs, having the ability to fold into G-quadruplexes. *H. sapiens'* GQS from Table 2 was aligned alongside the pre-mRNA sequence of the remaining orthologs (Figure 11).

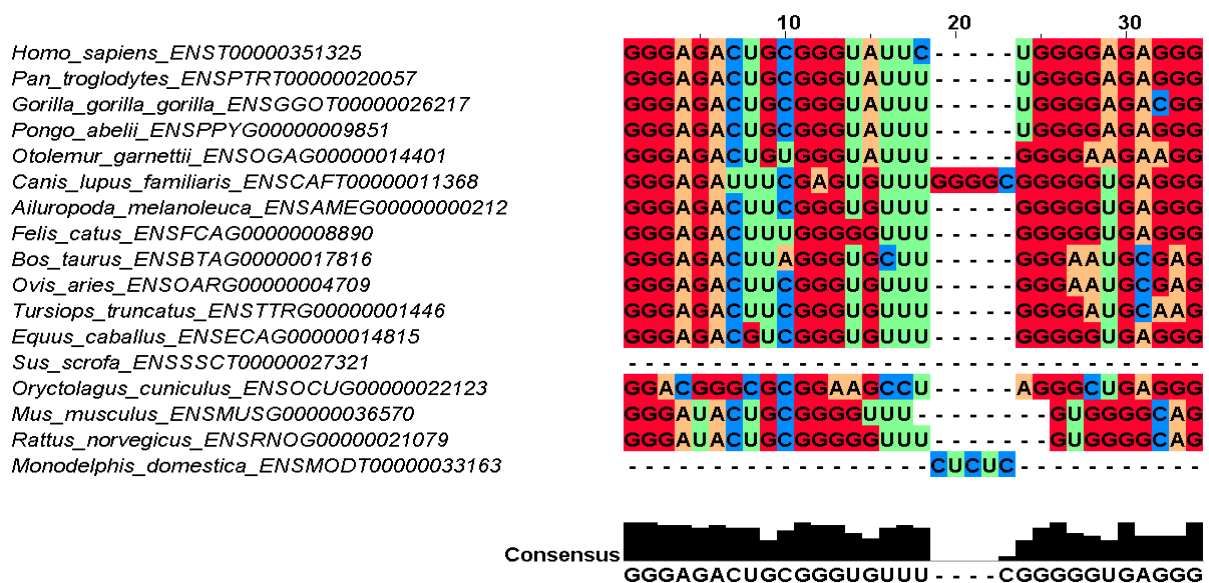


Figure 11: Highest scoring GQS for *H. sapiens* aligned with the remaining orthologs by MAFFT Version 7. Accession numbers are listed next to respective organism's name. Alignment of the *H. sapiens* GQS from Table 2 has indicated conserved sequences within most orthologs that can form G-quadruplexes. The consensus sequence was GGGAGACUGCGGGUGUUUCGGGGGUGAGGG and can form a G-quadruplex with a G-score of 40.

The conserved sequences from each ortholog from Figure 11 have been mapped (Appendix I) onto the *FXYD1* gene of the respective organism and are listed in Table 6.

Table 6: Genomic location and G-scores of the conserved sequences with respect to the highest scoring GQS of *H. sapiens*

Organism	Conserved sequence after aligning <i>H. sapiens</i> highest scoring GQS	Genomic location	G-score
<i>P. troglodytes</i>	GGGAGACUGCGGGUAAUUUGGGGAGAGGG	Intronic (6:7)	39
<i>G. gorilla</i>	GGGAGACUGCGGGUAAUUUGGGGAGACGG	Intronic (5:6)	20
<i>P. abelii</i>	GGGAGACUGCGGGUAAUUUGGGGAGAGGG	Intronic (6:7)	39
<i>O. garnettii</i>	GGGAGACUGUGGGUAAUUUGGGGAAGAAGG	Intronic (5:6)	20
<i>C. lupus</i>	GGGAGAUUUCGAGUGUUUGGGGCGGGGUGAGGG	Intronic (6:7)	20
<i>A. melanoleuca</i>	GGGAGACUUCGGGUGUUUGGGGGUGAGGG	Intronic (5:6)	40
<i>F. catus</i>	GGGAGACUUUGGGGGUUUGGGGGUGAGGG	Intronic (5:6)	40
<i>B. Taurus</i>	GGGAGACUUAGGGUGCUUGGGAAUGCGAG	Intronic (6:7)	0
<i>O. aries</i>	GGGAGACUUCGGGUGUUUGGGAAUGCGAG	Intronic (5:6)	0
<i>T. truncates</i>	GGGAGACUUCGGGUGUUUGGGGAUGCAAG	Intronic (5:6)	14
<i>E. caballus</i>	GGGAGACGUCGGGUGUUUGGGGGUGAGGG	Intronic (5:6)	40
<i>S. scrofa</i>	N/A	N/A	N/A
<i>O. cuniculus</i>	GGACGGGCGCGGAAGCCUAGGGCUGAGGG	Intronic (6:7)	19
<i>M. musculus</i>	GGGAUACUGCGGGGUUUGUGGGGCAG	Intronic (6:7)	14
<i>R. norvegicus</i>	GGGAUACUGCGGGGUUUGUGGGGCAG	Intronic (6:7)	16
<i>M. domestica</i>	N/A	N/A	N/A

From Table 6, the conserved sequences for almost every ortholog have the potential to form G-quadruplex and all the sequences are located in introns. The conserved sequences from *B. taurus* and *O. aries* are the only sequences that do not fold in G-quadruplex.

The consensus sequences obtained after aligning each GQS from Table 2 with the pre-mRNA of other orthologs are listed in Table 7.

Table 7: Consensus sequence obtained after aligning each sequence from Table 2 by MAFFT Version 7.0

GQS aligned with pre-mRNA of other orthologs	Consensus Sequence	G-score
<i>H. sapiens</i>	<u>GGGAGACUGCGGGUGUUUCGGGGUGAGGG</u>	40
<i>P. troglodytes</i> 1 st	<u>GGGAGACUGCGGGUGUUUCGGGGUGAGGG</u>	40
<i>P. troglodytes</i> 2 nd	<u>GGGUUGGAGGGCGGCGAGGGGUGGGG</u>	39
<i>G. gorilla</i>	<u>GGUGGCAAGGGU+G</u>	19
<i>P. abelii</i> 1 st	<u>GGGAGACUGCGGGUGUUUCGGGGUGAGGG</u>	40
<i>P. abelii</i> 2 nd	<u>GGGUUGGAGGGCGGCGAGGGGUGGGG</u>	39
<i>O. garnettii</i>	GGGCGCUGUGGGGGUGAGGC+GG	19
<i>C. lupus</i>	GGAGGAAGGCGGGAGAGGCA+GGGGCCAAGUGCCAGG GUUGGA	20 ¹ , 14 ²
<i>A. melanoleuca</i>	GGGAGACUGCGGGUGUUUCGGGGUGAGGG	40
<i>F. catus</i>	GGGAGACUGCGGGUGUUUCGGGGUGAGGG	40
<i>B. taurus</i>	GGGCGCGGGGGUUGGAGGGAGGG	37
<i>O. aries</i>	AGGUCAGGCAAAGGUGGGGGG	20
<i>T. truncatus</i>	GGGAG+UGGGAGGGGGAGGGCCUGGG	41
<i>E. caballus</i>	GGGAG+UGGGAGGGGGAGGGCCUGGG	41

<i>S. scrofa</i>	-----GGGG	0
<i>O. cuniculus</i>	ACUGGAAGAUGGAGGGUUCUGGG	18
<i>M. musculus</i>	ACUAGGCUGGGGGAGGGAGGGAGGGGGGGG	42
<i>R. norvegicus</i> 1 st	GCAGGUGGG+CCUUGGG	17
<i>R. norvegicus</i> 2 nd	GGAUGGAGGCCGGC	20
<i>R. norvegicus</i> 3 rd	GGCGCUGUGGGGG	0
<i>R. norvegicus</i> 4 th	GGCAC+GGGAGGUGAAG	18
<i>R. norvegicus</i> 5 th	ACUAGGCUGGGGGA	0
<i>R. norvegicus</i> 6 th	GGGGGGGAGGA	20
<i>M. domestica</i> 1 st	CCUGGC+GGGUGUGGGGUUUGG	20
<i>M. domestica</i> 2 nd	GCAAGGGU+GGGGGAAACCCUGCAAGAGAA	0

¹ The G-score obtained for the consensus sequence after aligning the highest scoring GQS of *C. lupus* is 20 after substituting the + with the base G.

² The consensus sequence after aligning *C. lupus*' highest scoring GQS has a G-score of 14 after substituting the + with the base A.

Besides *S. scrofa*, the consensus sequences obtained after aligning the highest scoring QGS from Table 2 for every ortholog, have the ability to form G-quadruplexes as seen in Table 6. Two out of the six QGSs from *R. norvegicus* gave consensus sequences that cannot form G-quadruplexes and one out of the two highest scoring GQS from *M. domestica* gave a consensus sequence that does not fold into a G-quadruplex.

3.1.4 Alternative splicing

The comparison between *H. sapiens'* *FXYD1* and the variant *FXYD1-009* mRNA and pre-mRNA sequences suggests that alternative splicing takes place.

- *FXYD1* mRNA FASTA sequence:

```
guggcagcugggccucacccccggcagggcugugcgugacccccugagugggggaaggcag
gcuguugccaugguggccugagcgcagcagaaauuccuccaggGACAAUGGCGUCUCUUGGC
CACAUUCUUGGUUUUCUGUGUGGGUCUCCUCACCAUGGCCAAGGCAGaaaguccaaaggaa
cacgaccgcuucacuuacgACUACCAGUCCCUGCAGAUCGGAGGCCUCGUCAUCGCCGGG
AUCCUCUUAUCCUGGGCAUCCUCAUCGUGCUGAgcagaagaugccggugcaagucaac
cagcagcagGACUGGGGAACCCGAUGAAGAGGGGAACUUUCCGCAGCUCCAUCCGC
CgucuguccacccgcaggcgguagaaacaccuggagcgauggaauccggccagGACUCCG
CUGGCACCUGACAUCUCCCACGCUCCACCUGCGCGCCCACCGCCCCUCCGCCGCCCUU
CCCCAGCCUGCCCCCGCAGACUCCCCUGCCGCCAAGACUCCAAUAAAACGUGCGUUC
CUCUCGA
```

FXYD1 amino acid sequence:

```
MASLGHILVFCVGLLMAKAESPKEHDPFTYDYQSLQIGGLVIAGILFILGILIVLSRRCRCKFNQQRT
GEPDEEEGTFRSSIRRLSTRRR
```

- *FXYD1-009* mRNA FASTA sequence:

```
uuuucugugugggucuccucaccauggccaaggcagAAAGUCCAAAGGAACACGACCCGU
UCACUUACGacuaccaguccugcagaucggaggccucgucaucgccgggauccucuca
uccugggcauccucaucgugcugaCCCCGCCCCUCGCGAGGGCGAGCUGGAGCUACAGCG
CCGCUUGGCGCCCGCCGGGAGGGAGCCUCAGCUUCUCCUACCUCUCCACGCCACAGGCA
GAAGAUGCCGGUGCAAGUUCAACCAGCAGCAGAGgacuggggaacccgaugaagaggagg
gaacuuuccgcagcuccaucggccGUCUGUCCACCCGCAGGCGGUAGAAACACCUGGAGC
GAUGGAAUCCGGCCAGgacucuccuggcaccugacauccuccacgcuccaccugcgcgcc
caccgccccuccgcgcgcccuucccagccugccccgcagacucuccugccgcca
gacuuccaauaaaacgugcguuccucucgaca
```

FXYD1-009 amino acid sequence:

```
XFCVGLLMAKAESPKEHDPFTYDYQSLQIGGLVIAGILFILGILIVLTPPLARASWSYSAAWRPPGGSL
SFSYLSTPTGRRCRCKFNQQRTGEPDEEEGTFRSSIRRLSTRRR
```


intron 4 from the *FXVD1* pre-mRNA, producing *FXVD1*. Alternatively, the binding of the sub units at 5'-GU and 3'-AG will result in a partially spliced intron 4 of the *FXVD1*-pre mRNA, producing *FXVD1-009*. Hence *FXVD1-009* is a consequence of alternative splicing of the intron 4 of *FXVD1* pre-mRNA.

A comparison of the pre-mRNA of *FXVD1* and *FXVD1-009* was performed by 1000 Genomes Transcript comparison option. *H. sapiens'* highest scoring GQS, GGGAGACUGCGGGUAUUCUGGGGAGAGGG, was compared in the two pre-mRNA transcripts for mutations. The result is shown in Figure 12.

FXVD1	3721	CTG	GGGAGACTGCGGGTATTCTGGGGAGAGGG	CTGGTTCC.
FXVD1-009	3721	CTGGGGAGACTGCGGGT	AATTCTGGGGAGAG	GCTGGTTCC.

Variation: rs201764718	
Position	19:35633462
Alleles	G/A
Types	Intron variant

Figure 12: Part of the pre-mRNA comparison of *FXVD1* (intron6) and *FXVD1-009* (intron5) that maps the highest scoring GQS of *H. sapiens*. The highest scoring GQS of *H. sapiens'* pre-mRNA is highlighted blue.

The GQS is present in both *FXVD1* and *FXVD1-009*. However, two variations within the sequence of *FXVD1-009* are present. Base A in the second loop that was a A/G variant and base G from the fourth quartet, which was a G/A variant as seen in Figure 12. The G/A variant is more likely to affect the G-quadruplex structure than the A/G variant as the A/G is a loop base instead of G/A from a quartet. The sequence of the variant-009 after G → A substitution is GGGAGACUGCGGGUAUUCUGGGGAGAGAG.

Analysis of the variant sequence by QGRS mapper revealed a GQS (GGAGACUGCGGGUAUUCUGGGG) with a G-score of 14, which is very low in stability. Further analysis by the Vienna RNA Package did not predict G-quadruplex formation by the variant sequence from *FXVD1*-009 pre mRNA. The results obtained after analysis by RNAfold and RNAsubopt are shown in Table 8.

Table 8: Dot bracket annotations of the MFE and secondary structures of the variant *FXVD1*-009 sequence (GGGAGACUGCGGGUAUUCUGGGGGAGAGAG) by RNAfold and RNAsubopt.

Dot bracket annotation	Free energy (kcal/mol)	Frequency of MFE	Diversity of MFE
.....(((.....))).....	-4.30	0.520	2.00
.....((((.....))).....	-4.10		
(((.....))).....	-1.70		
.....(((.....)))..	-1.50		
(((.....))).....	-1.40		
.((((.....))).....	-1.30		

The data presented in Table 8 indicate that RNAfold did not predict G-quadruplex formation for the variant sequence, even though the `-g` option was used in the command lines. GQS that were predicted to form low stability G-quadruplex with low G-scores from the *H. sapiens*' pre-mRNA were also predicted not to form G-quadruplex by the Vienna RNA Package (Data not shown). The MFE structure has free energy of -4.30 kcal/mol and structural diversity of 2.00, indicative of high instability.

The data obtained from the comparative analysis suggest the likelihood of the intronic G-quadruplex between exon 6 and 7 of *H. sapiens* *FXVD1* to play a major role in the splicing of the intron occurring between exons 4 and 5, impacting on the formation of *FXVD1-009*

3.2 G-quadruplex detection by Native PAGE

Comparison of R_f values of samples in the presence and absence of K^+ supports conformational changes in the +VE, Human_PLM and Bovine_PLM sequences (Figure 13). 30% Native PAGE gels were run at 140 mV with oligonucleotides of final concentration 3 μ M. The results obtained after exposure in the presence of SYBR Green I RNA stain S9430 and SYBR Green I nucleic S32717 are shown in Figure 13A-C.

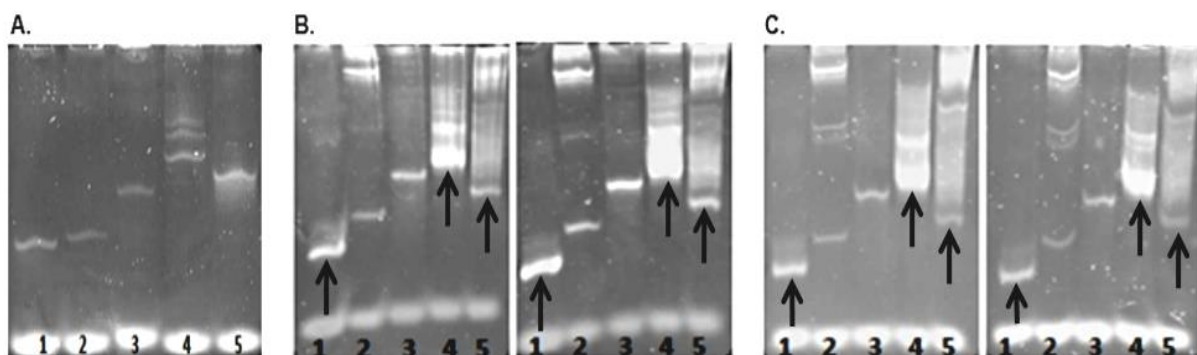


Figure 13: Native 30% PAGE of GQS oligos (Table 5) in absence and presence of K^+ . Lanes 1: +VE; 2:-VE_A; 3:-VE_B; 4:Human_PLM; 5:Bovine_PLM. **A.** 30% PAGE loaded with samples incubated in 0.02 M TrisOAc buffer solution only. **B.** 30% PAGE loaded with samples incubated in 0.02 M TrisOAc and 0.05 M K^+ buffer solution on two separate gels, duplicates. **C.** Two separate 30% PAGE, duplicates, loaded with samples incubated in 0.02 M TrisOAc and 0.10 M K^+ buffer solution. Arrows in **B** & **C** point putative G-quadruplexes. The control samples in lanes 1, 2 and 3 under K^+ free conditions and samples in lanes 2 & 3 in the presence of K^+ acted as markers.

Under K^+ free condition, the +VE and -VE_A controls migrated at the same rate on the gel. -VE_B migrated less than other controls but faster than Human_PLM and Bovine_PLM. Human_PLM was the slowest migrating sample. In the presence of 0.05 M K^+ , the +VE

control was the fastest migrating sample followed by the Bovine_PLM that migrated faster than -VE_B. In the order of fastest to slowest migrating sample: +VE > -VE_A > Bovine_PLM > -VE_B > Human_PLM is observed for samples in 0.05 M K⁺. Samples incubated in 0.1 M K⁺ migrated with a similar trend as samples incubated in 0.05 M K⁺. The tracking dye is at the bottom of the gels in A-C. The DNA species under K⁺ free conditions (Fig 13A) produced a distinct single band as well as Bovine_PLM, except for Human_PLM that produces 3 bands. In K⁺ containing buffer, the +VE and -VE_B controls produced single bands on the gels (Fig 13B & 13C), while -VE_A produced several bands and Bovine_PLM and Human_PLM produced smears.

The ratio of the distance migrated by each sample with respect to that of the tracking dye (R_f value) on the gel is represented graphically for 5 separate experiments.

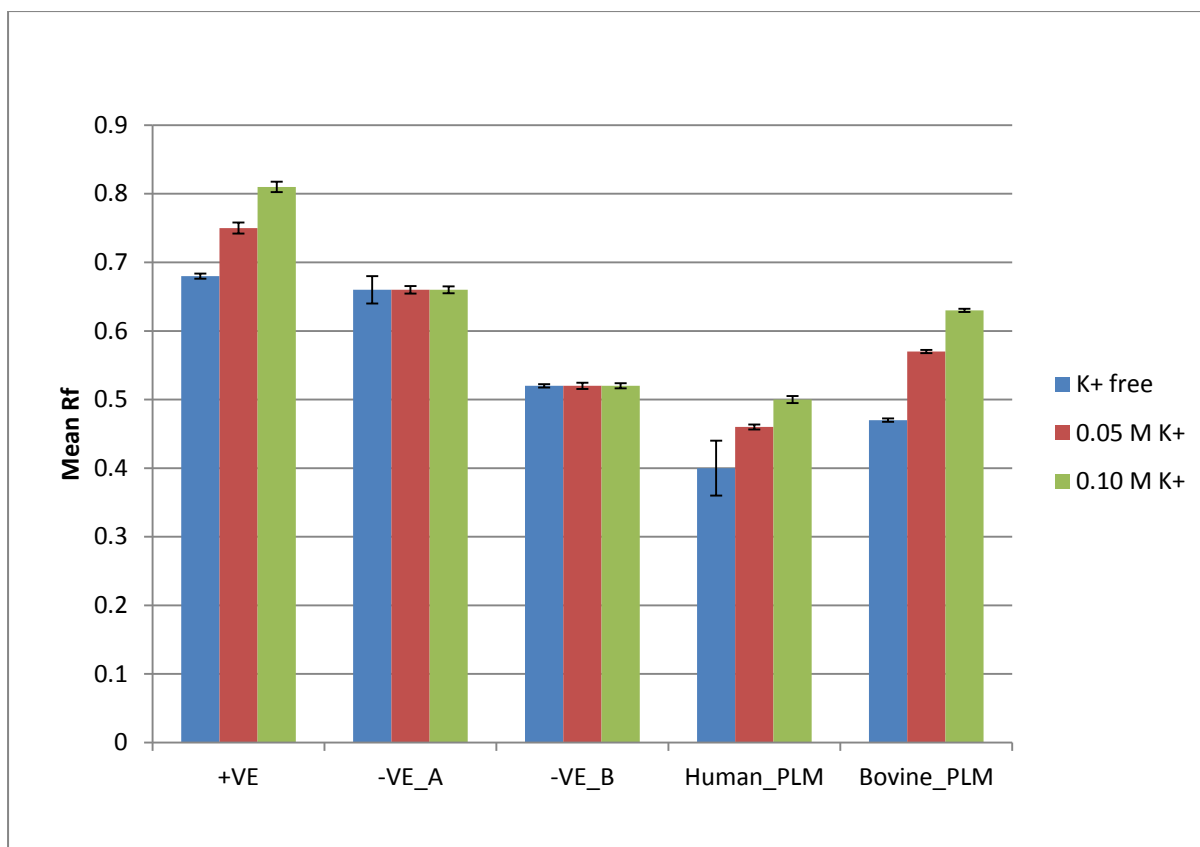


Figure 14: Comparison of the relative migration distance, R_f , obtained from native PAGE experiments for samples treated in K^+ free and K^+ containing buffer. The error bars show the standard error (n=5 experiments).

The +VE control, Human_PLM and Bovine_PLM samples migrated significantly faster when in the presence of K^+ than when in K^+ free buffer. At higher K^+ concentration the +VE, Human_PLM and Bovine_PLM samples migrated even faster. -VE_A and -VE_B samples in K^+ buffer migrated by the same rate in comparison to their respective counterparts in K^+ free buffer.

Table 9: Student 2-tailed-t-test of R_f values for samples in the presence of K^+ containing buffer against samples in K^+ free buffer(n=5)

Sample	+VE	-VE_A	-VE_B	Human_PLM	Bovine_PLM
Op-value for	4.18E-05	0.74044	0.45537	3.34E-06	1.97E-07
0.05 M K^+					
p-value for	4.23E-07	0.72447	0.34053	3.09E-07	5.33E-11
0.10 M K^+					

Table 10: Student 2-tailed-t-test of R_f values for samples incubated in different concentration of K^+ containing buffer(n=5)

Sample	+VE	-VE_A	-VE_B	Human_PLM	Bovine_PLM
p-value	0.00153	0.60751	0.67254	0.00032	3.83E-07

At a confidence level of 5%, the difference in migration for the +VE Control, Human_PLM and Bovine_PLM in the presence of K^+ compared to their respective K^+ free incubated counterparts are statistically significant as they support p values < 5% as seen in Table 9. – VE_A and –VE_B have p values > 5%, ruling out the fact that the differences in migration of these samples in the presence or absence of K^+ are significant. This significant difference in migration supports G-quadruplex formation in the +VE control, Human_PLM and Bovine_PLM samples. Comparison between similar samples at different K^+ concentrations (Table 10) supported p values < 5% for the +VE control, Human_PLM and Bovine_PLM suggesting G-quadruplex formation depends on availability of K^+ ions.

The slow migrating band of $-VE_A$ can be interpreted as intermolecular G-quadruplex formation between four strands of oligonucleotides; this is also supported by the fluorescence data shown in Figure 15.

3.3 Detection of G-quadruplexes by Fluorescence spectroscopy

The recorded spectrum of the controls, Human_PLM and Bovine_PLM sequences in the presence and absence of K^+ ions are shown below.

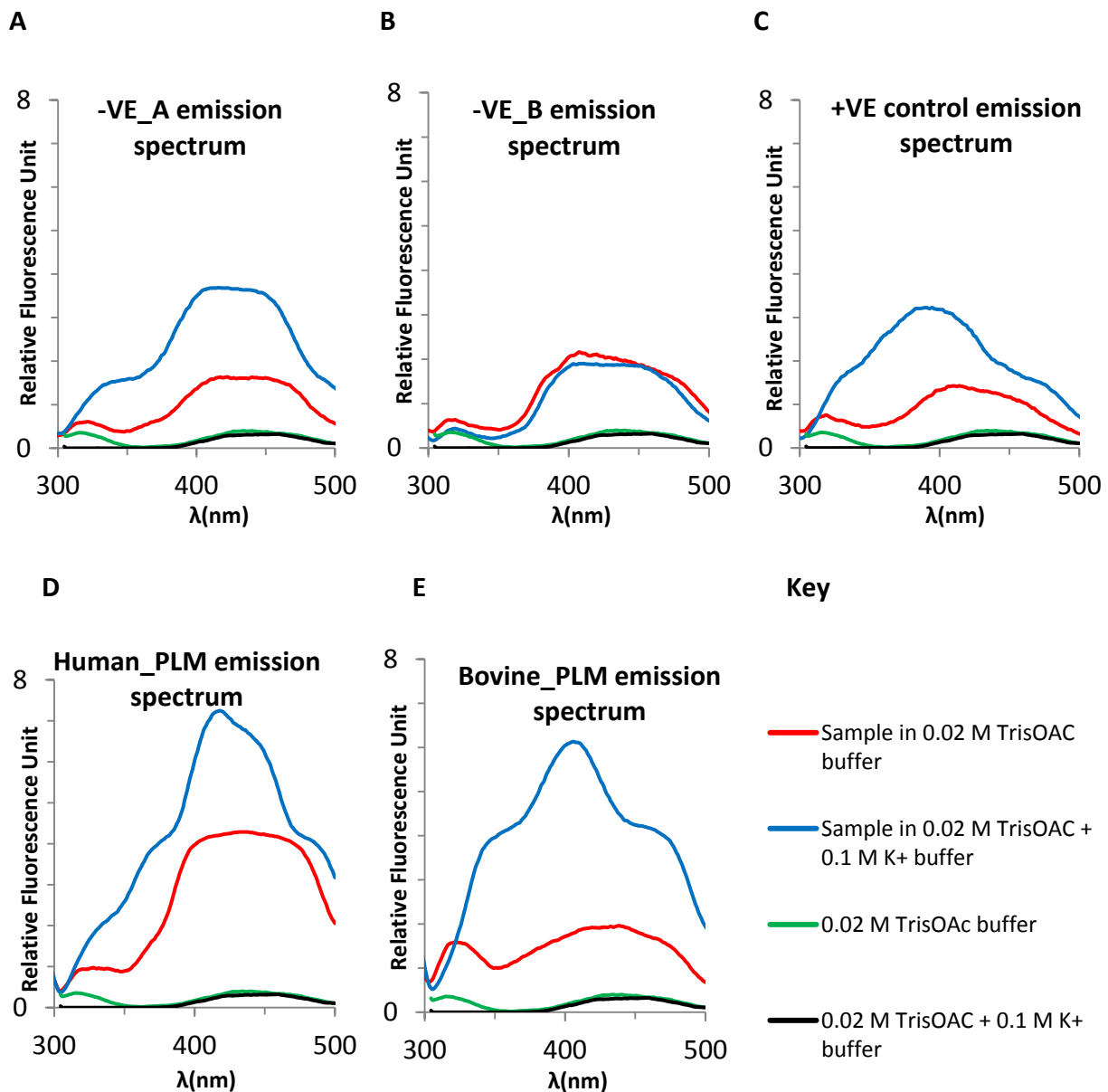


Figure 15: Emission spectra of samples recorded over the range 300-500 nm, excited at 260 nm. The oligonucleotide concentrations were 5.0 μ M for positive and negative control DNA samples 1.5 μ M for RNA samples.

The fluorescence intensity of -VE_A shows an unexpected increase upon addition of 0.1 M K^+ . This indicates the possibility that -VE_A can form G-quadruplex structures. As detailed in the discussion, the formation of an *intermolecular* G-quadruplex formed from four strands of DNA is possible with -VE_A. The fluorescence spectra of -VE_B (Fig. 15B) in the presence or absence of K^+ do not show significant differences. This is indicative that -VE_B cannot fold into a G-quadruplex as it was predicted by the *in-silico* studies. The emission spectra of the +VE control shows an increased fluorescence intensity in the presence of K^+ (Fig. 15C). This increase is most likely caused by intramolecular anti-parallel G-quadruplex structures formed by the +VE control. The increase of the peak maximum of the +VE control in K^+ buffer is ≈ 2.0 relative intensity units. The emission spectrum of Human_PLM over the range 300-500 nm (Fig. 15D) shows an increase of the fluorescence emission intensity upon addition of K^+ containing buffer. Notably, in the absence of K^+ , the Human_PLM RNA has a higher fluorescence emission intensity than other samples with a peak maximum of ≈ 4.0 , albeit there is a clear difference in K^+ buffer conditions with a maximum of ≈ 7.5 . Possibly canonical base-pairing due to secondary structure formation contributes to the higher fluorescence intensity in the absence of K^+ . The Bovine_PLM RNA sample in 0.1 M K^+ buffer shows a clear increase of fluorescence from 2.0 in K^+ -free conditions to ≈ 6.1 in K^+ buffer. The spectra of the buffers were also recorded and had a relatively low fluorescence emission compared to the oligonucleotides.

In order to assess potential fluorescence quenching effects of KCl on the fluorescence, emission spectra of quinine were measured with and without potassium ions in the buffer and at two different excitation wavelengths (250 and 350nm).

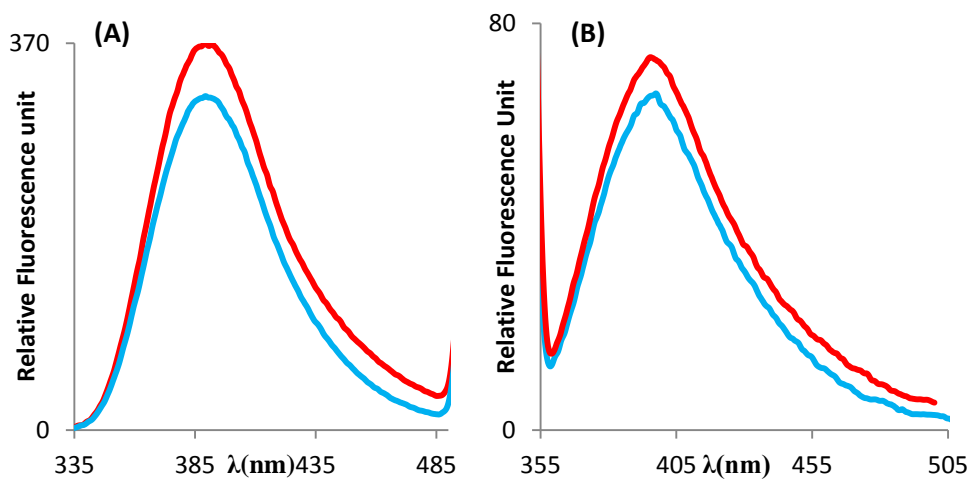


Figure 16: Emission spectra of Quinine at 0.6 ppm in the presence of 0.02 M TrisOAc buffer only (Red curve) or 0.02 M TrisOAc + 0.1 M K⁺ buffer (Blue curve). **(A)** $\lambda_{\text{ex}} = 250 \text{ nm}$, **(B)** $\lambda_{\text{ex}} = 350 \text{ nm}$.

The spectra shown in figure 16A and B indicate a small reduction of fluorescence due to the presence of 0.1 M KCl. It should be noted that this reduction effect is opposite to the fluorescence enhancement seen in the G-quadruplex fluorescence experiments.

4. DISCUSSION

4.1 Computational sequence Analysis

Computational analysis by QGRS mapper and Quadbase on *FXYD1* and orthologous pre-mRNA has revealed sequences that can fold into G-quadruplex. The G-scores generated by QGRS mapper for *FXYD1* and ortholog sequence GQS shown in Table 2 are comparable to that of the +VE control, indicative of a stable G-quadruplex, except for *R. norvegicus* and *G. gorilla* with G-scores of 21. Looking back at Kikin's folding motif, it can be seen that all the ortholog *FXYD1* GQS, excluding those of *R. norvegicus*, *G. gorilla* and the -VE controls, have three successive guanines. This indicates the existence of three stacks of G-quartets in the G-quadruplex of these ortholog GQSs as seen in the +VE control DNA. *G. gorilla*'s highest scoring GQS was GGUGGCGGUGG, with a G-score of 21 and as per Kikin's folding motif this particular sequence has only two stacks of G-quartets. Similarly, *R. norvegicus* has 6 GQS of G-score 21 and each GQS has only 2 stacks of G-quartets participating in G-quadruplex formation as seen in Table 2, hence accounting for low stability G-quadruplex from *R. norvegicus*. Stability of G-quadruplexes is enhanced by more G-quartets (Kikin *et al.*, 2006), while loop size has a smaller effect. GQSs having at least three guanine tetrads and loops of equal length connecting them, will be highly stable and have high G-scores (Kikin *et al.*, 2006). The GQS obtained for *S. scrofa*, GGGGGUGGGGGUGGGGGUGGGGG, has a G-score of 83, which makes its G-quadruplex twice as stable as that of the +VE control. *S. scrofa* has 5 G-quartets that stack on top of each other to form a G-quadruplex that has loops of equal length of 1 base each. This makes the G-quadruplex from *S. scrofa* highly stable. On the

other hand, both -VE_A and -VE_B have G-scores of 0 and this means that these sequences were not predicted to form any intramolecular G-quadruplexes.

Additionally, there were putative GQSs within the untranslated (UTR) regions of all the orthologs from the *FXVD1* pre-mRNA that have the potential to fold into G-quadruplexes but the G-scores for the majority of these GQS as seen in Table 3 do not compare well with the +VE control, resulting in G-quadruplexes that have low stability. As previously reported, the high occurrence of G-quadruplex in UTR regions leads to hypothesizing on their role as translational regulators (Huppert *et al.*, 2008, Bugaut *et al.*, 2012), the *FXVD1* gene in this instance. G-quadruplexes of low stability could support a rapid folding and unfolding of G-quadruplex ensembles and thus support the conformational heterogeneity within the UTR regions. Instead of inhibiting translation, this could support translation of the *FXVD1* gene. The 5'-UTR region contains the ribosomal binding site and low stability G-quadruplexes at that site can ensure that translation is not perturbed, as it would have been if highly stable G-quadruplexes or secondary structures are formed within that region. Alternatively, under stress conditions such as cell growth, mitosis etc., where cap-dependent translation is compromised at the 5'UTR, G-quadruplex formation can assist initiation of translation of the *FXVD1* gene via cap-independent translation (Bugaut *et al.*, 2012).

4.2 Stability calculations of secondary/tertiary structures

The +VE and Bovine_PLM GQS were both predicted to form highly stable G-quadruplexes by minimum free energy calculations using the Vienna RNA package. Bovine_PLM's G-quadruplex is the minimum free energy (MFE) structure, which is the most stable structure with a free energy of -8.37 kcal/mol in comparison to other secondary structures predicted. The +VE control was predicted to form a very stable G-quadruplex (-12.65 kcal/mol) with a frequency of 1.00 in the structural ensemble. This indicates that the +VE control was a suitable positive control for further studies. Two lower energy state secondary structures were predicted to compete against G-quadruplex formation for Human_PLM. The equilibrium constant of the G-quadruplex formed by the Human_PLM with respect to the two competing structures indicates a significant proportion of G-quadruplex structure present, which may increase upon increasing potassium concentration. Note that the energy model of the Vienna RNA package for G-quadruplex structures did not take the potassium ion concentration into account (Lorenz *et al.*, 2012). The data obtained from minimum free energy calculations suggest that Human_PLM will form a mixture of secondary and G-quadruplex structures.

4.3 Evolutionary conservation of G-rich sequences in *FXVD1* pre-mRNA

The evolutionary trait of G-rich sequences in the *FXVD1* gene was confirmed by the MSA experiment. The alignment of the *H. sapiens* GQS from Table 2, was found conserved among all orthologs except in *M. Domestica* & *S. scrofa* and the consensus sequence obtained has the ability to fold into G-quadruplex. Consensus sequences obtained from Table 7, with the exception of *S. scrofa* can form G-quadruplexes, indicating that G-rich sequences among the orthologs are conserved. The existence of evolutionary conserved GQS based on a pairwise alignment of two sequences has been proposed as a method of validation and emphasis of their functional significance (Menendez, Frees & Bagga, 2012). The presence of G-rich sequences in orthologs points to an evolutionary conservation of that feature, which supports the hypothesis that G-quadruplex formation is a control mechanism of *FXVD1* pre-mRNA processing.

4.4 Alternative splicing

G-quadruplexes have been reported to regulate gene expression *in-vivo* at the translational level via alternative splicing (Gomez *et al.*, 2004; Marcel *et al.*, 2011). The comparative analysis suggests that the G-quadruplex formed in intron 6 of the *H. sapiens'* pre-mRNA could be affecting the splicing pattern of intron 4 in the *FXVD1* pre-mRNA. The analysis suggests that the presence of a G-quadruplex in intron 6 is promoting the full splicing of intron 4. On the other hand the absence or presence of a G-quadruplex of low stability is causing partial splicing of intron 4, which will lead to the production of the variant *FXVD1-*

009. As reviewed by Clancy in 2008, the consensus 5'-GU and 3'-AG are the binding sites for spliceosome sub units, which determine splicing points in introns. The downstream G-quadruplex in intron 6 ensures that the sub unit U2 from the spliceosome complex binds to the most 3'-AG in intron 4 and ensures the latter is fully spliced. The absence or a lowly stable G-quadruplex in intron 6 causes the sub unit U2 to bind to an alternate 3'-AG, rather than the most 3'-AG, resulting in a longer transcript, *FXVD1-009*.

4.5 Laboratory experimental results support G-quadruplex formation

G-quadruplex formation in the +VE, Human_PLM and Bovine_PLM GQS were successfully detected by 30% native PAGE. Under K^+ free condition (Figure 13 A), the +VE control and -VE_A samples migrated almost a similar distance on the gels as they are both 22 bases long. The -VE_B, which is 29 bases long migrates slower than the +VE and -VE_A control sample under K^+ free condition. Under similar conditions, the 29 bases long Human_PLM and 24 bases long Bovine_PLM samples migrated slower than the control samples. The Bovine_PLM sample was expected to migrate faster than the -VE_B sample. Under the non-denaturing conditions used here, samples not only migrate according to their size but also according to their shape. RNA under normal physiological conditions form loops that makes RNA behave like longer molecules on gels in comparison to DNA molecules of same size (Rio, Ares, Hannon & Nilsen, 2010). In lane 3 from Figure 13 A, Human_PLM produced three distinct bands that moved at different rates on the K^+ free gel. It is proposed that the three bands are due to linear RNA and the two secondary structures predicted by minimum free energy calculations. Addition of K^+ (Figures 13 B & C) altered the migration properties of the +VE, Human_PLM and Bovine_PLM. The +VE control migrated fastest, while under K^+ free

condition it has the same mobility as -VE_A. Bovine_PLM also migrated faster than -VE_B, which would seem opposite under K^+ free conditions. Comparing the R_f of similar species under K^+ free and K^+ conditions from Figure 14 supports the fact that the -VE controls did not change structures and rather stayed in their linear conformations. *Intra*-molecular G-quadruplexes are compact in shape and confer high mobility rates in gels in comparison to linear species and *inter*-molecular G-quadruplexes (Williamson, Raghuraman & Cech, 1989; Bryan&Baumann, 2011). The dependence of R_f on the K^+ concentration strongly supports that intramolecular G-quadruplex formed by the +VE control, Human_PLM and Bovine_PLM sequences. The -VE_A sample (lanes 2 in Figure 13) showed in addition to the expected fast migrating band a slow migrating band at high molecular mass in presence of potassium. This can be attributed to the formation of *intermolecular* G-quadruplexes, which is possible in -VE_A. The two stretches of four consecutive guanines in the sequence of -VE_A (CGT**GGGG**AGATT**GGGG**AGCGCA) can participate in the formation of intermolecular G-quadruplexes (Figure 17). At a final oligonucleotide concentration of $3\mu\text{M}$, Moon *et al.*(2007) reported that intermolecular G-quadruplex formation is favoured.

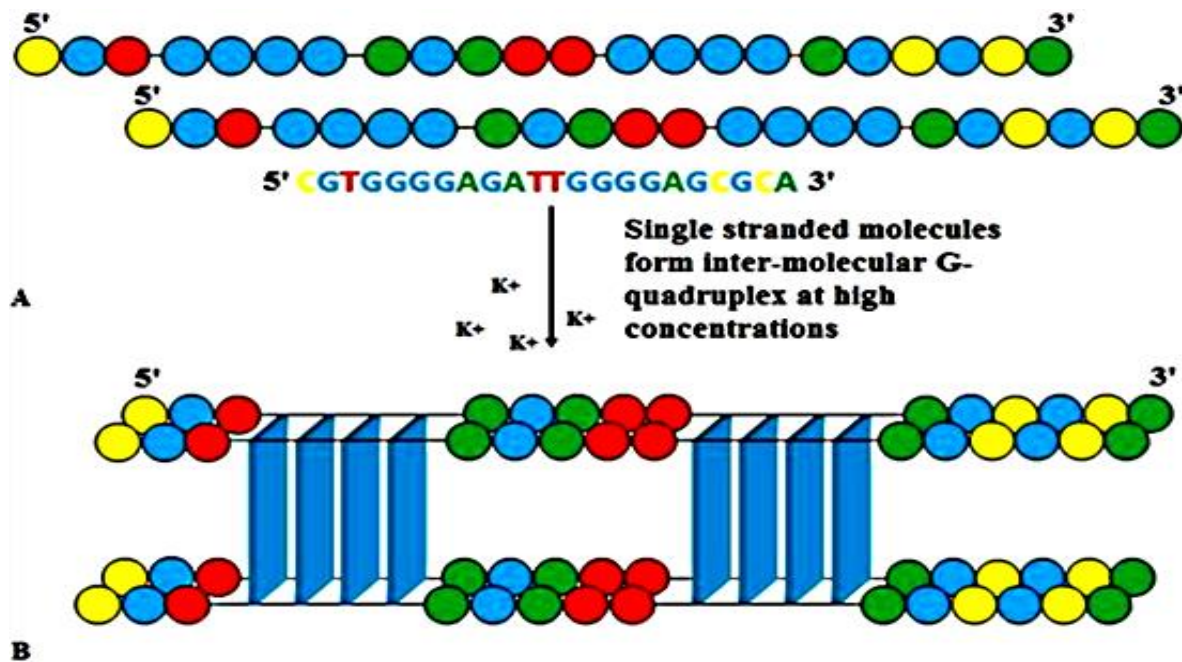


Figure 17: schematic illustration of the *intermolecular* G-quadruplex formed by -VE_A. **A.** single -VE_A species present in high amount, 3 μ M for the Native PAGE experiments, associate to form intermolecular G-quadruplex in the presence of K⁺. Circles represent unpaired bases and are colour coded according to -VE_A's sequence. **B.** Two sets of four consecutive guanines from four separate strands of -VE_A arrange into G-quartets (blue rectangles) to form a tetrameric parallel intermolecular G-quadruplex.

The proposed intermolecular G-quadruplex by -VE_A makes it difficult for the ensemble to move along the gel, resulting in slow migrating bands. In the K⁺ containing gel, the smeared bands of Human_PLM in lanes 4 (Figure 13 B & C) may be explained by the formation of other secondary structures due to Watson-Crick base pairing. The intramolecular G-quadruplex formed by Human_PLM is the fastest migrating structure in comparison to the other structures, as the G-quadruplex is compacter than the other structures proposed in Table 5. Similarly, the smear pattern by Bovine_PLM in the presence of potassium could be due to the formation of secondary structures predicted in Table 5.

Further confirmation of G-quadruplex formation was achieved by exploiting the intrinsic fluorescent properties of nucleic acid. The emission intensities of the +VE, Human_PLM and Bovine_PLM samples in the presence of 0.1 M K^+ was significantly higher compared to K^+ free buffer (Figures 15 A-E). This was due to the formation of G-quadruplexes in these species. G-quadruplex entities have been reported to have increased intrinsic fluorescence emission in contrast to non-G-quadruplex complexes due to the stacking of G-tetrads (Nguyen Thuan *et al.*, 2011; Kwok, Sherlock, & Bevilacqua, 2013). The higher fluorescence intensity of Human_PLM in K^+ free buffer could be due to the presence of other secondary structures as computed by the Vienna RNA package. Nonetheless, the fluorescence intensity in the presence of K^+ was clearly increased, which confirms the formation of G-quadruplexes. The -VE_A sequence showed higher fluorescence intensity in K^+ containing buffer compared to K^+ free buffer most likely due to the formation of *intermolecular* G-quadruplex (Figure 17), as was seen earlier in the native PAGE experiment. The presence of eight potential tetrads supports the high fluorescence intensity of the intermolecular G-quadruplex of -VE_A. Measuring the fluorescence emission spectrum of quinine in the same buffers, indicated that the K^+ containing buffer had a weak quenching effect on fluorescence. Hence, RNA samples in K^+ containing buffer were expected to show slightly less fluorescence than their respective counterparts incubated in K^+ free buffer, if they would assume the same structure. This was observed for the -VE_B control sample, which in the presence of K^+ had slightly reduced fluorescence intensity (Figure 15B).

In conclusion, using a computational scan of the *FXYD1* pre-mRNA potential G-quadruplex forming sequences (GQS) were identified in *Homo sapiens*, *Bos taurus* and other orthologs. Through energy calculations it was established that the G-quadruplex was either the most stable structure or existent in a significant proportion next to secondary structures. The stability of these G-quadruplex structures is likely higher *in vivo* considering the intracellular K^+ concentration of 120-150 mM. Using native PAGE and fluorescence emission spectroscopy the theoretical calculations were confirmed and the existence of G-quadruplex structures established. Multiple sequence alignment of ortholog GQS indicated that the G-quadruplex forming potential may be conserved in evolution, rendering it possible that it may occur *in vivo* as a mechanism to control phospholemman expression levels and ultimately the activity of the cardiac sodium-potassium ATPase.

4.6 Limitations and further work

Overall, the Native PAGE experiments were challenging due to the low molecular mass samples and electrophoresis in the presence of ionic species, which caused heating of the gel due to increased conduction. A high percentage acrylamide gel was used, as lower percentage gels would cause the +VE control's G-quadruplex to migrate faster than the tracking dye. This was observed in 20% and 25% acrylamide gels (data not shown). The heat generated during electrophoresis, mostly in the K^+ containing buffers may interfere with the electrophoresis and affect the migration of the samples. Often the heat caused the glass plate used to encase the gels to break and the gels were discarded. Heat also caused the voltage of the power supply to fluctuate, which also affected the process of electrophoresis.

The heat issue was addressed by using buffers pre-chilled at 4⁰C, which required a longer running time for the gels.

Apart from technical challenges and limitations, a more fundamental limitation is the relevance of the results obtained on short oligonucleotides for the longer pre-mRNA transcript *in vitro* and ultimately the existence of G-quadruplexes of *FXVD1* pre-mRNA *in vivo*. Once the existence of G-quadruplex structures *in vivo* has been established, the functional consequences on phospholemman expression need to be investigated. Therefore, the present study provides the basis for extensive further work in this area.

Further work should investigate the formation of G-quadruplex structures in longer oligonucleotides using gel electrophoresis, NMR, intrinsic fluorescence and fluorescence - resonance energy transfer (FRET). The formation of G-quadruplex should be investigated *in vivo* as previously described (Xu *et al.*, 2010). Single-molecule FRET can also be used to establish the dynamics and stability of the G-quadruplex, as for example in the work by (Okumus & Ha, 2010; Ying, Green, Li, Klenerman, & Balasubramanian, 2003). A modified construct of the Human_PLM sequence containing an acceptor molecule at one of its end can be used, alongside a complementary strand that will be covalently linked to a glass surface and also modified to contain a donor molecule. Hybridisation of the Human_PLM oligo to the complementary oligo, followed by the formation of a G-quadruplex will allow energy exchange between the donor and acceptor molecule and this can be detected by using Total Internal Reflection Microscopy (TIRM).

Alternative splicing of intron 4 of *FXYD1* has been linked to *FXYD1*-009 formation. G-quadruplexes have been reported in the past to influence splicing (Marcel *et al.*, 2011, Gomez *et al.*, 2004). Could G-quadruplex formation be the influential factor behind variant 009? Further work, similar to Marcel *et al.*, (2011), should address the consequences of G-quadruplex structure on the splicing of pre-mRNA. This can be addressed with constructs using the reporter gene Green Fluorescence Protein (GFP). A suitable construct would include encode an *FXYD1*-GFP fusion protein, while a stop codon is included in the particular intron under investigation. Alternatively the expression levels of mature mRNA species could be measured with quantitative PCR techniques.

5. REFERENCES

- Adrian, M., Heddi, B., & Anh Tuan, P. (2012). NMR spectroscopy of G-quadruplexes. *Methods*, 57(1), 11-24.
- Beaudoin, J. D., & Perreault, J. P. (2010). 5'-UTR G-quadruplex structures acting as translational repressors. *Nucleic Acids Research*, 38(20), 7022-7036.
- Beevers, A. J., & Kukol, A. (2006). Secondary structure, orientation, and oligomerization of phospholemman, a cardiac transmembrane protein. *Protein Science*, 15(5), 1127-1132.
- Beevers, A. J., & Kukol, A. (2007). Phospholemman transmembrane structure reveals potential interactions with Na⁺/K⁺-ATPase. *Journal of Biological Chemistry*, 282(45), 32742-32748.
- Biffi, G., Tannahill, D., McCafferty, J., & Balasubramanian, S. (2013). Quantitative visualization of DNA G-quadruplex structures in human cells. *Nature Chemistry*, 5(3), 182-186.
- Bossuyt, J., Despa, S., Martin, J. L., & Bers, D. M. (2006). Phospholemman phosphorylation alters its fluorescence resonance energy transfer with the Na/K-ATPase pump. *Journal of Biological Chemistry*, 281(43), 32765-32773.
- Bryan, T. M., & Baumann, P. (2011). G-Quadruplexes: From Guanine Gels to Chemotherapeutics. *Molecular Biotechnology*, 49(2), 198-208.
- Bugaut, A., & Balasubramanian, S. (2012). 5' UTR RNA G-quadruplexes: translation regulation and targeting. *Nucleic Acids Research*, 40(11), 4727-4741.
- Chang, T.-C., & Chang, C.-C. (2010). Detection of G-quadruplexes in cells and investigation of G-quadruplex structure of d(T2AG3)₄ in K⁺ solution by a carbazole derivative: BMVC. *Methods in molecular biology (Clifton, N.J.)*, 608, 183-206.
- Clancy, S. (2008) RNA splicing: introns, exons and spliceosome. *Nature Education* 1(1):31
- Crambert, G., Fuzesi, M., Garty, H., Karlsh, S., & Geering, K. (2002). Phospholemman (FX_YD1) associates with Na,K-ATPase and regulates its transport properties. *Proceedings of the National Academy of Sciences of the United States of America*, 99(17), 11476-11481.
- da Silva, M. W. (2007). NMR methods for studying quadruplex nucleic acids. *Methods*, 43(4), 264-277.
- Daehnel, K., Harris, R., Maddera, L., & Silverman, P. (2005). Fluorescence assays for F-pill and their application. *Microbiology-Sgm*, 151, 3541-3548.
- Du, Z., Zhao, Y. Q., & Li, N. (2008). Genome-wide analysis reveals regulatory role of G4 DNA in gene transcription. *Genome Research*, 18(2), 233-241.
- Ensembl.(2012).Chromosome 19:35,629,728-35,634,013.Retrieved November 38, 2012, fromhttp://www.ensembl.org/Homo_sapiens/Location/View?g=ENSG00000221857;r=19:35629728-35634013
- Ensembl.(2012). FX_YD1. Retrieved Novmber 26 2012, from http://www.ensembl.org/Multi/Search/Results?q=FX_YD1;y=0;site=ensembl_all;x=0;page=1;fall_species=1#
- Fuller, W., Howie, J., McLatchie, L. M., Weber, R. J., Hastie, C. J., Burness, K., . . . Shattock, M. J. (2009). FX_YD1 phosphorylation in vitro and in adult rat cardiac myocytes: threonine 69 is a novel substrate for protein kinase C. *American Journal of Physiology-Cell Physiology*, 296(6), C1346-C1355.

- Gomez, D., Lemarteleur, T., Lacroix, L., Mailliet, P., Mergny, J. L., & Riou, J. F. (2004). Telomerase downregulation induced by the G-quadruplex ligand 12459 in A549 cells is mediated by hTERT RNA alternative splicing. *Nucleic Acids Research*, 32(1), 371-379.
- Goncalves, D. P. N., Ladame, S., Balasubramanian, S., & Sanders, J. K. M. (2006). Synthesis and G-quadruplex binding studies of new 4-N-methylpyridinium porphyrins. *Organic & Biomolecular Chemistry*, 4(17), 3337-3342.
- Gray, N.K., & Hentze, M. W. (1994). Iron regulatory protein prevents binding of the 43S translation pre-initiation complex to ferritin and eALAS mRNAs. *EMBO J*, 13, 3882-3891
- Gu, H.-P., Lin, S., Xu, M., Yu, H.-Y., Du, X.-J., Zhang, Y.-Y., . . . Gao, W. (2012). Up-Regulating Relaxin Expression by G-Quadruplex Interactive Ligand to Achieve Antifibrotic Action. *Endocrinology*, 153(8), 3692-3700.
- Han, F., Bossuyt, J., Despa, S., Tucker, A. L., & Bers, D. M. (2006). Phospholemman phosphorylation mediates the protein kinase C-dependent effects on Na⁺/K⁺ pump function in cardiac myocytes. *Circulation Research*, 99(12), 1376-1383.
- Hong, Y., Haeussler, M., Lam, J. W. Y., Li, Z., Sin, K. K., Dong, Y., . . . Tang, B. Z. (2008). Label-free fluorescent probing of G-quadruplex formation and real-time monitoring of DNA folding by a quaternized tetraphenylethene salt with aggregation-induced emission characteristics. *Chemistry-a European Journal*, 14(21), 6428-6437.
- Huppert, J. L., Bugaut, A., Kumari, S., & Balasubramanian, S. (2008). G-quadruplexes: the beginning and end of UTRs. *Nucleic Acids Research*, 36(19).
- Johnson, J. E., Cao, K., Ryvkin, P., Wang, L.-S., & Johnson, F. B. (2010). Altered gene expression in the Werner and Bloom syndromes is associated with sequences having G-quadruplex forming potential. *Nucleic Acids Research*, 38(4).
- Kan, Z. Y., Yao, Y. A., Wang, P., Li, X. H., Hao, Y. H., & Tan, Z. (2006). Molecular crowding induces telomere G-quadruplex formation under salt-deficient conditions and enhances its competition with duplex formation. *Angewandte Chemie-International Edition*, 45(10), 1629-1632.
- Kikin, O., D'Antonio, L., & Bagga, P. S. (2006). QGRS Mapper: a web-based server for predicting G-quadruplexes in nucleotide sequences. *Nucleic Acids Research*, 34, W676-W682.
- Kostadinov, R., Malhotra, N., Viotti, M., Shine, R., D'Antonio, L., & Bagga, P. (2006). GRADB: a database of quadruplex forming G-rich sequences in alternatively processed mammalian pre-mRNA sequences. *Nucleic Acids Research*, 34, D119-D124.
- Kumari, S., Bugaut, A., Huppert, J. L., & Balasubramanian, S. (2007). An RNA G-quadruplex in the 5' UTR of the NRAS proto-oncogene modulates translation. *Nature Chemical Biology*, 3(4), 218-221.
- Kwok, C. K., Sherlock, M. E., & Bevilacqua, P. C. (2013). Effect of Loop Sequence and Loop Length on the Intrinsic Fluorescence of G-Quadruplexes. *Biochemistry*, 52(18), 3019-3021.
- Lech, C. J., Heddi, B., & Anh Tuan, P. (2013). Guanine base stacking in G-quadruplex nucleic acids. *Nucleic Acids Research*, 41(3), 2034-2046.
- Li, Q., Xiang, J.-F., Zhang, H., & Tang, Y.-L. (2012). Searching Drug-Like Anti-cancer Compound(s) Based on G-Quadruplex Ligands. *Current Pharmaceutical Design*, 18(14), 1973-1983.

- Lim, K. W., Alberti, P., Guedin, A., Lacroix, L., Riou, J.-F., Royle, N. J., . . . Phan, A. T. (2009). Sequence variant (CTAGGG)(n) in the human telomere favors a G-quadruplex structure containing a G center dot C center dot G center dot C tetrad. *Nucleic Acids Research*, *37*(18), 6239-6248.
- Lin, J., Yan, Y. Y., Ou, T. M., Tan, J. H., Huang, S. L., Li, D., . . . Gu, L. Q. (2010). Effective Detection and Separation Method for G-Quadruplex DNA Based on Its Specific Precipitation with Mg²⁺. *Biomacromolecules*, *11*(12), 3384-3389.
- Liu, W., Zhu, H., Zheng, B., Cheng, S., Fu, Y., Li, W., . . . Liang, H. (2012). Kinetics and mechanism of G-quadruplex formation and conformational switch in a G-quadruplex of PS2.M induced by Pb²⁺. *Nucleic Acids Research*, *40*(9), 4229-4236.
- Long, X., Parks, J. W., Bagshaw, C. R., & Stone, M. D. (2013). Mechanical unfolding of human telomere G-quadruplex DNA probed by integrated fluorescence and magnetic tweezers spectroscopy. *Nucleic Acids Research*, *41*(4), 2746-2755.
- Lorenz, R., Bernhart, S. H., Siederdisen, C. H. Z., Tafer, H., Flamm, C., Stadler, P. F., & Hofacker, I. L. (2011). ViennaRNA Package 2.0. *Algorithms for Molecular Biology*, *6*.
- Marcel, V., Tran, P. L. T., Sagne, C., Martel-Planche, G., Vaslin, L., Teulade-Fichou, M.-P., . . . Van Dyck, E. (2011). G-quadruplex structures in TP53 intron 3: role in alternative splicing and in production of p53 mRNA isoforms. *Carcinogenesis*, *32*(3).
- McCaskill, J. S. (1990). The equilibrium partition-function and base pair binding probabilities for rna secondary structure. *Biopolymers*, *29*(6-7), 1105-1119.
- Menendez, C., Frees, S., & Bagga, P. S. (2012). QGRS-H Predictor: a web server for predicting homologous quadruplex forming G-rich sequence motifs in nucleotide sequences. *Nucleic Acids Research*, *40*(W1), W96-W103.
- Mergny, J.-L., & Lacroix, L. (2009). UV Melting of G-Quadruplexes. *Current protocols in nucleic acid chemistry / edited by Serge L. Beaucage ... [et al.]*, Chapter 17, Unit 17.11-Unit 17.11.
- Moon, I. K., & Jarstfer, M. B. (2007). The human telomere and its relationship to human disease, therapy, and tissue engineering. *Frontiers in Bioscience*, *12*. doi: 10.2741/2412
- Moon, I. K., & Jarstfer, M. B. (2010). Preparation of G-quartet structures and detection by native gel electrophoresis. *Methods in molecular biology (Clifton, N.J.)*, *608*, 51-63.
- Morth, J. P., Pedersen, B. P., Toustrup-Jensen, M. S., Sorensen, T. L. M., Petersen, J., Andersen, J. P., . . . Nissen, P. (2007). Crystal structure of the sodium-potassium pump. *Nature*, *450*(7172), 1043-U1046.
- Musetti, C., Krapcho, A. P., Palumbo, M., & Sissi, C. (2013). Effect of G-Quadruplex Polymorphism on the Recognition of Telomeric DNA by a Metal Complex. *Plos One*, *8*(3).
- National Center for Biotechnology Information.(2014). Homo sapiens chromosome 19, GRCh38 Primary Assembly. Retrieved April 14 2014 from <http://www.ncbi.nlm.nih.gov/projects/sviewer>
- Nguyen Thuan, D., Haselsberger, R., Michel-Beyerle, M.-E., & Anh Tuan, P. (2011). Following G-quadruplex formation by its intrinsic fluorescence. *Febs Letters*, *585*(24), 3969-3977.
- Okumus, B., & Ha, T. (2010). Real-time observation of G-quadruplex dynamics using single-molecule FRET microscopy. *Methods in molecular biology (Clifton, N.J.)*, *608*, 81-96.

- Onyshchenko, M. I., Gaynutdinov, T. I., Englund, E. A., Appella, D. H., Neumann, R. D., & Panyutin, I. G. (2009). Stabilization of G-quadruplex in the BCL2 promoter region in double-stranded DNA by invading short PNAs. *Nucleic Acids Research*, *37*(22).
- Ou, T.-M., Lu, Y.-J., Zhang, C., Huang, Z.-S., Wang, X.-D., Tan, J.-H., . . . Gu, L.-Q. (2007). Stabilization of G-quadruplex DNA and down-regulation of oncogene c-myc by quindoline derivatives. *Journal of Medicinal Chemistry*, *50*(7), 1465-1474.
- Palacky, J., Vorlickova, M., Kejnovska, I., & Mojzes, P. (2013). Polymorphism of human telomeric quadruplex structure controlled by DNA concentration: a Raman study. *Nucleic Acids Research*, *41*(2), 1005-1016.
- Pandey, S., Agarwala, P., & Maiti, S. (2013). Effect of Loops and G-Quartets on the Stability of RNA G-Quadruplexes. *Journal of Physical Chemistry B*, *117*(23), 6896-6905.
- Paramasivan, S., Rujan, I., & Bolton, P. H. (2007). Circular dichroism of quadruplex DNAs: Applications to structure, cation effects and ligand binding. *Methods*, *43*(4), 324-331.
- Parham, W. A., Mehdirad, A. A., Biermann, K. M., & Fredman, C. S. (2006). Hyperkalemia revisited. *Texas Heart Institute Journal*, *33*(1), 40-47.
- Phong Lan Thao, T., Mergny, J.-L., & Alberti, P. (2011). Stability of telomeric G-quadruplexes. *Nucleic Acids Research*, *39*(8), 3282-3294.
- Presti, C. F., Jones, L. R., & Lindemann, J. P. (1985). Isoproterenol-induced phosphorylation of a 15-kilodalton sarcolemmal protein in intact myocardium. *Journal of Biological Chemistry*, *260*(6), 3860-3867.
- Randazzo, A., Spada, G. P., & da Silva, M. W. (2013). Circular Dichroism of Quadruplex Structures. *Quadruplex Nucleic Acids*, *330*, 67-86.
- Redman, J. E. (2007). Surface plasmon resonance for probing quadruplex folding and interactions with proteins and small molecules. *Methods*, *43*(4), 302-312.
- Rio, D. C., Ares, M., Jr., Hannon, G. J., & Nilsen, T. W. (2010). Nondenaturing agarose gel electrophoresis of RNA. *Cold Spring Harbor protocols*, *2010*(6), pdb.prot5445-pdb.prot5445.
- Rogers, J., & Wall, R. (1980). A mechanism for rna splicing. *Proceedings of the National Academy of Sciences of the United States of America-Biological Sciences*, *77*(4), 1877-1879
- RSCB PDB. (2012). Structure of an intramolecular G-quadruplex containing a G.C.G.C tetrad formed by human telomeric variant CTAGGG repeats. Retrieved November 28, 2012, from <http://www.rcsb.org/pdb/explore/explore.do?structureId=2km3>
- RSCB PDB. (2012). Structure of the Na,K-ATPase regulatory protein *FXVD1* in micelles. Retrieved November 30, 2012, from <http://www.rcsb.org/pdb/explore/explore.do?structureId=2JO1>
- Rubis, B., Kaczmarek, M., Szymanowska, N., Galezowska, E., Czyrski, A., Juskowiak, B., . . . Rybczynska, M. (2009). The biological activity of G-quadruplex DNA binding papaverine-derived ligand in breast cancer cells. *Investigational New Drugs*, *27*(4), 289-296.
- Samatanga, B., Dominguez, C., Jelesarov, I., & Allain, F.H.-T. (2013). The high kinetic stability of a G-quadruplex limits hnRNP F qRRM3 binding to G-tract RNA. *Nucleic Acids Research*, *41*(4), 2505-2516
- Scaria, V., Hariharan, M., Arora, A., & Maiti, S. (2006). Quadfinder: server for identification and analysis of quadruplex-forming motifs in nucleotide sequences. *Nucleic Acids Research*, *34*, W683-W685.

- Shay, J. W., Zou, Y., Hiyama, E., & Wright, W. E. (2001). Telomerase and cancer. *Human Molecular Genetics*, 10(7), 677-685.
- Shapiro, M. B., & Senapathy, P. (1987). Rna splice junctions of different classes of eukaryotes - sequence statistics and functional implications in gene-expression. *Nucleic Acids Research*, 15(17), 7155-7174
- Shinoda, T., Ogawa, H., Cornelius, F., & Toyoshima, C. (2009). Crystal structure of the sodium-potassium pump at 2.4 angstrom resolution. *Nature*, 459(7245), 446-U167.
- Siddiqui-Jain, A., Grand, C. L., Bearss, D. J., & Hurley, L. H. (2002). Direct evidence for a G-quadruplex in a promoter region and its targeting with a small molecule to repress c-MYC transcription. *Proceedings of the National Academy of Sciences of the United States of America*, 99(18), 11593-11598.
- Song, Q., Pallikkuth, S., Bossuyt, J., Bers, D. M., & Robia, S. L. (2011). Phosphomimetic Mutations Enhance Oligomerization of Phospholemmann and Modulate Its Interaction with the Na/K-ATPase. *Journal of Biological Chemistry*, 286(11), 9120-9126.
- Stegle, O., Payet, L., Mergny, J.-L., MacKay, D. J. C., & Huppert, J. L. (2009). Predicting and understanding the stability of G-quadruplexes. *Bioinformatics*, 25(12), 1374-1382.
- Sun, H., Li, X., Li, Y., Fan, L., & Kraatz, H.-B. (2013). A novel colorimetric potassium sensor based on the substitution of lead from G-quadruplex. *Analyst*, 138(3), 856-862.
- Teriete, P., Franzin, C. M., Choi, J., & Marassi, F. M. (2007). Structure of the Na,K-ATPase regulatory protein *FXYD1* in Micelles. *Biochemistry*, 46(23), 6774-6783.
- Thandroyen, F. T., Morris, A. C., Hagler, H. K., Ziman, B., Pai, L., Willerson, J. T., & Buja, L. M. (1991). Intracellular calcium transients and arrhythmia in isolated heart-cells. *Circulation Research*, 69(3), 810-819.
- Tluckova, K., Marusic, M., Tothova, P., Bauer, L., Sket, P., Plavec, J., & Viglasky, V. (2013). Human papillomavirus g-quadruplexes. *Biochemistry*, 52(41), 7207-7216.
- Tseng, T.-Y., Chien, C.-H., Chu, J.-F., Huang, W.-C., Lin, M.-Y., Chang, C.-C., & Chang, T.-C. (2013). Fluorescent probe for visualizing guanine-quadruplex DNA by fluorescence lifetime imaging microscopy. *Journal of biomedical optics*, 18(10), 101309-101309.
- van der Velden, A. W., & Thomas, A. A. M. (1999). The role of the 5' untranslated region of an mRNA in translation regulation during development. *International Journal of Biochemistry & Cell Biology*, 31(1), 87-106.
- Viglasky, V., Bauer, L., Tluckova, K., & Javorsky, P. (2010). Evaluation of human telomeric g-quadruplexes: the influence of overhanging sequences on quadruplex stability and folding. *Journal of nucleic acids*, 2010.
- Vummidi, B. R., Alzeer, J., & Luedtke, N. W. (2013). Fluorescent Probes for G-Quadruplex Structures. *Chembiochem*, 14(5), 540-558.
- Williamson, J. R., Raghuraman, M. K., & Cech, T. R. (1989). Mono-valent cation induced structure of telomeric dna - the g-quartet model. *Cell*, 59(5), 871-880.
- Wilson, K. S., & Vonhippel, P. H. (1995). Transcription termination at intrinsic terminators - the role of the rna hairpin. *Proceedings of the National Academy of Sciences of the United States of America*, 92(19).
- Wong, H. M., Payet, L., & Huppert, J. L. (2009). Function and targeting of G-quadruplexes. *Current Opinion in Molecular Therapeutics*, 11(2), 146-155.
- Wong, H. M., Stegle, O., Rodgers, S., & Huppert, J. L. (2010). A toolbox for predicting g-quadruplex formation and stability. *Journal of nucleic acids*, 2010.

- Wong, W. C., Zhuang, J. Y., Ng, S. L. L., New, L. L. L., Hiew, S., Guo, J. J., . . . Li, T. H. (2010). Conformational organizations of G-quadruplexes composed of d(G(4)T(n))(3)G(4). *Bioorganic & Medicinal Chemistry Letters*, 20(15), 4689-4692.
- Wu, Y., & Brosh, R. M., Jr. (2010). G-quadruplex nucleic acids and human disease. *Febs Journal*, 277(17), 3470-3488.
- Wuchty, S., Fontana, W., Hofacker, I. L., & Schuster, P. (1999). Complete suboptimal folding of RNA and the stability of secondary structures. *Biopolymers*, 49(2), 145-165.
- Xu, L., Xu, Z., Shang, Y., Feng, S., & Zhou, X. (2012). Structural polymorphism of human telomere G-quadruplex induced by a pyridyl carboxamide molecule. *Bioorganic & Medicinal Chemistry Letters*, 22(8), 2988-2992.
- Xu, Y., Suzuki, Y., Ito, K., & Komiyama, M. (2010). Telomeric repeat-containing RNA structure in living cells. *Proceedings of the National Academy of Sciences of the United States of America*, 107(33), 14579-14584.
- Yan, Y.-Y., Lin, J., Ou, T.-M., Tan, J.-H., Li, D., Gu, L.-Q., & Huang, Z.-S. (2010). Selective recognition of oncogene promoter G-quadruplexes by Mg²⁺. *Biochemical and Biophysical Research Communications*, 402(4), 614-618.
- Ying, L. M., Green, J. J., Li, H. T., Klenerman, D., & Balasubramanian, S. (2003). Studies on the structure and dynamics of the human telomeric G quadruplex by single-molecule fluorescence resonance energy transfer. *Proceedings of the National Academy of Sciences of the United States of America*, 100(25), 14629-14634.
- Yuan, G., Zhang, Q., Zhou, J., & Li, H. (2011). Mass Spectrometry of G-quadruplex DNA: formation, recognition, property, conversion, and conformation. *Mass Spectrometry Reviews*, 30(6), 1121-1142.
- Yuan, L., Tian, T., Chen, Y., Yan, S., Xing, X., Zhang, Z., . . . Zhou, X. (2013). Existence of G-quadruplex structures in promoter region of oncogenes confirmed by G-quadruplex DNA cross-linking strategy. *Scientific Reports*, 3.
- Zhang, C., Liu, H.-h., Zheng, K.-w., Hao, Y.-h., & Tan, Z. (2013). DNA G-quadruplex formation in response to remote downstream transcription activity: long-range sensing and signal transducing in DNA double helix. *Nucleic Acids Research*, 41(14), 7144-7152.
- Zhou, Z., Zhu, J., Zhang, L., Du, Y., Dong, S., & Wang, E. (2013). G-quadruplex-Based Fluorescent Assay of S1 Nuclease Activity and K⁺. *Analytical Chemistry*, 85(4), 2431-2435.
- Zhu, H., Xiao, S., & Liang, H. (2013). Structural Dynamics of Human Telomeric G-Quadruplex Loops Studied by Molecular Dynamics Simulations. *Plos One*, 8(8).
- Zuker, M., & Stiegler, P. (1981). Optimal computer folding of large rna sequences using thermodynamics and auxiliary information. *Nucleic Acids Research*, 9(1), 133-148.

APPENDIX I

GQS mapping from Table 2 and conserved sequence from Table 6 in the *FXYD1* pre-mRNA of each ortholog

Alternate exon sequences are represented in uppercase characters, where purple characters are UTR sequence bases and black characters represent translated sequence. Intron sequences are denoted by lowercase blue characters. The highest scoring GQS from Table 2 are underlined, while conserved sequences from Table 6 are highlighted yellow to map their position in the gene for each organism.

Key: UTR region
Intronic sequence
Exonic translated sequence

Mus musculus

GGGUGGAGCAUCCAGUUCUGGGCCAGGGGUCCAAGUGCUUAGCUCCUAGGGUGCACAGCU
GGACAUUUGGGGGUCUUCUGUCAACAGGGGACAGCGUGAAUGGGgugagcguccccagccc
ucccuccgggccccucagcuccccuagcugggaggccuauuuugggaacaagaguggccagc
cuguggcuucucagggcaggccugacccaagagggaggagagaguguggggacagggguugca
caggggcgggagaguagagacuccuccuuuuucagcggccacugcgcagaccccuggcagg
gggugaggcucagauacucauuuguauaggucuguuucugucucuguuuggggggcacagaa
ggcccagagcgagagaauugucuaaugucuaaaccucgpcucucuaaucaacaguugggg
agaggguguuuguuugcuccuguuccagcuacaccacucuguguguguguguguaccuguac
auaaaugugucugugcccguaugugugucccugaaaacaacaucugacuucucucagggcaugg
gccgccugucacucacuggccuaaagucuuuguugugaaagaugucacccagagguggacaaa
gagaggganguuccccuuuucucacagcuucaagaaaaggagaugggguggccuguagggga
uguggcuccuggcugggcccaccccagcaguguuauacaggaccccugagucuuuggggg
gggagcuguugccauggguggcccugugcagcaaaauccuccgggugaagugggagauuu
uauaccaggggucagggagagagcgggcaggcggccgagggcaggagagcugggacggccug
gguacagagagaccacugguugagguguguaggggcagguggggcugggcauguccugcugu
augucgccuaguguuuccaccuauuguccagaggcagcuugcuucccuacaagguagguuu
ugagacucugggaccagcuaacggauugggaguagccugugggagccaccccacccccagg
acucugccucucccaucugucuuugcugcuguguaugcuguggucuccugguccuauuuuu
gaguuguuuuagggacaugguuuugggugaagcaaggagccauucaacuugaauggcugac
acuuaaguccuuaggccguccuugacuuaaccccacggguucagAUCCUCUUUAGGAGGGAA
AGAGAGCAGGGCAGAGGACAUUUCUUGACCCUGGCUGACUCCUAGGGCAAUGGCAUCUCCC

Canis lupus familiaris

GGGAGGGGAGACCGCUGAGGGCGGCGCAGGACCAGCUCUGGAACAGGGGGUCCAAAGUGCUC
ACCCCGGCACAGCCGGACGUUUGGGGGCCUUCUUUCAGCAGGGGACAGCCUGACUGGGgug
agcguccccugcccuccccccagggccucaccccuggccuggccacgccaccuauuuuggga
gcaggaguggccagcccguggcuucccagggcaggccagacccaagaggaagggagugugguu
gggacggccguggggguucccagggagccgagugugggugcgacucccccucccugcugcug
cgugugcaggcugggguggguuuugagcacugauguguguaggucggguggcgucacuuuug
gggggacuggaggcucagaugaagaguaucguuuuagugacugugucuccacccaugucu
ugcucaaaccagagguuuggggaguaggcgugucuccauuccagccccauugcguaugugu
gugugucugugugucugugugucugugugucuccuggccuggcaucugucuccgucucu
cagccccgcugcucugggcucaugccacucgcccuggguguccgcccugugagagauguca
cccagaggcaggcggaggggauguuuuccuuguucuaacaauuccagaagagaaggggggu
ggccuuucccccaggggacgcccuguaagcgauguggcagccgggcccucaccccggcagaguug
ugcgugacccccgagugggggaaggaaggcuguugccaugguggccugugugaggcaauuc
cuccagggugaagugggagauuuuauaccggggucaggagagagccggccagcggccgag
gccaggggagccgggauuuacacggacacagcgaggcccugugugugggaggguggcccu
gggcgugucuuugggucgagugucgcucaccccucacggcgugcgucugucucccaccugg
uggggugagccauccugcucuccacgggguaaggugugggaaccugggggcccgcugucagg
aggcccaggccuugggagcccccggugggucugugugugucucaccccugcccucgcugugug
ucguaccacccccacggugguuuguuuggggacaccguguccacaugaagcaguggccaag
cuggaugaugggugcuuuuggaauuaagcccuggacucugauuuuaccccuuggguucaag
ccccauuggugagggagacgaggaacacauuucugaccuugcugcucccagGACGAUGG
CACCUCUCCACCACAUCUUGGUUCUCUGUGUGGGUUUCCUCACCAUGGCCACCGCAGgugag
ucuagggcgguagcccacaaccaccucagcccacaggggaggccagggaggggaaagcccu
ucaagagaaccaacuuggagacuccaaccuccaccagucaguugggguaaccaggaaacugg
ggacuucgcguggggcccaaaccagcuaguauuuggggcaggggagcggaucaaggucag
gcaaaggcggauuggggauggaggccucuaaccucaaauagacagaaucauugacaacaggg
gauaagacaggaagcgggggaguuaggagccccugccccaccagcacagggcagaugag
gcggcuaaggccaggggagggugggagccugcucagggcccagcggucgcgagacucucag
cccacgggaguaaagccccagagggucucuuuacgcccucccugugcagaguccaggaa
gcagccaaccucugacuuccuucucuuuccagAAGCGCCACAGGAACACGACCCGUUCACCU
ACGgugaggggagggagaggcaucucaggggagccgggagggcgcauggccuaggugugccc
guccuguccucauaccucucucuccuuguccaccugucucucgggucggguguuuguauc
ucggucacucuccggucucucgcgucucucagagaucuggcucucugacucccuguuuugau
cugcccucugucugugucucugugugucugucuaucuggucccucucugagucucuuuccu
gucaccucugcguaucuauggcuauccucugcugugccucccucucucccucugcgguc
cccucaccucuccaccauccucucuaucuccuuguuuccugccuccucccccgccugcccu
gcccaccuccuccucuccuucgcaaccocgcuugaucuccucccugaucccgcucccauu
ccuccuuacaccguucuccucuccccucccggguccuccucgccccuccuccuccuccuucc
uccucccucccugcccucacccuccucccugccgcccacagACUACCAAUCCUGCGGAUC
GGAGGCCUCAUCAUCGCCGGGAUCCUCUUCAUCCUCGGUAUCCUCAUCGUCCUGAgugagua
ccccagccccugccuccagccccgcgggugccguggugcgugcccggccucgcccgggg
ucuccgccccgccccgcccucgccccgccccgcccgcuuagccccgcccacgucccgccc
ugccgcccucgccccaccccugccaccccagccccgccccuccgcccucgccccgcccacgccc
ccugccgccccgcccuaagccccgcccuccgccccgcccuaagccccgcccuccgccccgccc
ccgccccgccccgcccuccgcccucgccccgcccuaaccuccgcccucuccgccccucccag
cccaggcggcucaccagcgcgcucggugcccgcccggagcugaaucccggccuccuccua
ccccacccgcagGCAGAAGGUGCCGGUGCAAUUCAACCAGCAGCAGAGguaagaggcccc
uccgggucucacucaccuacuucgcucuaagaggggcgucgggggugaggcagggauc
caccagaccgcagccggagcccuuccgcaaaauguaauaagcccuacuauugugucca

cccgaucucccaucagcgcgacuauguauuaagcaccuacuaugugccauggcccaagccuggcc
cugggaccaagcgaggaaaaaccucccgccuuccuggccgagcuccagccuaguggagg
cgguggccguggguuccaacagccccacagauagaaaaucacaaagcgugauaacacaaag
ugcaggaaagaagaaacggcggugaaaugagaucaucucacacgcggcccaguuuagcuuag
agucuuguuccuagcucuugauuccucucgaauaaaauguuaaagcauggacaanguaug
aauauguuagaacaauuauagauauuaucuaaaguaguagcuaauuuuacuggguguguac
cacgugucagauacgguuucacuuccucugggagggaggugcuguuauuaaccccuuugac
agaugaggaaacuaaggcacagggagguaaagucacuuguucaagaucacucaaguagaag
augggggguucuggguuccaaccaggccaucucauggcagucugccaaguccccaugacu
auccuccccuaccaacuacauccucgccccaaauccgcgaggguacucacuguaaacc
agcucagaagccccugccagcacagaagcugcuccugggugcuccuauuucuaagcggacc
ccgagccugcucuucguccauaucugggccuaguuaacaccaaucugggaaaggaggcuugua
cugggggguuccuagaagggcagccucuccccuuuccaucccgaaaucccucugccucugu
cuucccagGACUGGGGAACCCGACGAAGAGGAGGGAACUUUCCGCAGCUCCAUCGCGCguga
gucuggggagacugcggguauuuuugggagagggcugguuccaaggacccuuuuccuggcc
cucccuggcugcguagaggggaagggcuggaucugaaagcggagggcggggaguugccccgcc
gccccccaccugcccaggaacuggggauGCCucuccagaaugacccccgaucuccguguu
ccccccagGUCUGUCCACCCGCAGGCGGUAGAAACACCUGGAGCGAUGGAAUCGGCCAGgu
gcugcagcucugacacggcggugggaggggaaggaggagggaaggaaaggcgggagagggagg
ggccaagugccagggguugaagggcggcggagggguggggcuggacguccccccucgccucuc
accuuuucaccucacagGACUCCCUGGCACCUGACAUCUCCCACGCUCCACCUGCGCGC
CCACCGCCCCUCCGCCGCCCUUCCCCAGCCUGCCCCUGCAGACUCCCCUGCCGCCAG
ACUUCCAAUAAAACGUGCGUUCUCUCGACAGCACUUUGUCGGUCUCGGUCCUCAGCGCGA
AAGCCCAGCGCCACUGGGCCCCAGCA

Bos taurus

GGAGACCGCUGAGGGCAGCGCAGCCAGCUCUGGGCCAGGGGUGCAAAGUGCUCGGCCCCGG
GGCACAGCCGGACGUUUGGGGGCCUUCUUUCGGCAGGGGACAGUCUGACUGGGgugagcguc
ccccgccccuccuccagggccucaccccugnnnnnnnnnnnnnnnnnnnnnnnnnnnnnnnnnn
nn
nn
nn
nn
nnnnnnnnnaaagaugucacccagagggcagggcaggggauguuuuccugucucacugcuu
ccagaagaggagaaggggugggccuuuccacgggggagcugggggcagugggcagccag
ccucaccccgggagggguugugcaugaccccacaguggggggaggaaggcuguugccauggu
ggccugugcgaggcaaaauuccuccaggggugaagugggagauuuuauaccagggucaggca
gagagcgggcccagcggccgagggcagggagagcgggcuauuacggacacagcaaggccgugg
ugugugggagggggccuugggcccugggcugucucgucccuggcagugucugucucu
ccaccugggguggggugagggcaucugcucucccugccaggggagggggaaccuggggg
cuacagugagggaggccccggccugcgggagauccuugugggucugugugugccucaccccgu
ccuugcugcugggugaccucuuuguguggguuguuugggagcgcuguuuccugaugaagc
agggggcgccucuguuucucaggggagaccagccggaugauagaugcuuuuggaauaaguc
ccuggacugucucugacuuaaccgcuuggguucagggcccagugggggagacugagggcac
gcauuuccugaccuuugguauuccccagGACAUGGCAUCUCUCAGCCACAUCUUGGUUCU
UGUGUGGGUCUCUUGCCAUGGUCAACGCAGgugagucugggggaggcagcccacuaccacc
ucagcccaggggugguaaggguaagggaaaauucugcaagagaaacaagcuggagccucca
gucugaacugagucucaguggggucucaugugggguccagucacaggcugguauucuggggga
ggggagagggaugccccaggucgggcaaagggggagggugggauggaggccggcuucccguga
augauggaucacagacaaccuggaagagauggagagcugaggcugucaggugccuccugc
cccauuccggacagugcagagaggcagccaagaccagagaggggugggagccuacucagag
uccaacaguccccagacuccugccccgagacuguaaaacuccacagggucugugaugccg
cucucuguccaggguccaggaagcauccaaccugauuuucucucucuuuccagAAGCAC
CACAGGAACACGACCCAUCACCUACGGgugagggaggggcaucuuucucuggggucugggcu
ugguuagccugcccuaucucucucuguuucugucuccaucauucucuaaggccucucgguguuu
acaucuuuggcauucucauucuuuauucucuuugauuuggcucucugacucuuucggucucgau
cucccuuuguccugucucucugagucucugucucucuaauuugugucccucucugucucucu
gauucauucuccuuuaccucuuaguauccacggccucuccucuguuugccaccugccuuuc
uccucuccugccccccuuuccucuccaucauccuuccuuacucgauugcuuccuccucc
ucugccuguccaccuccuaccuuuucuccugauccccuuccccacaucgcuccucc
ucccgcacugauguccuuuccuccucuuucccauccuuccucuuugccccuuccuccca
uucugccccuuuccuauccuuccucuccucucccugcauucaccuccuccgugcauucac
ccgcccuccugcugcccacagACUACCAAUCCCUGCGGAUCGGAGGCCUUAUAUCGCCGGG
AUUCUCUUCAUCCUGGGCAUACUCAUCGUCUAAAgugagucccccuauccugccuucagucg
cuuccggugucugcccagccccgcccaccucccgcuccgcccuaacccccgcccacucg
ugcccuggccccgcccuuuguuucuguccaccaccuuuccuccugggcccugcaccuguu
cugcccugcccucagccacgucccaguuucugcccuucccccauucccgccuccggccccg
cccgguccuuauuccugccugcccucgggucgccccgcccucuaucccccgcccggccccg
cccacuuauauucccgcuucuggccccgcccgguuuccuauccccgcccggacacgcccc
cauuucuaucccccgcccucggccccgcccugcccugcccaccuuauuccucagacacgc
cagcccgggcaagcgagaucuguggcucgucugcgcugugcggcuuagagggggaucucag
cacacuccucuccacgccccaccacagGCAGAAGAUGCCGGUGCAAUUCACACAGCAGC
AGAGguaagaagccucucuggaccucucuccuccgcucuaaaggagcguugggggugag
accagaaguccacucauuccacagccagauccuucggcaaaauauguauuaaacaccuacuac
gugcccagcccacagccaggccuuggccaccaagccacgaguuaacugcccucucugucugag

Rattus norvegicus

GAGAACUGGGACUGCCUGAGUACGGAGAGACCACUGGCUGAGguguguaggggcaggugagg
cugggcauguccuguuugucucacagcauuccaccuguguccggagauagcuugcuucccu
ucaagggguagguuuggggacucugggaccaccugucuguuggggguagccugugggaagccc
cugaggagucugcccuccaccucugccucaauaucuguaugcuguguagucuccugccc
cauuauaggacuuguuuagacuugguuuggggugaagcagggggagcuagucaaguugaaug
gcugacaguuaguccuuaggccgcccuugacuuaacccccaugggguucaggcccuuuauag
aaggggaagagagcagagcagaggacauuuuugaccucggaugacuccuuagGCAUAGGC
AUCUCCCGGCCACAUCUGAUUGUCUGUGUGUCUCCUCUCCAUGGCCAGUGCAGgugagu
caaaggagguaccagcaucucagccaggugggguggcagaggcagggaaaagcccccaag
aagaccaagugggagaccctaaacuagaucaccaugugacaggagauaggggucuccacua
ggcucugaucauggcuggcaucuaggggagaggggaagaugccugagugagguaaaaguggg
aggggauggaagguaggucucugggugacagaaaauugaacaaccugcaaggugucagggug
ccgggccagugccggagguuccagggugcagaauaggcuggaaaccugccgacggcucagua
gcaccctaacuccgggcucaagaagauaggcagagcccucacuaccuuuccugccacagac
cccaggagcuacucuaauucggaucuuuuuuucuuucuaagAAGCUCCGCAGGAACCAGAU
CCAUUCACCUACGgugagggguuucgagagggggucuggguguucuaucucuccucuccuc
cucacacacacaca
cacacacacacacacucaggcacacucucuccacucucuccugcucuaguugucugag
acucccuugccugucuaauugaccucucugucucacugggacugcacuguugggggagauggg
ugccccauccccuacggagugggcauccucgcauuccuuccccccuuuccaccaccuccuc
cuccuccuuuccuacccuguccucuccuccuccucacacaucugcucuuccccuuuccuc
uccuccuccuggcccugcaaacuaucuccuuccccauugggucaccuccuccggggcugccc
acagAUUACCACACCCUGCGGAUCGGCGGCCUCACUAUCGCUGGGAUCCUCUUAUCUUGGG
CAUCCUUAUCAUCCUUAgugagugucugcaccugucucuccacccccgcuccagccuucc
uccccaagccccacuccagcaacacacacagccugugcacuauacacgcccacacagggcu
cagucuccaaacacuucccacaucuccaccucagacuccaaccucgcaacacacagacccca
ccccaccucaaaaccacgccccucaacuccaccaccagaccacgccccacaucuccuuccuc
cuccagcccugcccagguccaccuccucgcccuccuccaguuuggaggagagccuagggga
ugcuggagcaagaggggaucucagccuauaccuccacuccacagGCAAAAGAUGCCGGUG
CAAUUAACCAACAGCAGAGgugagugguccucuggaccuccucgcuuccuccgagug
gagagggcgugggggcgaggcggaauugcaccuucugcagucgaacacguauuaagcgc
uuaguguguguuuaaccuaagccaggcuccugggucggagcgauggucaaagcuccucucu
gccuggcucagcgcaccagccagugggggcccugggcuccaccagccccgcagauggaaacu
caagcugggugagggcgaagcugggcagaagcagccgcgugaaaugagauaccucacaggg
cggcccaguuuagcuccaguccggauccucgcgaggaauccucugaaaauaacuuuaaa
gcacaggcaacguaggcaugccuucugcugucuaagacgaucacagaugccuuccaccgac
ccucuagcaugguugagugcgcaccacgagccaggcgcgguuuucuaauuauguaucccuac
cccaccgggugaggugcgcuccaucauccaucccguuugugcauauagaggaaacugagggca
cggggagguaaaggugacuuaagggucacucacuggaccctaaugucccaaacucccaagaccu
gugaccguccucucccaacaauucaagugccuuccccaacacccccggaggccuccaccg
cgcaggcugggagcaccuccugccgcaccucugaaacagcagcgggaagcuucuguuucugac
ggaccgugucuaugucaaguccacggugggggucuggaaauaaggccugcaguggggcuucu

cagaagcggcuaccucuccugguccauccgaauuccucugucuguuccuucccagAACUGGG
GAACCCGACGAAGAGGAGGGAACUUUCCGCAGCUCCAUCCGCCgugaguucg**gggauacugc**
ggggguuuguggggcagcuguuuuuaagagccccucuucugggcuuagaauuggguuuggcg
gagaguuaucccugguugcagacucucccugaccccagaacucucugcauccucucagGUC
UGUCCACCCGCAGGCGUAG**AACCUCACCUGGCUCCAGGAAACUCAGCCAG**guccugcagu
ugagggaggaaggagggagagagguggcggguuggaggaggcaaggggcaaagugccag
ugugggagcguggcgaggagagcuugccacucacucucucacccccgcag**AGCCCCUUGG**
CACCUGACACCUCUCCCACCCAGCUGCUCGCCUGUGACCACCUCAGCGUCCCUGCAUCA
GCCUGCUUCUCGGACACCCUUGCUGCUCAGACCUCCAAUAAAACUCGGUUUCCUUCUUG

uccucuccccucuuuccuuccucuccccucucuccuuccucuccccucuuuccuuccu
ccccucucuccuuccucuccccucuuuccuuccuuccccacucucucucuccuccuc
ccuccuccacucuccucuccccaccccguuucuuuccaugcucccccaugguuccuuug
ucuuccucuccacccccaggACUGGGGAAACCUGAUGAAGAAAAGGGUACUUUCCGCAGU
UCCAUCCGCCGU

Felis catus

AUGGCAUCUCUCCACCACAUCUUGGUACUCUGUGUGGGUUUCCUCGCCAUGGCCAACGCAGg
ugagucugggguagguagcccgcuaaccaccucagccccgagggaggggaggggaagccuuuc
aagagaaccaaguuggagacuccaacuuaaacagagucaguggguaccaggaaguuggagg
uuucacgugggggaggggaggggaggaugcccagggcagacaaagguggagggugggauugga
gccccucuucccgacagggacagaaucaggacaacacgggaugagggcgggaagcuguagca
guuaagugaccaccugccccccccccaggacagugcagaugaggcagcuaagagccagaga
gggguggacagccuguucaggguccaauaguccccagacucucagcccaggacaggaagcc
ccaaaaggucucuuuaugccccuuccugcccagggccccaggaagcauccaaccuugacu
ucuuucucuuuccagAGGCUCCACAGGAACACGAUCCAUUCACCUAUGgugagggagggagg
ggcauuuaugcuugggaguugggaggguggguggccuggguuugccgguccuguucccacuc
cuccucgucucucucuuuccuuuaucucugacucaguauuuauaucucugucagucuccuuc
cucucuuucucuuugucucucagaaaggcucucugacuccuucuuuguuuuuauucucccuuguc
ugugucucugugucuccgugugucuaauugacccccuccugucucucugauucucuuucucc
uuuuaccucucaaugucuuacggcucuauccucugcggccaucuccuuucucccucuguc
cccuccuccucuccaucauccccccuacuucuuuguuuuccuccuccuccuccugcccugccu
accucuuuccuuuuccuuccacccccuccucucccauuccucucuuuccuccacacu
guuuccuccucucauugaucucucugcucuccuccugauccuccuugccccuuccuccca
uucugccccucuccuguccuuccuccuccuccuccugucucacucuccuccugccgcca
cagACUACAAAACCCUGCGGAUCGGAGGCCUUAUCAUCGCCGGGAUCCUCUUAUCCUGGGU
AUCCUCAUCGUCCUGAGUGAGUACCCCCACCCUGCUACCUCAGCCCCGCAGGUGCCGUGU
UUCGUCCCcgnnnnnnnnnnnnnnnnnnnnNCAACCAGCAGCAGAGguaagaggcccucggg
gcucucacucuccuccuuccgcucuaagaagggcgcugggagugaggcagggaguccacucga
cccacagccagagaccuucggcaaauacguauuaagcaccuacuacgugccaagccgcaag
ccaggcccuggggaccaaaccggcgaauaacugaacugcccuccuccugccuggcugagcucca
gcccagugggggcgggcgccguggguucccgacgccccacaaauaaaaucacaaagcgug
auaagugcugucaaagaaggagccacggcgaaauagagauaccgcgcuuggcggcccaguuu
agcucagaguccuguuuccagcucuuugacucaucucuaaaauaaaaauguaaagcacugua
gaaucccuuccgugugaaaacaauucuaaauguuuuuuacagaauagcuaauguuuagu
cccacgugcuaaaagguauuguuuuuacguguaauaacguuuuugacuccucacaccccuugc
augagacugucguuaacagccucguuuuacgaggaggaaaccgaggcgcagggaggugaag
ucacuugcccagaucaucucuaagaagaugagggguucuggguuucuaaccuaggcugucucca
ggccgucuguccucaaagcccuuccggccaucccuccccccaccaacuuccagucucuucccag
cacuccgggagggcacuuggagcgcguccugccacacgcuaaacugcuccuggggugcgcgccg
auuuucuguuucuggcggcccccgagccugcuccucgcccggucucuggcccucaguacggg
ggucugugaaaugagggcuguaucuggggggguuccugggagcaucugccucucuuuuuucac
cccacguccuucugccucucuuuccagGACUGGGGAACCGGAUGAAGAGGAGGGAACUUU
CCGAGCUCCAUCCGCCgugagucugg**gggagacuuuugccgguuuugggccugagccg**cugguu
ccaagaaccccuuccuguccucucugggcgugcggagggagggacuugacccgacagcga
agguccgggaguuucccugucgcuccccccuccgcgggagcuggggugcccuccugacacc
cgaacucuccguguuuccccucagGUCUGUCCACCCGCAGGCGGUAG

gugaaaugggggcugcacugggguuuccggguguagcugccucucuccuuuuccauccca
auuccuucugcaucucuuucucagGACUGGGGAACCUGAUGAAGAGGAGGGAACUUCCGC
AGCUCAAUCCGCCgugaguuuggggagacuucgggguguuuuggggaugcaagcugguuccaag
aaccuuuccugguccuccguggggcgcguggagcggggggcuugaucugaaaccgagguc
ggggaguugcccugcugugcuccaccuuccagaggagcuggggugcccuccugcuaaccg
aacucuauguguuccccuuagGUCUGUCCACCCGCAGGCGGUAG

Equus caballus

GGACGUUGGGGCCUUCUUCCGCAGGCGACAGCCUGAUUGGGgugagcgucccccgcccuc
ccuccagggccucccccugcgcucugggcggccuauuuugggagcaggaguggccagcc
uguggcuucccagggcaggccagacccaagaggaagggaguguggggaaguugggguuccc
caaaggugggagugugggugccgcuccuuccuccugcggcuccgugugcaccggcug
gguguggguuuuggacacucacguguguagggccggugcugacugugugggggaccaga
ggcccagaugacgaguaaugugugccugugucuccaccuacguccugcuccaaccagaagu
ugggggagugggcuugucuccauucuaaccccacugcggugugugacuguguguccgucc
cugccccuggcaucugucucucagccgcaccggccugggcccugucaccggcc
cuguggugucugcucgggaaagaugucaccagagccggggcggaggagcuguuuuucccuc
ucccauugcuuccaagagagcagcaaggguggccuuuccacggggacagccuguggcacug
uggcagccgggcccucaccccgcagggcugggcaugaccccagugggggaaggaaggcugu
ugccaugguggccugugcagggcaaaucuccagggugaagugggagauuuuuaccccg
ggggcaggcagagagcgggcccggcggagggcaggagagcggggauaucgcagacacaug
aggcugcggugugcugcagggggccuugggcguguccuggccgugucauccucacggg
gugucugucucuccaccgugggguguggcaccuugcuuucccacuagggcagcugugggaa
uucuggggccugcugcggggaggccccguggacgggugaugucucaccccuguccuugcugu
caugugacacccaucauguggguuuuagugacacuguguucccaugaagcagaggguac
cccuguuucuuugggguggccaagcuggaugacagagggcuuuuggaauaaguccuucuaug
ucucugacuuaaccccugggguucaggccccagugguggagggacgaggguaaaaauuccu
gaccuuuggguguucccagGACAUGGCAUCUCUUGGACACCUCUUGGUUCUCUGUGGGUC
UCCUCAGCAUGGCCAACGCAGgugagucuuuggggagggagcccaccaccaccucacccc
aggguggcaggggugagggaaaccuugcaagagaacugaguuggggacuucacccuaaacug
aguuauguagggcaccaggaaacuggggcuccacaugcaguccagucacaggcugguauuu
gggggaggggaucaggcaaaggugggacgggaugguggccagcuucccaugaaggauuga
aucuuagccuguaauaagaaggggagcuggggagucaggggcccucuguccucgggac
agugcagaggguccagguaagagccagagaggggugggcccgcugcucaggguccagucacc
ccaaacucucagcccaggaagguaaagcccacagcggucacuuuaugcccucuccugucca
ggaucccaggaucccaggaagcauccugaucucucucucucuuuccagAAGCUCCACAGGAA
CAUGAUCCAUCACCUAUGgugagggaggggcauccaucuuugggaguuugggagugggguu
uggguuuugccuguccuguccucauucacucucucuuucuuucuccucucuccaugucucug
acccccagcguuuauaucucugucacucuccuucucucucuuucccuugaucuggcucucug
acucugucuuugaucuccccuugucugucugcucucucugucucuuucugugugucugccuc
cuuauuuugaucucucccugucucucugauucuuucucuuucuccuuuuaccucucaguauc
caugcccacuccucugcugccuucugcccuuucucuccucccuguucccucacuccucucca
ucaccccccuuacucccuguuuccucucugcccugcccagcuucuccccuuccuuucccuc
caccucuccucucucuaaucucccuucuccucucccauauaucugcuccauccucucaug
acuuccuuccuuccuucccuccuucccauucugcccucuccgauccuuccucucccucc
cugcccucacuguccuccuugugcccguagACUACCAUACUGCGGAUCGGAGGCCUCAU
CAUCGCCGGGAUCCUCUUCAUCCUGGGCAUCCUCAUCGUCCUGAgugaguacccccgacccc
accgccuccagcccucugcggguuuccgcccagcuccgcccuguucccgcccgcucucca
accucgcccguauccacucggccucgcccucuguucccgccccgccccgucuccucggccc
cgccccuguucccguccugccucaucuccuagaccccgccccuauucccgccccgcccua

cuccauaggccccgcccgcggccccgccucuacccccgaggccccgagucucgcaagcuccag
cuggagcacgagcgccgcgcccgcgggagccgacgcucagcccgguccccccuuc
ccccacagGCAGAAAGUGCCGGUGCAAUUCAACCAGCAGAGGguaggaggccuccgg
cccgcacucaccuacucccgucuccagaggggcgucgggggugagccagagccccgugcgcaa
aucugcauaagcgccuacuaugugccuggccccgaggcgggcgucgggaccagccgcgcc
uucaccgcccggccuggcugagcuccagcccagcgcggggcgggggccguggguuccaac
aaccacgaauguaaaaucacaaagcgugguaagcgucgcaaaggaaggagccgggcgaaa
ugagaucaccucacuugcuggcccaguuagcucggaguccuauuccuagcucuuugauuca
ucuuuaaaauaaaauuuaaagcccaggcgagguaugaauaccuuccaaguuaaagcauu
agagauguuuuuauaaaauaauagcuaauacugguuggguguguccuccgugccagauacugu
cugacuguguguuaucuuagugaccccucccgccacgucuaugagguaggugcugcucucag
ccucauuuuacagaugaggaaaccgaggcacgggaggugaagucacuagcccaggauacuc
ggcuagaagacgaggauucuggguuuucuaaccuaggccguccuccgggagggugcccccaag
ucccuuuggucaucccuccccccgccagcucccaguccuuccccccggcacucggcacucgg
gagaugcucccugucaccgcguggagcgcuccccgccacgccugaaccugcuccugggggc
gccgccuccucgcccaccgcugggcccucgggacacgggucuaugaaaugaggcugcccuggg
cauucggggagcggccgcucucuccuuuuccaucccaauuccuucugccucuccuuucc
agGACUGGGGAACCUGAUGAAGAGGAGGGAACUCUC CGCAGCUCCAUCCGCCgugaguugg
ggagacgucggguguuugggggugaggggacguuuccgagaacccccuuccuggcccuccuug
gcugcguggagggaagggcuuggucugaaaccgaaggcggggaguuccccccgcugcccacu
ccacagcagcggugugacucccugacaccgaacucucuguguccccccagGUCUGUCCACC
CGCAGGCGGUAGAAACAGCUGGCGGAUGAACCCAGCCAGguccugaacucugacugggcu
gcgggagcagugagggggaggagggggcguggggucggggggcuggggggguggcugggaggg
cucuccugccucucacccguuucacccccauagGAUCCCCUGGCACAUGACGCCUCCCACCC
AGCCCCGAGCGCCACCGCCACCAGGACUGUCAUCUCCCCGAGCCUGCCCCACAGACUCG
UCUCUGCCGCCAGACUCCAAUAAAACGUGC UUCUCUCUG

Ailuropoda melanoleuca

AUGGCGCCUCUCUACCGCAUCUUGGUUCUCUGUGUGGGUUUCUCACCACGGCCAACGCAGg
ugagucuggggguacuuaagccccaccaccccagcccaaggaggcaaggggugaggggaag
cccuucaagagaaccaaguugggagacuccaaccuaaaugagucaguuggggguaccaggaaau
uggggguuucacauggggccacucacaagcuaguauuuggggguagaggagcggaugcaagc
ucagggcgaagguggacgguggggauggaggcccacuuccucagaugacagaaucaucugacaa
cacgggguaagacaggauuugggggaguuaggugccccugccccaccacaagauggugcag
augaggcagcuaagaccagacaggguggggagccugcucagggcccaacagucgccagacu
cucagcccaggagaguaaagccccagaaguucucuuauguccuucucuauccagaguccc
aggaagcauccaaccucugacuucuuucucuuccagAAGCUCCACAGGAACACGACCCAUU
CACCUAUGgugagggcaggaagaggugucuauccgcgggaggguggggagggcgccuggccuggg
uuugcccauccuguccucauuacuccucucucuuucuccaucucucuuucugacucagugu
cucucucucucucucucucagaucucugacuccuuguuuugaucuccccuugucugucucuc
ugugcgccugucuaucugauccucucugucucucugagucuccuucuccuuaaccucuca
guaucuuauggcucuauccucugcucugccuccuuucuccucucuguccccuacuccuc
uccaccauccuucacuucuuuccuuguuuccucucuccuccugcccgccaccuccuccu
uuccuuccaccucucucuccugauccucuccuccuuccuccuuaucuuucuuucc
ccugacugaucuccucuaaccuccuccuccugguccuccuugcccacuccucccauuc
ugccccucuccuauccuccccccuccuccuccugcccuacucuccuccuccugccguccacag
ACUACCAAUCCCUGCGGAUCGGAGGCCUCAUCAUCGCCGGGAUCCUCUUCAUCCUGGGUAUU
CUCAUCGUCCUGAgugaguacccccaccgcuaccuccagccccgcaaccucgagca
gagccggcgacgagcgccacucggugcccgcuaagagcugaauucagccucguccuccuc
cuacccccaccacagGCAGAAGGUGCCGGUGCAAUUCAACCAGCAGCAGAGguaagaggc
cccuccgggucucacucaccuacuucgcucuaagaggggaggggaggggaggggaggggaggu
ccaccgccccgcagccagagaccuucagcaacuauuaaagcaccuacuacguuccaa
accccaagccaggcccggggacaaaugggugaauagauaaaucgcccuccuccugccuggcug
agcucccagccccgugggggagggcgccgugggguuccaacagccccacaaauuaaaauaac
aaagcgugauaagugcugugagagaaagagccacggcgaaugagaucaccgcacuuggcgg
cccaguuuagcucagcuguccuagcucuuuaguucaucuuuaaaauuaaaauuaaag
caauguaugaauaccuucuccauguuaaaacaauuaagacaugcuuuuaaaauuaagcuua
uauuuagucccaauugccagauacuguuuuauuguguaauuauuuuacuccucacacc
cuuguaugaggucggugcuguuuaaccucauuuuacugaugaggaaaccgagggcacaggg
aggugaagucacuugcccaagaucacucaacuaggagauaagggguucuggguuucuaagccua
ggcugucuccaggccggcugcccucaaguccuucagcaccuccuccccaccaacuuccggc
ucuuccccaaccuccgggagggcacuuggagcaccuccugccacaagcuuaaaccgcuccug
ggugcgccugauuaucuaagcggacccccgcgcucuccucgccaucucuggcccucaguac
agggggguguguaaauagaggcugcagggggcauucagggggcgccugccucucuccuuuu
ucaucccuaauucuuucugccagGACUGGGGAACCUGAUGAAGAGGAGGGAACUUUCCGCAG
CUCCAUCCGCCgugaguuugggagacuuccgggucuuuuccgggucagggcagguuccaagaa
ccccuuuucuggcccggacagggggcgaggagggggcuugaucugaaaccagaggucugg
gaguuccccugcuguuccccgcuccgcaggaacuggggugccccuccugacaccggaacucu
cuguguucccccucagGUCUGUCCACCCGCAGGCGGUAG

Pongo abelii

AGGCUUCCAGGCAGGCCAACCCAAGAGGGAGGGAGUGUGGUUGAGGCAGUGGGUUCUGCAG
GGUGGGGAUGUGGGCGACUCCUCCUGCCCUGCUGGUGCGUGUGCACCCUGGCAGGGUGUGGA
GUUUGGACACACACGUGUGUAGGGCUGGUUGCGUCACUGCGUGGGGGCACCGGAGGCCAGA
GGAGGAGUACUGGAUGCCUGACGGUGUUACACCCACGUCUCCUGCUCAACCAGAAGUUUG
GGAGAGguuguuguccauguccauuccggccccacuguguguguguguguguguguguaucc
cugccccagcauguguuuucuaucucucaggccccacugggucugggcccuaugucacuugccu
gacauccgauugugaaagaugucacccagaggcgggcagaggggucugucuuuuucuuuuuu
guugcugcccagggaggagauugggguggacuucccacaggggagccuguggcgauguggc
agcugggcccucaccccggcagggcugugcgugacccccugagugggggaaggcaggcugug
ccauggguggccugagcgagcagaauuccuccagggugaaguggggagauuuuuauaccccggg
ucaggccgggagcgggcgggcgagagggcagggagcugggaaucgcggggcauagugagg
ccgggcauguaggcaggugggacuugggcgugcccugcugucuccugcuccguguuugugug
aggcagcgccuccucugcccugccaggguaaggucugggaauccgggggcccugcugcgggaggu
ggaggccuaagggaggccccagggacugugugucucaccccuguccugcuacguuguguu
guugugugaccccacugggagguuuguuuuggugacacuguguccccacgaagcuggggua
cccguuucucuaugcuuggagccaccaagcuagaggacgaacgcuuucugugauucggucccca
gacugucucugacuuaaucccuuggguucaagcccugugugggagagcaagggcacacacug
ccuaauccguggugucccccccagGACA AUGGCAUCUCUUGGCCACAUCUUGGUUUUCUGUG
UGGGUCUCCUCACCAUGGCCAAGGCAGgugagugcaggggaggcugccccgcuaccaccuca
gccccagggauuggcgggcggggaccgaagaaccaaguuggagacccaaccuagacugagucg
gcugggguaaccaagaaguugggggucgccacaugggguccagucacaggcugguauuuggg
ggaggggagaggaagccccagaucaggcaaaagauggggugggauugggggucgaaauccuggu
gggaaucugggucacagacagccugccgugagucagggagcuggggcaguuaggugccgcc
ugccccuucugggacagugcaaaaggaggcagcugggacccagagagggugggagccugccu
agacaccucagacucucagcccagcagggcagagccccaguggucuccuauugccccucu
cugccaggaccccaggaagcauuaaccccugauuucucucucuuuccagAAAGUCCAAAGG
AACACGACCCGUUCACUUAUGgugagcggggggucuaauuuugagucuuugggggagagccug
gcuuugcuggucguuugauuucccccucgcccucccccagaguccaguauugauaucuguca
uucuccuucccucuaauuuguccuuccucucugauuccaccugucugcaucuuuccugucuc
gugucuaucugugucgucugucugugugauaccucucugguugucuuucucuuugccuggguc
gucucagccucucguggcccuaucucugcuucuuuccauucucucucccgucuguccucuc
cucccugccccgucuccuuccuuaucaccccucuccucucccugggucccccacuucc
uccuuccauaucugucuccccuuaauuauucuuuuuccccccuucugccugcuggucuuuc
ucccuguccuccucccauuuaccccucuccuauucuccuccucuccuccugcccuc
accuucccugcucugcugcucacagACUACCAGUCCCUGCAGAUAGGAGGCCUCGUCAUCGC
CGGGAUCCUCUUAUCCUGGGCAUCCUCAUCGUGCUGAGugagugccccuagcccccgccu
cuaccccgcucucccuggccccgcucuccuagccccgccccucccgccccaaaccucc
caggccuugccccgcuaaccugccuuggcucccuggccccggucucgccucuaagccccgc
cccgucccccaagccccgcccccgcgggcgagcuggagcgacagcgccguuggugccc
gccaggaggggagccucagccucuccuaccucuccacgcccacagGCAGAAGAUGCCGGUGCA
AGUUCAACCAGCAGCAGAGguaagacgcccuaucacgcccuccuucgcccgcuccugcucua
gagggggcgcgggugaggcggggaguaccccugacccgcagcccgaucucccaucagcgacu
auguauuaagcaccuacuaugugccauggcccaagccuggcccuggggaucagcgagga

aaccucccgcccuuccuggccgagcucccagccuaguggaggcgguggccguggguuccaac
agccccacagauagaaaaucacaaagcgugauaacacaaaaugcaggaaagaagaacggc
ggugaaaugagaucaucucacacgcggcccaguuuagcuuagaguccuguuccuagcucuuu
gauuccucuuugaauaaaauguaaaagcauggacaauguaugaauauguuagaacaauua
gauauuaucuaaaguaguagcuaauuuuauuggguguguaccacgugucagauacgguuuc
acuuccucuggggagggaggugcuguuauuaaccccacuuugacagaugaggaaacugaggcac
agggaggguuaaagucacuuuguucaagaucacucaaguggaauauggggaaucuggguuuc
caaccagggccaucucauggcagucugccaaguccccacgacuaucccucuccuaccaacu
cacaucccugccccaaauccgaggagguacucaccguuaaccagcuuagaagccccuguc
agcacuaaagcugcuccugggugcuccucauuucuaagcggaccccagccgcucucuccguc
auaucuggggccuaguuaacccaucugggaaaggaggcuuguacugggggguuccuagaagg
gcagccucuccccuuuccaucccgaaucccucugccucugucucccagGACUGGGGAAC
CCGAUGAAGAGGAGGGAACUUUCCGCAGCUCCAUCCGCCgugagucuggggagacucgqqu
auuuuqggagagqcugguuccaaggaacccuuuccuggcccuccuggcugcguagagg
gaggggcuggaucugaaagcugaggggugggaguugccccgcccggggcccaccugcccag
gagcugggggaugccucucaugaaugacccccgaucuccguguuccccccagGUCUGUCCACC
CGCAGGCGGUAGAAACACCUGGCGGAUGCAAUCCGGCCAGgugcugcagcucugacacggc
ggugggaggggaaggaggagggaaggaaaggcgggagaggggggccaagugccaggguuq
aagggcggcagggguggggcuggacgucccccucgcccucacccuuuuucccucacag
GACUCCCCUGGCACCUGACGUCUCCACGCUCCACCUGCGGCCACCGCCCCUCCGCCGC
CCUCCCCAGCCUGCCCCGCAGACUCCCCUGCAGCCAGAAUCCAUAUAAAACGUGCG
UUCUCUCGACUGCACUUUGUCGGUCUCGGUCCUCAGCGCAAAGCCAGCGCCCCUGGAC
CCCAGCAGGGGGCGCCCCACCCUAGAGGAUUGUGCGGGGACGACGGUGGUGGGCGGGGGCGG
GGNNNNNNNNNNNNNNNN

aaagcggagggcgggggaguugccccgccgcgggccccaccugcccaggagcugggggaugccu
cuccagaaugacccccgaucuccguguuccccccagGUCUGUCCACCCGCAGGCGGUAG

Sus scrofa

GAGGGGUGGGGUGGGGUGGGGACACCGCUGAGGGCGGCGGUCCAGCUCAGGGCCAG
GGGGUCCAGCCGGCCGUUUGGGGGCCUUCUUCAGCAGGGGACAGCCUGACUGGGgugagcg
ucccccccuccuccaggccucaccccuggccuggccgggagccuauuuugggagcagaag
uggcgcccaggcaggccagacccaagaggaaggguguguguuugggucguuggggcucccc
aggggugggagugugggugcagcuccuccuuucgcccuguggcugcgugugcaccucggcugg
gugugcgguuuggacacucacguguguagcucggggcugcguccuuguuugggggccccggga
ggcccagaugaggaguacugugugccuguggcuccaccucgagucucuccaaccagaagu
uuggggagugggugugucuccacuccagccccacugugcgcgugcauguaugcgugagu
gccccggccccaggcaucugccuugggucucucagcccugcuggccuggggccuccuguca
cucgcccugguguguccacugugaaagaugucaccagagacaggcaaaaggggauuuuuu
ccccguucuccucacuccaggagaggagaagagguggccuuuccacgggggagccugug
gcuuguggcagccaggccucaccccggcaaugacccccgaggcaggaggggggguaggaaa
gcuguugccaugguggccugugcgaggcaaaauccuccagggugaagugggagauuuua
cccagggucaggcagagaguggccaguggccgagggcaggagagcugggaucuuucagaca
cagcgaggcaguuuugcaagcaggugggucuuuggguguguccuggcugucuggggcucug
gcaggcuggccgucucucugccaggguggggugaggcaccuccaccaccggaguaggugugg
ggaucuggggccugcugugggggaagcccgggcuucgggaggucccuguggauuuugugu
gucccccugccugguccuuguccuugcugccauaugacccccccccauugggugggagu
uugggugagacuguguccuggugaagcagggggugccuuguuuccagggcgaccaagcuag
auggaugcuuuuggaauuaagucucuggacuguaucuaacccuuggguucaggccccagu
gguaggggaacaaggguaacacacuccugacccuuggugcucucccagGACAAUGGCAUCUCU
CAGCCACAUCUUGGUUCUCUGGGUCGGAUCCUCACCGUGGUCAACGCAGgugagucugcgg
gaggcagcccaccacucaccucagccccaaaggguggcaagcguagggggaaagccugcgaga
gaacuaaguuggagacucggucuaucuaaguccguugaggagccaggaaaugggggucuc
acaugggguccagucacaggcugugugugggggaggggagaagaugccccaggucaggcaa
aaauggaggggugggagggaggcgggcuuccgugaacgauggagucagucgauggacaaccug
uaaugagaugggagcugaggcaguuaaugccugcccugcccugcccaggacagugcaga
gggguggcugggaccagagcggggguggggugggggguggggggggcgcgccugcucaga
guccaacagucuccagacucucagcccagaaaugcgaacccccaaaaggaccucguuacgcc
ccucccuguccaggauccagggagcauccaccucugaugucuuucucucuuuccagAAGCU
CCACAGGAACACGACCCAUUCACCUAUGgugagggagggaggggcccucuuucugggggagcu
ggcuggguggggguggggggcugggcugaguuagccuguccucucuccccccaucucucucug
uuucugucuccaccugucucuaagacucucaguguuuaucccucugucauucucauucucuc
cuuucucaugaucuggcucuaucuuugaucucuuuggcuguuucucucugucucucagugagu
cccugucucucugucucucugauucucuuucuccuuuccccucucaguaucccauggcccag
ccuccacuuccuccuggcuuucuccucuuuccugccccccuauccuuuccauaccuccccc
aucucccuuguuuuccuccuccucuuugcccugcccaccuccucuuuccuuuuucuuuac
auccucuuuucuccaucuccugucucucgucucuccuccuccucuuauugaucuccuuu
cuccucuucccggauccuuccuccuggccccuuccuccuauucugcuccucuccuggcuuu
ccuccuccccuccugcauucaccguccucccugcuguccacagACUACCAUCCUUCGGA
UCGGAGGCCUCAUCAUCGCCGGAUCCUCUUCAUCCUGGGCAUACUCAUCGUCUUGAguggg
uacccccacacugccuccagccaugcuucugcgugucugcuccagccccgcccugucccc

gccccgccuccaaccgccucuauccagcccuuggccccgcccuuguuucugcccugcac
cuguucugcccugggccccgucucugucucgccuucggaccgccucgccccuuccuaucc
ccgccucggccccgccccuguccugccccaccuuauccccgccccccagccucucugc
ccuggcucgcgcgcgagcucuggcuggcugugcggcacugagcagaauaucagcgcgcucuu
ccucacacccccaccacagGCAGAAGAUGCCGGUGCAAGUUCAACCAGCAGCAGAGguaaga
ggccucuguggaccucacucuccuacucggcucuaaaggggagcugggggugaggccgga
aguccacucaauccacagccagagacaccggcaaauauguacuaagcaccugcuaugugccc
agccccgagguagccugggaccaagccacgaaauaaguaaacuccuugccuggcugagcucc
cagcccaguggggcgugggaguggguuccaagagaccacaaauaaaaucacaaagcg
ugauaagugcugugaaagagCCUCGGCAAAAUGAGAUCACCUCACUUGGCGGCCAGUUUAG
CUCGGAGUCCUGU

ccugauacaucuccuuuccagGACUGGGGAACCUGAUGAAGAGGAGGGAACUUUCCGCAGU
UCAAUCCGCCgugagucuggggagacuucggguguuugggaaugcgaguugauuccaagaag
ccuuugcgggccuccuccugggcgaggggggucgcggggaggggcuugaucugccugccgu
gccccgaccuuucagaggagcuggggugccccucuugacuuccggauucucugucuuccucc
ucagGUCUGUCCACCCGCCGGCGGUAG

APPENDIX II

***FXVD1* variant 009 pre mRNA sequence ENSEMBL Transcript ID: ENST00000589121**

Key: UTR region
Intronic sequence
Exonic translated sequence

UUUUCUGUGUGGGUCUCCUCACCAUGGCCAAGGCAGgugagugcaggggagggcugcccgcua
cccaccucagcccagggguggcggugggggaccgaagaaccaaguuggagaccccacccuag
acuaagucggcuggggguaccaagaaguugggggucuccacgugggguccagucacagggcug
guauuugggggaggggagaggaagccccagaucaggcaaagaugggguggaugggggcugaa
uccccgauggggaauaacugggucacagacagccugccgugagucagggagcuggggcaguuag
gugccaccugccccaucugggacagugcagagggggcagcugggaccagagagugugggca
gccugcccagacaccucagacucuaagcccagcaaggcagagccuccaguggucuccuau
gccccuccugccaggaccccaggaagcauucaaccccugauuucucucucuuuccagAAAG
UCCAAAGGAACACGACCCGUUCACUACGgugagcggggggucuaauuuugaguccuggggg
agagccuggcuuugcugguccuuugauucccccucgccccccccagaguccaguauugau
aucucugucauucuccuucccucuaauuuuguccuuccucucugauuccaccugucugcaucu
uuuccugucugugucuaucugugucacugucuaugugauaccucucugguucucuuucucuu
gccugcgucugucucagcaucucguggcccauccucugcuucucuccgucucucucuccccc
uguccuccucucccugucccccucccuccuuccuauacaccccuuuccucucccugguac
cccacuuuccuccucccauauaucugcucuccccuuaauuauucuuacuucccccccucugccugc
ugguccuuucucccuguccucccuccuucccauuuaccccucuccuauucuccucccugucuu
cccugcccucaccuucccugcucugcugcucacagACUACCAGUCCUGCAGAUCCGGAGGCC
UCGUCAUCGCCGGGAUCCUCUUAUCCUGGGCAUCCUCAUCGUGCUGAgugagugcccucag
cucccgcccucuaaccccgcucucucccuggccccaccucucucuggccccgcucucccuggc
cccgcucucccuagccccccucucccuggccccgcucucccuggucccgccccucccugg
ccccgccccgccccaaaccccucccaggccuugccccgcuaaccugccuugguuccccggcc
cccggucucgcccucuaagccccgccccgucuccccaagCCCCGCCCCUCGCGAGGGCGAGCUGG
AGCUACAGCGCCGCUUGGCGCCCGCCGGGAGGGAGCCUCAGCUUCUCCUACCUCUCCACGCC
CACAGGCAGAAGAUGCCGGUGCAAGUUAACCAGCAGCAGAGguaagacgccccuccccgccc
cuccuucgcccgcucccugcucuggagggcgccgcgggugagggcggggaguaccccugacccg
cagcccgauccccgucagcgacuauuguauuaagcaccuacuaugugccauggcccaagccug
gccugggaccaagcgaggaaaaaacucccgcccucccuggccgagcucccagccuagugg
aggcggguggccguggguuccaacagccccacagauagaaaaucacaaagcgugauaacaca
aagugcaggaaagaagaacggcggugaaaugagaucaucucacacgcggcccaguuuagcu
uagagucuuuguuccuagcucuuugauucccucucgaauaaauguaaaagcauggacaaugu
augaauauguuagaacaauuauagauuuuaucauaaguaguagcuaauuuuacugggugug
uaccacguguuagauacgguuuacucucccuggggagggaggugcuguuauuaaccccuuu
gacagaugaggaaacuaaggcacagggagguaaagucacuuguuacaagaucacucaagugg
aagauggggggguucuggguuuccaaccaggccaucucauggcagucugccaaguccccaug
acuaucccucccccaccaacuucacaucccugcccccaaacccgaggguacucacugua
accagcuuagaagccccugccagcacauaagcugcucccugggugcucccuaauucuggcgg

accccgagccugcucuucguccauaucugggccuaguuaacaccaaucugggaaaggaggcuu
guacuggggggguuccuagaagggcagccucucuccccuuuccaucuccgaaaucccucugccuc
ugucuucccagGACUGGGGAACCCGAUGAAGAGGAGGGAACUUUCCGCAGCUCCAUCCGCCg
ugagucugggggagacugcggguauucuggggagagggcugguuccaaggaccgcuuuuccg
gccucccuggcugcguagaggggaagggcuggaucugaaagcggagggcggggaguugccc
gccgcgggcccaccugcccaggagcuggggaugccucuccagaaugacccccgaucucggu
guucccccagGUCUGUCCACCCGCAGGCGGUAGAAACACCUGGAGCGAUGGAAUCCGGCCA
Ggugcugcagcucugacacggcgguggggaggggaaggagggaggaaggaaaggcgggagaggg
agggggccaagugccagaguugaagggcggcgagggguggggcuggacgucucccccucgcu
cucacccuuucacccucacagGACUCCCCUGGCACCUGACAUCUCCCACGCUCCACCUGCG
CGCCCACCGCCCCUCCGCCGCCCUUCCCCAGCCUGCCCCGCAGACUCCCCUGCCGCC
AAGACUCCAUAUAAAACGUGCGUUCUCUCGACA